UNIVERSITA` DEGLI STUDI DI NAPOLI

FEDERICO II

Facolta` di Ingegneria

Dipartimento di Ingegneria Chimica, dei Materiali e della Produzione Industriale

PHILOSOPHICAL DOCTORATE THESIS

IN MATERIALS AND STRUCTURES ENGINEERING

major in **Biomaterials**

XXVI CYCLE

Peptide-conjugated hydrogels for cell and tissue recognition

Tutor : **Prof. Paolo Antonio Netti**

Coordinator: **Prof. Giuseppe Mensitieri**

Candidate

Antonio Paciello

ACCADEMIC YEARS 2011-2014

"Here, you see, it takes all the running
you can do, to keep in the same place.
If you want to get somewhere else,
you must run at least twice as fast as that!"

Lewis Carroll - Alice in Wonderland

ACKNOWLEDGEMENT

It would not have been possible to write this doctoral thesis without the help and the support of many kind people around me, but only for some of them it is possible to give a particular mention here.

Above all, I would like to thank my Family for its great patience at all times. My parents, brothers, sister, brother and sisters-in-low and my five nephews have given me their unequivocal support throughout, as always, for which my mere expression of thanks likewise does not suffice.

I would like to thank my PhD advisor, Prof. Paolo Antonio Netti, full Professor at Universita` di Napoli Federico II and Scientific Coordinator of the Center for Advanced Biomaterials for Health Care of Istituto Italiano di Tecnologia (IIT@CRIB) in Napoli, for supporting me during these past years, and above all for having believed in my scientific gifts. This thesis would not have been possible without his help, support and encouragement.

I would like to thank again Prof. Netti for engaging me in a very interesting project named "*Novel smart hydrogels HA-based with non-covalent adhesive properties for tissues healing applications*". This technological project has also allowed me to relate with the research and development activities in the industrial world.

I would like to thank Dr. Mariagabriella Santonicola for her good advices, support and friendship. Dr. Santonicola has been my PhD Supervisor for the first 18 months of my doctoral thesis, when she was Team Leader at IIT@CRIB. Our collaboration continued also later when she joined Sapienza Universita` di Roma as Assistant Professor. I am very grateful for her precious guidance and contribution to the project "*Novel supramolecular PEI-based hydrogels for plasmid release and photo-patterning at near infrared wavelengths"*.

I would like to acknowledge Istituto Italiano di Tecnologia and Universita` di Napoli Federico II for supporting me with a scholarship in these three years of PhD training.

I am most grateful to Dr. Fabio Formiggini for his good advices, assistance and training for confocal microscopy and his lesson on image editing; Maurizio Mangiulli for his friendship and precious help in the laboratory work; Dr. Angela Maria Cusano for her precious contribution in plasmid DNA entrapping and releasing experiments.

I would also like to thank my colleagues and friends Dr. Raffaella Della Moglie, Massimiliano Porzio and Elisa Vaselli for providing support, kindness and friendship that I needed; Dr. Giuseppe Amalfitano for his collaboration on the project "*HBOC emoglobin-based as novel oxygen carrier*" not reported in this thesis; Dr. Paola Vergara for her friendly moral support.

I would like to thank Francesco for his patience at all times and for his kind affinity during this thesis draft.

I would like to thank my cousin Biagio for his affection and support in every time.

I would also like to thank my old friends, when I attended undergraduate degree in chemistry, Prof. Daniela Montesarchio, Cinzia, Rosita, Giovanni, Mariantonietta, Caterina, Elsa and Concetta for their great friendship and affection also after many years; and my "flying" friend Mariano who always relies on our friendship when he is "elsewhere" on the earth.

Last, but by no means least, I thank my friends cats and, in particular, my little crafty Caty over all for her patience when she arrived at meal time and I was completely grasped for the writing of this PhD thesis.

Sincerely thanks

Antonio

CONTENTS

LIST OF ABBREVIATIONS

aECM = artificial extra cellular matrix

Arg, R = L Arginine

Asn, N = L Asparagine

Asp, D = L Aspartic Acid

ATR = Attenuated Total Reflectance (FTIR)

CBF = Collagen Binding Fragment

CIBF = Collagen type I binding Fragment

CIBF-biotin = Collagen type I binding Fragment N-terminal biotynilated

cMB420 = DVS crosslinked hyaluronic acid microbeads prepared using 420 µl of DVS per 10 ml of the 2.5% HA solution

CT = Corneal Topographer

Cys, C = L Cysteine

D_2O = deuterium oxide

DCM = Diclhoremethane

DMF = Dimethyl formamide

DNA = deoxyribonucleic acid

DOPA= L-3,4-Dihydroxyphenylalanine

DTT = ditiotreitiol

DVS = Divinyl sulfone

ECM = extra cellular matrix

EDAC = 1-Ethyl-3-(3-dimethylaminopropyl)carbodiimide hydrochloride

EDC = 1-Ethyl-3-(3-dimethylaminopropyl)carbodiimide

ESEM = Environmental Scanning Electron Microscope

fcMB = fluorescent DVS crosslinked hyaluronic acid microbeads

fcMB350 = fluorescent DVS crosslinked hyaluronic acid microbeads prepared using 3500 µl of DVS per 10 ml of the 2.5% HA solution

fcMB350-CIBF = fluorescent DVS crosslinked hyaluronic acid microbeads prepared using 350 µl of DVS per 10 ml of the 2.5% HA solution and conjugated with CIBF

fcMB420 = fluorescent DVS crosslinked hyaluronic acid microbeads prepared using 420 µl of DVS per 10 ml of the 2.5% HA solution

fcMB420-CIBF = fluorescent DVS crosslinked hyaluronic acid microbeads prepared using 420 µl of DVS per 10 ml of the 2.5% HA solution and conjugated with CIBF

fcMB420-CIBF-biotin = fluorescent DVS crosslinked hyaluronic acid microbeads prepared using 420 µl of DVS per 10 ml of the 2.5% HA solution and conjugated with CIBF biotynilated

FTIR = Fourier Transform Infrared Spectroscopy

Glu, E = L Glutamic Acid

Gly, G = L Glycine

HA = Hyaluronic Acid

HBPs = hyper branched polymer

HCl = Hydroclhoric Acid

His, H = L Histidine

KCl =Potassium Chloride

LSCM = Laser Scanning Confocal Microscope

Lys, K = L Lysine

MAAH = Methacrylic anhydride

Met, M = L Methionine

Mid-IR = Mid-wave infrared

MP = Microbeads

MSCs = Mesenchymal stem *cells*

NaCl = Sodium Chloride

NaOH = Sodium Hydroxide

Ne = Neon

NHS = N-Hydroxysuccinimide

NIR = Near infrared

OCT = Optical Coherence Tomography

PAAc = poly acrylic acid

pDMAEMA = poly(2-dimethylaminoethyl methacrylate)

PDMS = Polydimethylsiloxane

PEG = poly ethylene glicol

PEI = poly ethilen imine linear

PEI-branched = poly ethilen imine branched

PEI-MA = poly ethilen imina methacrylated

PEO = poly ethylene oxide

Phe, F = L Phenylalaline

pLL = poly-L-Lysine

PNIPAM = poly *N*-isopropylcrylamide

PRK = Photorefractive Keratectomy

Pro, P = L Proline

PVA = poly vinyl alcohol

RNA = ribonucleic acid

SAXS = Small Angle X-ray Scattering

Ser, S = L Serine

SH = Tiol group

TEA = Tri Ethilen Amine

Thr, T = L Threonine

Trp, W = L Teyptophan

Tyr, Y = L Tyrosine

UV = Ultraviolet rays

Val, V = L Valine

Wd = weight dried

Ws = Weight swollen

XIIIa = Fibrinoligase and fibrin-stabilizing factor

LIST OF FIGURES

Spreading is dependent on the ligand concentration as demonstrated by fluorescent microscopy (A, Scale bar: 100 *ím) with double staining* of cell nuclei (blue) and f-actin cytoskeletal elements (red), and quantified by cell surface areas (B). (Lutolf et al. *Macromolecules* **2007**)

Figure 1.9. - The strategy to create biomolecular channels in agarose hydrogel matrices uses the chemical modification strategy in (a) and a focused laser, resulting in alternating volumes of cell-adhesive (peptide) channels separated by non-adhesive (agarose) volumes (Schoichet M. et al. *Nature* **2004**).

Figure 1.10. – a) representative XY cross-section image of green fluorescently labelled oligopeptide channels (scale bar:200 μm); b) representative image of the green fluorescently labelled oligopeptide channels constructed from a series of XY cross-sectional micrographs over a 0.5 mm depth (scale bar:200 μm) (Schoichet M. et al *Nature* 2004).

Figure 1.11. - Schematics demonstrating photoinduced patterning of an existing poly(ethylene glycol) diacrylate (PEGDA) network at the microscale (A) and macroscale (B). The following description applies to both schematics. Step 1: Precursor solution containing the mono- or diacrylate derivatized moiety to be patterned is layered onto a base PEGDA hydrogel and allowed to diffuse into the hydrogel network. Step 2: A laser beam generated by a Ti:sapphire laser tuned to 720 nm is scanned across an *x–y plane within the hydrogel, with the laser shutter being opened only in the user-specified regions* of interest (ROIs) shown in the ROI template to the right of the hydrogel being patterned in (B). In TPA, conjugation of the molecule to be patterned to the hydrogel substrate occurs only at the laser focal point. The microscope stage is incremented axially and patterning is continued within the specific ROIs at this next *x–y plane. This sequence of steps is repeated until the desired 3D patterns have been formed. Step 3: Unbound precursor* is allowed to diffuse out of the hydrogel network (West J. et al. *Adv. Mater.* **2006).**

Figure 3.1. – Collagen Binding Fragment assay of CIBF-biotin after detection with streptavidin stained with ATTO 647 N dye: a) white light transmission and b, c) fluorescence images of CIBF binding on collagen type I fibrillated on mica; d) white light transmission and e, f) fluorescence images of CIBF binding on porcine derma; f) white light transmission and (g, h) fluorescence images of CIBF binding on human derma; i) white light transmission and l, m) fluorescence images of CIBF binding on human cornea.

Figure 3.2.– Synthetic scheme and action mechanism of DVS-crosslinked microbeads HA-based: a) preparation of fcMB by single emulsion technique; b) amide group formation between MB-COOH and peptide-NH_2; c) final microbeads (fcMB-CIBF) specialized for specific and selective recognition of collagen type I in eukaryotic tissue; d) tissue covering mediated by fcMB-CIBF; e) microbeads deformation upon peptide interaction forces and HA layer formation; e) representative molecular binding between peptide and site-binding on collagen.

Figure 3.3. – DVS-crosslinked microbeads HA-based stained with ATTO 647N dye, morphological characterization:

- LSCM: a) white light transmission and b) fluorescence images.
- SEM: c) microphotographs of loaded fcMB (Magnification 937X and EHT = 10.00 KV).

Figure 3.4. – Swelling behaviour of microbeads: Top) the relationship between diameter versus velocity of stirring is reported for both different crosslinked swollen and dried microbeads; bottom) swelling equations of fcMB350 and fcMB420 are respectively reported, assuming that the slope of the line coincides with the swelling factor.

Figure 3.5. – fcMB-CIBF-biotin, ATTO 647 N labelled streptavidin binding assay: white light transmission and fluorescence images of a, b) fcMB unfunctionalized show adsorption of fluorescent streptavidin; c) shows a

fluorescent crown formation due to molecular recognition between biotin and streptavidin.

Figure 3.6. – LSCM analisys: a) bright-field, b) fluorescence and c) white light transmission images of CIBF-biotin and collagen recognition as well as biotin and Strepdavidin coated microspheres (480, 520) Dragon Green.

Figure 3.7. – Collagen covering ability of fcMB-CIBF with different conjugation degree. Overlapping of white light transmission and fluorescence images: fcMB420-CIBF prepared using 50 mg of fcMB420 and a) 1.5, b) 2.5 and c) 3.1 mg of CIBF.

Figure 3.8. - LSCM characterization of fcMB-CIFB abilities to cover human derma and cornea of the eye: fluorescence images show a, d, g) non-adhesive capability of unfunctionalised fcMB; adhesive abilities of fcMB420-CIBF and fcMB350-CIBF on b, c) fibrillated collagen, e, f) human derma and h, i) human cornea.

Figure 3.9. – LSCM fluorescent images: a) and b) show the photo-frame overlapping on overall z-stuck of 75 µm of human cornea treated with fcMB420-CIBF and fcMB350-CIBF: both microbeads show abilities to form a layer of about 34 and 20 µm respectively. OCT analysis of untreated c) and treated d) human cornea with fcMB420-CIBF: in according to fluorescence analysis, OCT images show the formation of the layer with a thickness of about 34 µm. CT analysis for untreated e) and treated human f) cornea show the light scattering relative to a slow water evaporation from formed HA layer.

Figure 3.10. - Images acquired by optical microscope show:

- b) single microbead deformation (magnification 10X) with frontal observation and four different focuses;
- c) microbeads deformations (magnification 20X) in axial observation.

Figure 3.11. - Illustrative picture of supposed microbeads deformation mechanism:

- top) view of deformation along x-axis;

- bottom) view of deformation along z-axis.

Figure 3.12. - Optic microscope picture. From the right to the left: camera, objective, simple, light filter and visible light source.

Figure 3.3. - Recognition, adhesion and HA layer formation of fcMB420-CIBF loaded on human derma. Photo-frame images were collected using a homemade optical microscope. The layer formation was completed after 420 seconds.

Figure 4.1. – a) General synthetic scheme of supramolecular hydrogels by methacrylation of branched PEI: **a)** indicative reaction scheme of branched PEI (M_w ~ 25 kDa) with methacrylic anhydride and triethylamine in dichloromethane; photograph of hydrogel after swelling in water **b)** PEI-MA 3; **c-e)** PEI-MA 4 and **d**) PEI-MA 5.

Figure 4.2. - ATR-FTIR absorbance spectra of dried branched PEI and methacrylated PEI hydrogels (PEI-MA) collected under ambient conditions.

Figure 4.3. - ^{1}H NMR spectra at 700 MHz of methacrylated branched PEI hydrogels in D_2O at 25 °C. The peaks at 2.5-3.0 ppm were assigned to protons of PEI backbone, the characteristic peak at 1.70-1.75 ppm (a) to methacrylated secondary amines [–NH–COC(CH_2)CH_3] and the peak at 2.0-2.1 ppm (b) to methacrylated tertiary amines [>N– COC(CH_2)CH_3].

Figure 4.4. – Histogram of percentage of secondary (in blue) and tertiary (in red) methacrylated amines via H^1-NMR calculated: evidence of secondary amines of starting branched PEI more reactive of primary amines and periodic characteristics of methacrylation reactions varying only methacrylic anhydride molar ratio with respect to total amount of amines.

Figure 4.5. - Confocal fluorescence microscopy images of PEI-MA 4 stained with ATTO 657N imaged by a HeNe excitation laser at 633 nm, detecting 650-750 nm emission band: images show the conformational arrangement of PEI-MA 4 hydrogel at 4 ˚C (left) and 40 ˚C (right), that are typical for supramolecular hydrogels.

Figure 4.6.- SAXS data/analysis, spectra in the region of the scattering vector q between 0.1 and 0.3 $Å^{-1}$. PEI hydrogels show structure with dimensions of around 9 nm, assumed as lamellae organization.

Figure 4.7. - Confocal fluorescence microscopy imaged sequences (b-d-f) show a z-stack of 10-μm-thick sections across 50 μm of PEI-MA 3, 4 and 5 respectively and white light transmission images (a-c-e) showing the porous microstructure of the supramolecular PEI-MA hydrogels labeled with Alexa Fluor® 350 dye. g-h-i) overlapping sequences shows a z-stack of 300-μm-thick sections across of hydrogels samples. All scale bars are 50 μm.

Figure 4.8. – Titration curves by 0.1 N HCl for the branched PEI (red line), PEI-MA 3 (blue line), PEI-MA 4 (black line) and PEI-MA 5 (green line).

Figure 4.9. - Confocal fluorescence microscopy imaged sequences (left) and white light transmission images (bottom) showing the porous microstructure of the supramolecular PEI-MA 4 hydrogel labeled with ATTO 647 N dye; different pores size and distribution at varying pH values were observed: from open structure in image a) to close structure in image i) with increasing pH value. All scale bars are 30 μm. Fluorescence images (m-n-o) showing overlapping sequences with a z-stack of 10-μm-thick sections across 300 μm. All scale bars are 50 μm.

Figure 4.10.– plasmid DNA entrapping and release kinetics using elution buffer obtained from 10 mM NaCl in 50mM NaOH with final pH of 12.57.

Figure 4.11. – Electrophoresis experiments on agarose gel to demonstrate that DNA integrity is preserved during entrapment as well as upon elution step. 1-2) DNA sample T_0 ; 3-4-5) PEI-MA 4 supernnatant during entrapping DNA; 6-7-8) PEI-MA 5 surnatant during entrapping DNA; 9-10) PEI-MA 3 surnatant during entrapping DNA; 11) DNA molecular weight ladder; 12) Eluted DNA from PEI-MA 4 and 13) Eluted DNA from PEI-MA 5.

Figure 5.1. - Preparation of photoactive supramolecular hydrogels by methacrylation of branched PEI: **a)** reaction scheme of branched PEI (M_w ~

25 kDa) with methacrylic anhydride and triethylamine in dichloromethane; **b)** photograph of PEI-MA hydrogel after swelling in water overnight; **c)** laser patterning.

Figure 5.2. a) ^{1}H NMR spectra at 700 MHz of methacrylated branched PEI in D_2O at 25 °C. The peaks at 2.5-3.0 ppm were assigned to protons of PEI backbone, the characteristic peak at 1.70-1.75 ppm (a) to methacrylated secondary amines [–NH–COC(CH_2)CH_3] and the peak at 2.0-2.1 ppm (b) to methacrylated tertiary amines [>N– COC(CH_2)CH_3]. b) ATR-FTIR absorbance spectra of dried PEI and methacrylated PEI (PEIMA) collected under ambient conditions.

Figure 5.3. - Confocal fluorescence microscopy images (left panels) and white light transmission images (right panels) showing the porous microstructure of the supramolecular PEIMA hydrogel labeled with Alexa Fluor® 350 dye. The sequence shows a z-stack of 10-μm-thick sections across 50 μm of hydrogel sample. All scale bars are 100 μm.

Figure 5.4. – Fluorescence and white light trasmission images of photopatterning by two-photon near-IR activation at λ = 1000 nm. Left: fluorophores photobletching, right: direct photopatterning of PEI-MA hydrogels in solutions. a) methacryloxyethyl thiocarbonate rhodaamine B shows labile photobleaching and pronounced pattern, b) Alexa Fluor®350 carboxylic acid succinimidyl ester shows pronounced photobleaching and pattern, c) 6 aminofluorescein shows labile photobleaching and pattern probably due to low yield of Michael-type addition and d) ATTO 647N free carboxylic group shows resistance to photobleaching but exaltation of fluorescence of the dye bound in pronounced pattern.

Figure 5.5. - Top: white light transmission images of direct photopatterning of PEI-MA hydrogels in solutions of (a) biotin-COOH and in comparison with experiments in (b) biotin-NH_2 solution where no patterning can be observed. Bottom: white light transmission images of direct photopatterning

of PEI-MA hydrogels in solutions of RGD. c) Hydrogel surface without photoactivation, b) direct photopatterning and c) direct photopatterning of hydrogel at micro spatial resolution.

Figure 5.6. - White light transmission images of PEI-MA hydrogel in solution without functional probes. No imprinting is visible before and after multiphoton laser irradiation at wavelengths of 680 nm (top) and 1000 nm (bottom). Scale bars are 100 μm.

Figure 5.7. - White light transmission images of direct photopatterning by two-photon near-IR activation at λ = 1000 nm of PEI-MA hydrogels in solutions of (a, b and b1) biotin-COOH; a1, a2 and b2) fluorescence images and sequential patterning of PEI-MA hydrogels with biotin-COOH and recognition using strep-ATTO-647N; c) grayscale histograms corresponding to fluorescence intensities from selected ROIs (70×70 μm^2) showing the effect of the additional patterning on the intensity signal from the fluorescent dye.

Figure 5.8. - Fluorescent images of direct photopatterning of PEI-MA hydrogels in solutions of biotin-COOH by two-photon near-IR activation at λ= 680 nm and 1000 nm and recognition of the biotin-patterned hydrogel interface with fluorescent streptavidin (strep-ATTO-647N). Image shows fluorescent intensity relative to photoactivation with different wavelenghts of the laser source.

LIST OF TABLES

1. INTRODUCTION

Peptide-conjugated hydrogels for cell and tissue recognition: state of art

Biomaterials is *"...a substance that has been engineered to take a form which, alone or as part of a complex system, is used to direct, by control of interactions with components of living systems, the course of any therapeutic or diagnostic procedure..."*[1]

The development of biomaterials for tissue engineering and regenerative medicine applications has recently focused on the design and synthesis of biomimetic materials that are capable of eliciting some specific responses to cell and tissue mediated by biomolecular recognition, which can be manipulated by altering design of the material. Biomolecular recognition of materials by cells and tissue has been achieved by surface and bulk modification via chemical or physical methods, with bioactive molecules as short peptide sequences that can incur specific interactions with cell receptors or tissue binding-site. Starting point for designing interactive materials is to functionalize surfaces with factors that promote the adhesion and survival of selected cell types, involved in the wound healing or tissue regenerative process[2]. Hydrogels represent one the most popular materials used in tissue engineering and regenerative medicine for their versatile properties. They can mimic the tissues composition regarding biological and mechanical sustainability. These soft materials can be obtained by several chemical and physical procedures using synthetic or natural materials. In the last decades, hydrogels have aroused particular attention for scientific community, because they can be specialized to mimic remarkable biological processes. Hybrid hydrogels are usually referred to as hydrogel systems with components of at least two distinct classes of molecules, for example, synthetic polymers and biological molecules, interconnected either covalently or noncovalently.[3-4] Peptide and/or protein segments have been also used to introduce degradability,[5-6] temperature-induced phase transition,[7] and sensitivity to the

presence of biologically active molecules[8] into the hybrid hydrogel structure. Thus, when they are designed to give dynamic responses, in these cases defined also smart materials, they can be used as potentially synthetic ECM to that one natural alternative, which can interact with cell receptors or with sequences for binding sites of the biological tissues. Peptides, instead, are the smallest bioactive entities contained in a protein and they are responsible, in particular way, of full chemical interactions and spatial arrangement, which together supply the biological recognitions. Bio-hydrogels can thus be applied to a very broad spectrum of research and clinical functions, ranging from surgical adhesives to materials for tissue and cell culture. For example, biomimetic hydrogels can provide biological cues for cell–matrix interactions to promote tissue growth, diagnostic sentence of biomolecules, cells screening and adhesive interactions on tissues injury.

1.1. Peptide for cell and tissue recognition: using biology as a guide.

In nature, the viability of biological systems is sustained via specific interactions among the tens of thousands of proteins, the major building blocks of organisms from the simplest single-celled to the most complex multicellular species. These molecular interactions are accomplished with molecular specificity and efficiency leading to the formation of controlled structures and functions at all scales of dimensional hierarchy. Through evolution, Mother Nature developed molecular recognition by successive cycles of mutation and selection. Molecular specificity of probe-target interactions, ligand-receptor, antigen–antibody, is always based on specific peptide molecular recognition[9]. Using biology as a guide, is now possible understand, engineer, and control peptide interactions and exploit them as a new design tool for novel materials and biosystems. In scientific literature many papers have highlighted recent advances in the use of peptides, as essential part for the design of new soft or smart biomaterials. They can be

very practical for new material synthesis and device fabrications for a wide range of applications in regenerative medicine and tissue engineering. Peptides and proteins have superior specificity for target binding as seen in the antibody recognition[10] and this biological recognition function, for example, can be used to induce signal transduction pathways in cells[11-12], to recruitment of biomolecules[13], to promote cellular adhesion[14-17] and cell and tissue penetration[18-19] and also as specific diagnostic markers for tissue and cell recruitment and identification type[20]. The use of peptides at interfaces holds many advantages compared to entire protein immobilization or physisorption. Whole proteins, as example fibronectin and vitronectin, or protein fragments have been chemically conjugated or physically adsorbed over surfaces to developed improved materials[21]. A major limitation related to simple use of whole proteins is that they can denature, causing a significant conformational change and consequently reduced affinity for a particular cell or tissue. Furthermore, the protein can be bonded or adsorbed in an orientation that makes the cell binding domains inaccessible to cell or tissue surface receptors. Therefore, the use of peptides, as minimal bioactivated sequences that possess binding affinities similar to that of the parent protein, are an attractive approach, since both the surface density and orientation can be more simply controlled. In addition, if compared to proteins, peptides are easily synthesized and purified, are relatively inexpensive, do not rely on tertiary structure for bioactivity, are less susceptible to enzymatic degradation, are less likely to elicit an immunogenic response, and do not denature. One of the most popular peptides, widely described in literature is RGD (Arg-Gly-Asp). The RGD sequence is the cell attachment site of a large number of adhesive extracellular matrix, blood, and cell surface proteins, and nearly half of the over 20 known integrins recognize this sequence in their adhesion protein ligands[22]. Such peptides promote cell adhesion when conjugated onto a surface, and inhibit it when presented to cells in solution. In this way, the RGD can be chemically

conjugated to polymeric materials to give a biomedical platforms where the biomaterial-recognition activity of adhesion proteins can be reproduced by short synthetic peptides[23]. This minimum motif cooperates with synergistic amino acid sequences like Pro-His-Ser-Arg-Asn (PHSRN), which help to maintain appropriate spatial conformations of ligands as well as receptors[24-25]. Other short peptide fragments like YIGSR and IKVAV, which are derived from laminin, REDRV, and LDV from fibronectin, are also known to mediate different cellular responses[26-27]. Some tissue hierarchical structures are originated from molecular recognition between peptides sequences to give self-assembly as, for example, in the case of collagens fibres. They are assembled, in supramolecular manner, from triple helix peptides in micron-size with precise recognition between peptides[10] and successively fibres are highly stiffened after crosslinking formation in extracellular spaces, mediated by appropriate enzymes. Collagen is the major component of the extracellular matrix of connective tissues and provides structural support: collagen can also affect cell behaviour and gene expression through interactions with other matrix proteins and cellular receptors. For example, integrins domains α1β2 and α2β1 are the major collagen receptors on the surface of eukaryotic cells[28]. In other hand, those cell-integrin receptors are able to recognize on collagen specific binding site for molecular recognition and cellular attachment. Adopting techniques based on screening of recombinant fragment peptide pool, is been possible to isolate collagen binding fragment (CBF) able to recognize some molecular determinants on collagen type I in specific and selective way[29-31]. One of the sequences isolated, NH_2-Gly-Cys-Glu-Asp-Ser-Glu-Thr-Arg-Thr-Phe-Tyr-COOH, in particular way, showed high binding affinity with collagen type I binding site and, for example, can be utilized in molecular recognition of collagen tissue.

These versatile functions of peptides are extremely practical for relevant applications, as already above mentioned, in widely field of scientific interest in biomedicine and tissue engineering but also including nanoreactors,

sensors, electronics, and stimulus-responsive materials which essentially bridges the nano-world and the micro-world.

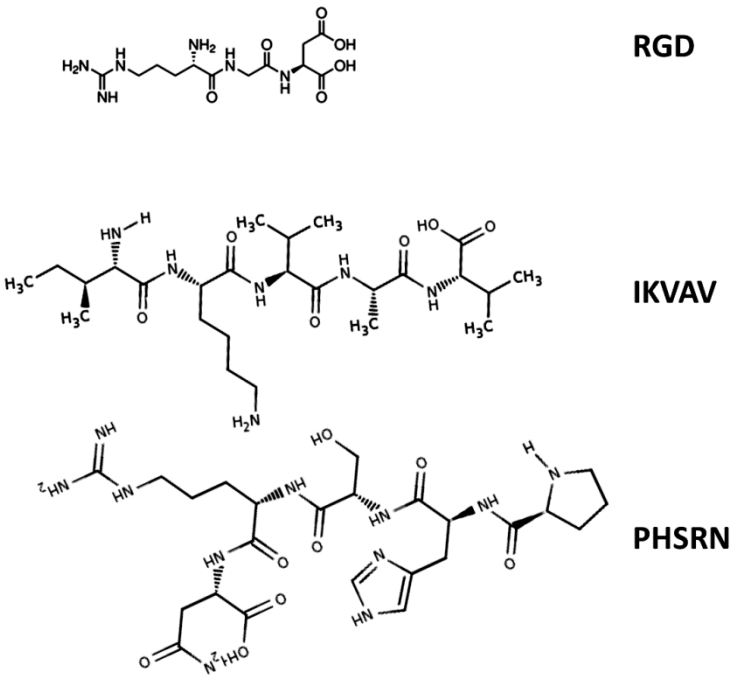

Figure 1.1. - Chemical structures of several bioactive peptides

1.2. Hydrogels material: using chemistry to manipulate matter.

Hydrogels are polymeric materials distinguished by high water content and diverse physical properties[32]. Hydrogels, due to their unique properties, flexible methods of synthesis, range of constituents, and desirable physical characteristics, are preferable materials using for many applications in regenerative medicine and tissue engineering. They can serve as scaffolds that provide structural integrity to tissue constructs, control drug and biomolecules delivery to tissues and cultures, and serve as adhesives or barriers between tissue and material surfaces[33]. Due to the various possible definitions of a hydrogel, different methods of classification are possible. They can be classified into different categories depending on the preparation method, the nature of chemical bounding formed, the chemical o physical

interactions between polymer chains and the mechanical and structural characteristics. Hydrogels, in agreement to first scientific definition, are physically or chemically cross-linked polymer networks that are able to absorb large amounts of water[34]. The second definition is related to hydrogels as macromolecular networks swollen in water or biological fluids[35]. Furthermore, classification can be made according to the physical structure: amorphous, semicrystalline, hydrogen-bonded, supramolecular, or hydrocolloidal. They are prepared by chemical polymerization or by physical self-assembly of synthetic or natural occurring polymeric building blocks. Most commonly, these building blocks are macromolecules in a variety of architectures, including cross-linked polymers, entangled fibrillar networks, colloidal assemblies, amphiphilic assemblies and supramolecular assemblies[36] (Figures 1.2., 1.3., 1.4.). Typical examples of synthetic and natural polymers that are used to form hydrogels for biomedical applications are poly-acrylic acid (PAAc)[37], poly (vinyl chloride) (PVA)[38], poly (ethylene glycol) (PEG)[39], poly (ethylene oxide) (PEO)[40], poly-N- isopropylacrylamide (PNIPAM)[41], collagen[42] and many different polysaccharides as hyaluronic acid (HA)[43], chitosan[44] and sodium alginate[45]. Crosslinked hydrogels network can be obtained using many different chemistry reactions[46]. The most popular methods of hydrogels network formation is photopolymerization, combined to curing agent (photoinitiator), of polymers modified with double bonds (acrylate or methacrylate groups)[47]. Other interesting hydrogels preparation method is given by thiol-ene photopolymerization reaction. This reaction is a highly efficient, radical mediated reaction between a thiol and an alkene groups on polymers material. A radical source, or photoinitiator in the presence of light, extracts an hydrogen from a thiol forming a thiyl radical which can add across a carbon–carbon double bond[48]. Other again interesting chemical mechanism for the crosslinked hydrogel is defined "autocrosslinking". This method is widely utilized to reticulate polysaccharides having free primary hydroxyl groups. A particular example

is given by vinyl sulphone (DVS) to reticulate structure through sulfonyl bis-ethyl linkages between the hydroxyl groups of hyaluronic acid forming ether bounds[49]. In literature are reported many further methods for crosslinked hydrogels preparation by condensation reactions of multifunctional reactants. Examples of the reactant groups include reactions of isocyanates and amines[50] or alcohols[51] to form urea or urethane bonds, amines or thiols and vinyl groups to form amines or sulfides by Michael additions[52-54], amines and active esters such as N-hydroxy succinimide to form amides[55-56], acids or acid chlorides and alcohols to form esters[57] and aldehydes and amines to form Schiff bases[58]. In the last years, a further class of hydrogels, defined supramolecular hydrogels, have raised a remarkable interest from scientific community. The supramolecular crosslinking of polymer chains in water by specific, directional and dynamic non-covalent interactions, such as hydrogen bonding, π–π stacking, metal complexation, ionic, and solvophobic interactions, has led to the development of novel supramolecular polymeric hydrogels. These aqueous polymeric networks constitute an interesting class of soft materials exhibiting attractive properties such as stimuli-responsiveness and self-healing arising from their dynamic behaviour and they are crucial for a wide variety of emerging applications[59-60]. In addition aqueous supramolecular chemistry has unlocked a versatile toolbox for the design and fine-tuning of the material properties of these hydrogels, even if the relationship between molecular structure, biocompatibility and mechanical properties of supramolecular hydrogels still remains a challenge[61]. A supramolecule is a system of two or more molecular entities held together and organized by means of inter-molecular non-covalent binding interactions[62] and in the cases of polymers material, they are modified *ad-hoc* with chemical entities able to recognize their molecular determinants to give molecular recognition and successfully interactions, thus the functional polymeric precursor (polymeric building blocks) can easily assembly to form supramolecular hydrogel[59] (figure 1.5.). Various

supramolecular structures as hydrogels, also including micelles, vesicles, tubes, fibers and films, which have been prepared through the primary self-assembly processes, have aroused the scientific attention due to the great advantages in biomedical applications[63]. In particular, self-assembly of amphiphilic hyperbranched polymers (HBPs) represent a newly emerging class of materials, because exploiting their abilities to give precise hierarchical structures is possible to mimic those ones biological like ECMs. For example, hyperbranched polymer vesicles have demonstrated great potential to be used as model membranes to mimic cellular behaviours, such as fusion, fission and cell aggregation[64].

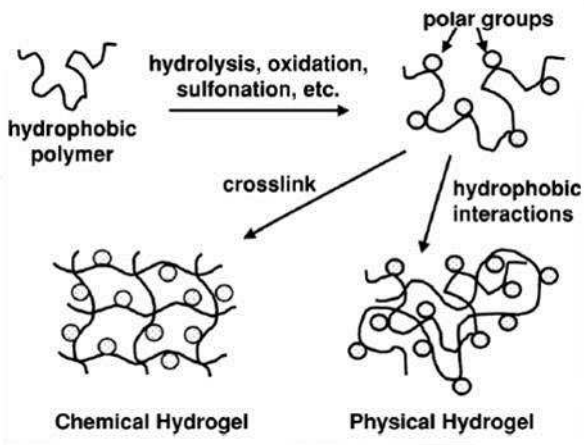

Figure 1.2. - Schematic hydrogels formation by chemical modification of hydrophobic polymers. Examples of these types of hydrogels include (a) the partial hydrolysis of the acetate groups to –OH groups in conversion of PVAc to PVA, and (b) the partial hydrolysis of PAN to a polymer containing varying concentrations of acrylonitrile, amide and carboxyl pendant groups. In either case the resulting gel may be subsequently covalently crosslinked. (Hoffman, A. S. et al. *Advanced drug delivery reviews* **2012**)

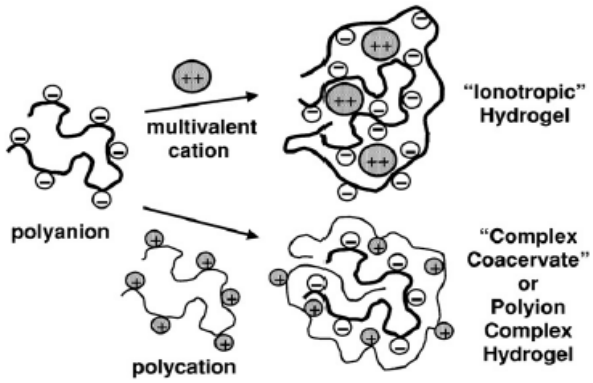

Figure 1.3. - Schematic of methods for formation of two types of ionic hydrogels. An example of an 'ionotropic' hydrogel is calcium alginate, and an example of a polyionic hydrogel is a complex of alginic acid and polylysine. (Hoffman, A. S. et al. *Advanced drug delivery reviews* **2012**).

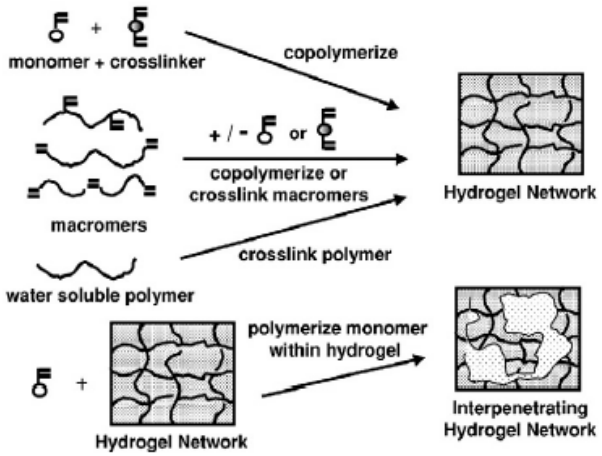

Figure 1.4. - Schematic of methods for formation of crosslinked hydrogels by free radical reactions, including a variety of polymerizations and crosslinking of water-soluble polymers. Examples include crosslinked PHEMA and PEG hydrogels. (Hoffman, A. S. et al. *Advanced drug delivery reviews* **2012**).

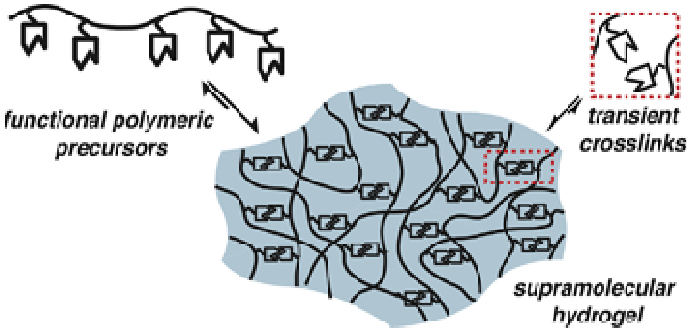

Figure 1.5. - Supramolecular hydrogel self-assembly (Hoffman, A. S. et al. *Advanced drug delivery reviews* **2012**)

1.3. Peptides conjugated to hydrogels: several bioconjugation chemistry strategies

The remarkable ability of biological molecules to recognize, sort, and process complex sources of information continues have inspired novel approaches to the fabrication of smart macromolecular systems. Extensive studies have been performed to render materials biomimetic. The surface or bulk modification of biomaterials with bioactive peptides is a simple way to make biomimetic materials[65]. By combining the complex functions or recognition abilities of biological systems, synthetic chemistry strategies, photoctivation

chemistry and abilities of several macromolecules to give supramolecular materials, have been designed micro and nanometer architectures that integrate features such as specific for potential applications in biomedicine, clinical diagnostic and tissue engineering including the wounds repairing. In biological systems, most biochemistry reactions occur at the surface/interface with order and precision. The understanding of these surfaces and their reactions represents an important avenue to improve and develop biocompatible biomaterial surfaces, which means designing biomimetic material surfaces[66]. Bioconjugation involves the linking of two or more molecules to form a novel complex having the combined properties of its individual components. Natural or synthetic compounds with their individual activities can be chemically combined to create unique substances possessing carefully engineered characteristics. A peptide able to bind discretely to a target molecule within a complex mixture, may be covalently bonded with another molecule or capable of being detected to form a traceable conjugate[67]. However, is possible to apply different bioconjugation chemistry strategies, showing particular attention for the choice of the reaction conditions regarding solvents and peptides solubility properties, which often represented important limitations. Peptides can be activated introducing at N-terminal or C-terminal regions or on site-specific modification at Arg, Asp, Cys, Gln, Glu, Gly, His, Lys, Met, Phe, Ser, Thr, Trp, Tyr and Val residues not involved for peptide bioactivity, with chemical reactive entities [68]. Bioconjugation chemistry strategies today, fortunately offer a wide range of possible procedures useful to covalently bond a peptides or biomolecules to dried and swollen hydrogel already formed or by single building blocks as precursors of final hydrogel. Examples of specific chemistries useful to bioactive surfaces hydrogels or incorporate peptides into biomaterials, as also reported in Figure 1.6.,[69] including commercially accessible crosslinkers[67], Michael addition of cysteine-containing peptides to vinyl sulfones, acrylate or maleimide conjugation[70-71], coupling with succinimidyl carbonate and

related formation of polyurethane linkers[72], amine/carboxylic acid coupling using EDC/EDAC and NHS,[73-74] chemoselective chemistries such as "click" chemistries[75-76] and native chemical ligation.[77-78] Otherwise, photoactivatable UV-initiated cross-linking and *in situ* synthesis represent an alternative procedure to covalently bond a peptide to polymers previously activated with acrylic, methacrylic or succinimidyl ester groups[79-81]. One of the most important considerations related to smart biomaterials development is given by spatial presentation of biological signal in the cell and tissue recognition[82]. In other hand, the assessment of subtle changes in peptide structure affecting cell and tissue signaling requires a model system that allows the control of peptide sequence, conformation, orientation, presentation and provides the ability to systematically tether multiple ligands to an interface. Current microfabrication methods for 3D hydrogel matrices with controlled intrinsic structure mainly include photolithographic patterning[83], microfluidic patterning[83] and electrochemical deposition[84]. These tecniques have been significant developments to regulate spatial and temporal distribution of biomolecules in various materials, even if the most micropatterning techniques are applicable only for two-dimensional patterning[85]. In the last decade another very interesting techniques for immobilize peptides and other biomolecules on or into hydrogels is showed by photochemical immobilization strategies using two-photon irradiation[86-87].

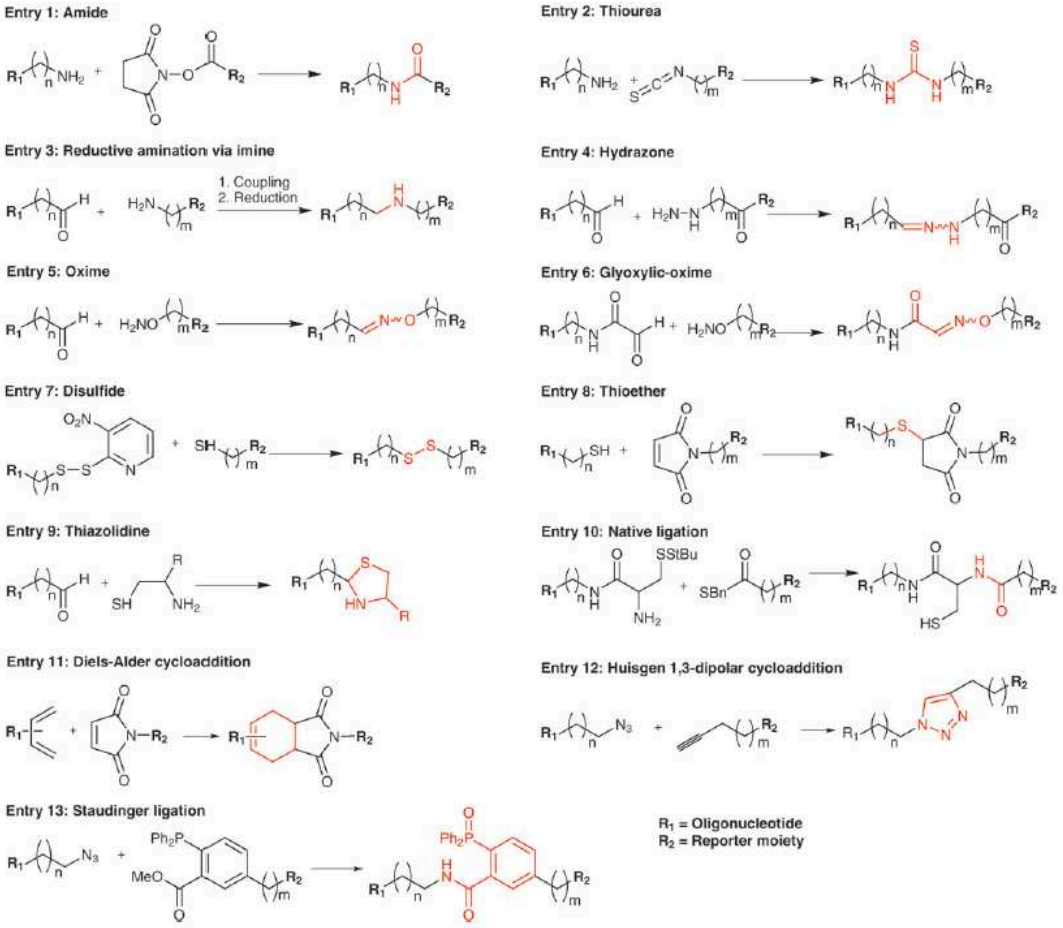

Figure 1.6. - Several chemistry strategies for immobilize peptides

1.4. Peptide-conjugated hydrogels: properties and applications

Biomimetic hydrogels are involved in many biomedical applications, on the strength of the related biological and specific fields of interest[88]. They can be engineered to resemble the extracellular environment of the body's tissues in ways that enable their use in medical implants, biosensors, and drug-delivery devices[89]. In order that, cell or tissue compatible hydrogels are used as biomedical devices, they essentially may be designed by mean a strategy of corresponding control over physical properties and bioactivity to influence specific interactions with cellular or tissues systems and for modulate cell behaviour may be included spatial and temporal patterns bioactive

molecules[85]. The interrelationship between the hydrogel processing, structure, properties and performance results be complicated by a performance criteria characterized by a multitude of molecular interactions at the cell/material interface, including transport properties such as sustained release, tissue interactions such as bioactivity, and chemical stability such as degradability[32]. With tissue-recognition compatible hydrogels, the interrelationship between hydrogel and tissue depending by spatial disposition of bioactive signal and mechanical sustainability of the hydrogel. In any cases the peptide-conjugated hydrogel may present five important properties for biomedical applications, which are degradation, bioadhesion, bioactivity, transport (for example, controlled release of bioactive molecules or oxygen), and biomechanical compatible properties[90]. Hydrogels can be cast into practically any shape, size, and form[91] and can be easy conjugated with peptides on hydrogels surface or they can be internalized into network previously conjugated to starting polymers. The spatial and local peptide immobilizations to hydrogel allow investigating many biological aspects related to cell and tissue recognition. This aspect is a fundamental approach used in the tissue engineering because to understand living cellular behaviour represents an essential aspect for tissues regeneration features. In other hand, in tissue regeneration, biomaterials are designed to contain precisely positioned bioactive ligands that instruct cell behaviour. Since RGD peptides have been found to promote cell recognition in 1984[92], still representing a major recognition system for cell adhesion, numerous materials have been RGD functionalized for academic studies or medical applications. Therefore, immobilization of RGD on hydrogel structures instructs many cell types to attach to the material via cell-surface proteins called integrins, because formation of focal adhesions only occurs, if the ligands with stand the cells contractile forces[93]. Relatively to the way which hydrogels are bioactivated, for example only on surfaces or into network, they find different employment for elucidating biological behaviour of cells and tissues. Peptide-conjugated

hydrogel on surfaces in two-dimensional patterning allows of their ability to spatially control surface chemistry and topography at the micrometer level, and thus is possible evaluate their ability to tailor cell microenvironment. In other hand, patterning method can find use in tissue engineering in the elucidation of fundamental structure–function relationships of recognition cell and protein arrays for biotechnology[83]. In addition to patterning strategies, also surface grafting techniques[94-95], self-assembled monolayers[96], and polymer–peptide hybrids, have effectively tethered single peptides to interfaces for the study of cell adhesion phenomena. Peptide-conjugated hydrogels two-dimensional bioactivated have showed significant developments to regulate spatial and temporal distribution of peptides in cell-recognition or tissue-recognition but deduce several limitations in the related application for regenerative medicine due to lack of bioactivation internal to hydrogels network. However, to provide to this limitations much progress has been made introducing cell-recognition or tissue-recognition sites into biomaterials to obtain artificial extra cellular matrix (aECM). aECMs are designed to mimic the natural ECM of the biological tissues. The natural biological ECM has important signalling and regulatory functions in the development, maintenance, mechanical integrity and regeneration of tissue[97]. The ECM structures are very complicated systems where take place every fundamentals chemical, biological and mechanical living relationship. ECM recognition sites and components, in synergy with soluble signals provided by growth factors and hormones, participate in the tissue-specific control of gene expression through a variety of transduction mechanisms[98-100]. Furthermore, the ECM is itself a dynamic structure that is actively remodelled by the cells with which it interacts[101]. For example, bioinspired materials as aECM, can be used as carriers for transplanted cells that are subsequently grafted into tissue defects[102], and also as cell infiltration matrices to induce regeneration and remodeling in vivo[103]. Collagen and fibrin are clinically well-established and FDA-approved matrices for wound

healing to treat burns and chronic wounds, and as tissue sealants, respectively. Many cell-compatible hydrogel materials have since been modelled on these seminal concepts for the hybrid- materials preparation. Therefore, protein derived as collagen and fibrin can be used to instruct aECM to adhere at damaged tissues for in vivo experiments[104]. For example, three-dimensional aECM was prepared using fibrin-peptide conjugated to PEG using factor XIIIa as cross-linking for peptide-derivatized PEGs and simultaneously incorporating RGD as cell-recognition site[6] (Figure 1.7. and 1.8.). The natural ECM is a dynamic matrix that is constantly changing in composition and structure as tissues develop, remodel, repair, and age. One the most important property of aECM is given by degradability of the constituents, becouse when the cells producing matrix needs to substitute artificial construct with a biological tissue of neo formations[105]. Therefore, in the aECM application can be used another interesting bioactive property of several peptides, which showed susceptibility to the degradation operated by cellular MMPs. Proteolytically responsive synthetic hydrogels were pioneered by Hubbell and co-workers[106]. They used poly(ethylene glycol) (PEG) macromeres that are cross-linked by oligopeptides that mimic collagenase substrates found in natural ECM proteins. The end-linked PEGco-RGD hydrogels were formed by Click chemistry, in which a Michael-type addition reaction between the di-thiolated oligopeptides and vinyl sulfone groups on the PEG is carried out in the presence of cells and/or tissues. Also for three-dimensional peptide-conjugated hydrogel there are several limitations. Fundamental limitation of aECM prepared utilising peptide-polymer as building blocks consist in the random immobilization of bioactive signals into the hydrogel network. In tissue regeneration is always indispensable considered the spatial distribution control of bioactive signal because a precise spatial distribution represents an important parameter for cell-guidance behaviour in tissue genesis and regeneration[107]. In the last decade another very interesting techniques for immobilize biomolecules on

or into hydrogels is given by photochemical immobilization strategies using two-photon irradiation[86-87] (Figure 1.9.). Combining photolabile hydrogel matrices with focused light provides to directly modify the local physical or chemical properties in three-dimensional. For example S-NBC-modified agarose hydrogel with incorporated peptides modified with succinimydil ester, can be activated by light to give click chemistry reaction (Figure 1.10.) without further chemical additives[108]. Another example of hydrogel used as model materials for the generation of internal 3D patterns is given by poly(ethylene glycol) (PEG)-diacrylate (Figure 1.11.). PEG macromers, not only, undergo rapid polymerization in the presence of photoinitiators but the unbound biomolecules is allowed to diffuse out of the hydrogel network and after can be covalently bounded via two-photons irradiation[85]. This immobilization strategy allowed to go beyond limitations related to two-dimensional conjugation patterning and, in addition allows the fine spatial control of biological signals position into hydrogel network nearly to reproduce their distribution as in natural biological matrices.

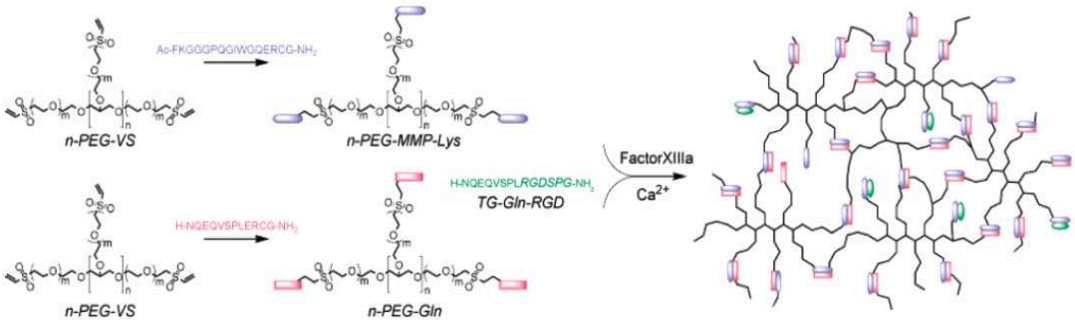

Figure 1.7. - Factor XIIIa-catalyzed PEG hydrogel formation. The transglutaminase enzyme factor XIIIa was used to cross-link two multiarm PEGpeptide conjugates, n-PEG-MMP-Lys and n-PEG-Gln (here, n) 8), in combination with a cell adhesion peptide, TG-Gln-RGD, to form multifunctional synthetic hydrogels. (Lutolf et al. *Macromolecules* **2007**)

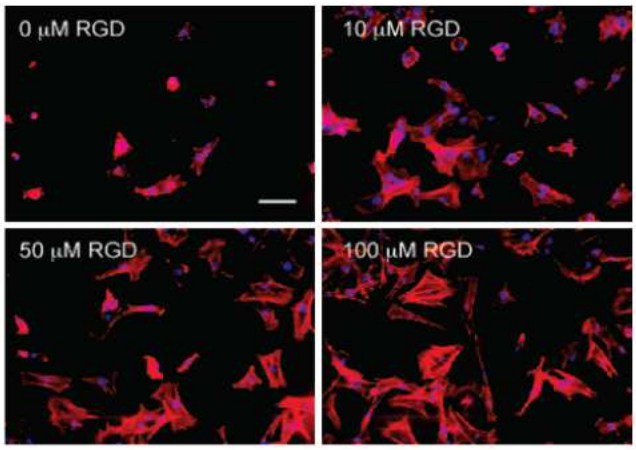

Figure 1.8. - Incorporation of the integrin-binding RGD ligand in the formof TG-Gln-RGD renders gel networks adhesive for primary fibroblasts.Spreading is dependent on the ligand concentration as demonstrated by fluorescent microscopy (A, Scale bar: 100 *ím) with double staining* of cell nuclei (blue) and f-actin cytoskeletal elements (red), and quantified by cell surface areas (B). (Lutolf et al. *Macromolecules* **2007**)

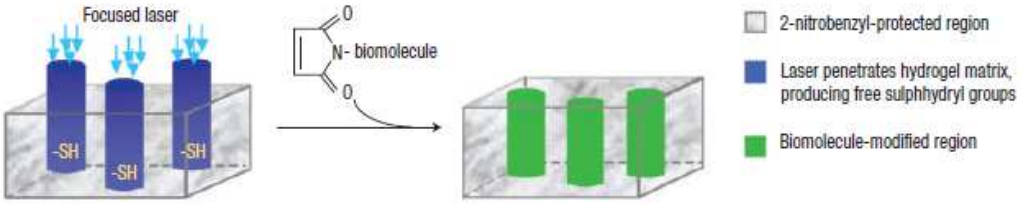

Figure 1.9. - The strategy to create biomolecular channels in agarose hydrogel matrices uses the chemical modification strategy in (a) and a focused laser, resulting in alternating volumes of cell-adhesive (peptide) channels separated by non-adhesive (agarose) volumes. (Schoichet M. et al. *Nature* **2004**)

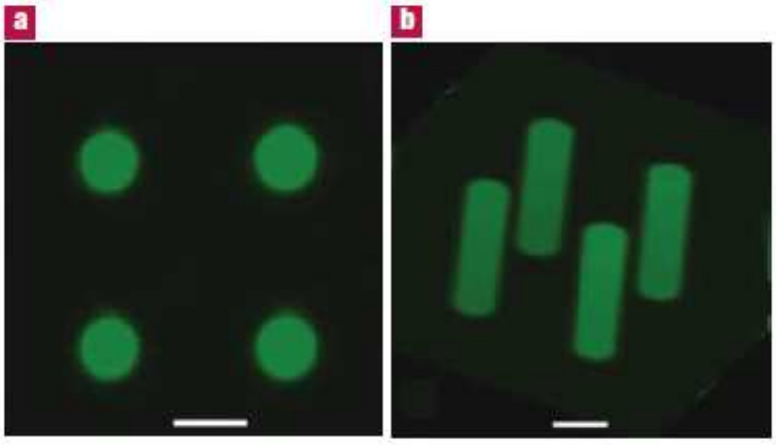

Figure 1.10. – a) representative XY crosssection image of green fluorescently labelled oligopeptide channels (scale bar:200 μm); b) representative image of the green fluorescently labelled oligopeptide channels constructed from a series of XY cross-sectional micrographs over a 0.5 mm depth (scale bar:200 μm). (Schoichet M. et al *Nature* 2004)

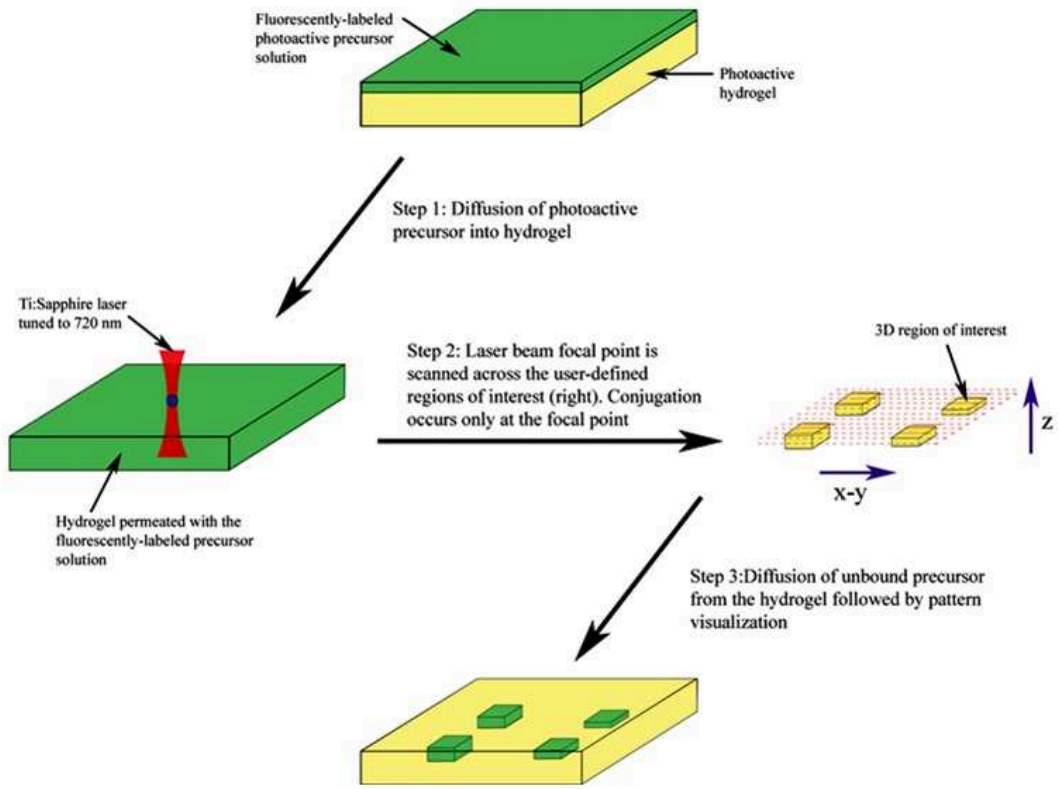

Figure 1.11. - Schematics demonstrating photoinduced patterning of an existing poly(ethylene glycol) diacrylate (PEGDA) network at the microscale (A) and macroscale (B). The following description applies to both schematics. Step 1: Precursor solution containing the mono- or diacrylate derivatized moiety to be patterned is layered onto a base PEGDA hydrogel and allowed to diffuse into the hydrogel network. Step 2: A laser beam generated by a Ti:sapphire laser tuned to 720 nm is scanned across an *x–y plane within the hydrogel, with the laser shutter being opened only in the user-specified regions* of interest (ROIs) shown in the ROI template to the right of the hydrogel being patterned in (B). In TPA, conjugation of the molecule to be patterned to the hydrogel substrate occurs only at the laser focal point. The microscope stage is incremented axially and patterning is continued within the specific ROIs at this next *x–y plane. This sequence of steps is repeated until the desired 3D patterns have been formed. Step 3: Unbound precursor* is allowed to diffuse out of the hydrogel network. (West J. et al. *Adv. Mater.* **2006)**

1.5. Hydrogels like tissue adhesives for wounds repair

Recent hydrogels designs are based on biological rationale and therapeutic demands. The applications of hydrogels as ocular materials,[109-110] as wound-healing materials,[111] have been discussed in the literature. In particular, hydrogels are been also addressed to tissue adhesives in surgical repair,

because opportunely bioadhesion properties allows cells and tissues to adhere to hydrogels. Synthetic polymers such as poly(ethylene glycol), poly(vinylalcohol), and poly(lactic acid) are excellent hydrogel components due to their ease of synthesis and modification, and low cost. Natural polymers such as collagen, hyaluronic acid, and cellulose are also good hydrogel components due to their biocompatibility and ease of modification, and can provide biological signals to facilitate wound healing[112-113]. In order to obtain chemically cross-linked hydrogels, these polysaccharides have been modified with a variety of functional groups. Hyaluronic acid has been modified with adipic dihyrazide[114] and methacrylate groups[115] to enable cross-linking. Chondroitin sulfate has been modified with adipic dihydrazide[116], methacrylate[117], and aldehyde groups[118]. Polysaccharide hydrogels were produced by reaction of adipic dihydrazide-modified hyaluronic acid[119] or chondroitin sulfate[114] with aldehyde-functionalized poly(ethylene glycol). Alternatively, hydrogels were formed from the exposure of methacrylate-modified polysaccharides dissolved in buffer with a photo-initiator to high intensity light[116]. Researchers have also added varying amounts of poly(ethylene glycol)-diacrylate before cross-linking of methacrylate-modified polysaccharides for improved mechanical properties[117]. Hydrogel-based adhesives are the other main type of adhesive under investigation for ocular wound repair. First promoted for use as contact lenses in 1960 by Wichterle and Lim[120], hydrogels have since been adapted to a wide variety of biomedical applications such as intraocular lenses, artificial organs, maxillofacial reconstruction, vitreous substitutes, cartilage repair, and drug delivery[121]. Hydrogels have also been investigated for use as barriers following tissue injury in order to improve the healing response[81]. For example, hydrogels as barrier with cell-adhesion modified have been used to promote enhanced osteogenic differentiation of MSCs for bone repair[122], to provide an essential foothold for neurite outgrowth in axonal regeneration[123], and to understand the regulatory role of mechano-transduction in stem cell

fate determination[104]. Hydrogels used as barriers applications have included in vascular injury in the cases of thrombosis and restenosis[124] and post-operative tissue adhesion formation[125]. For prevention of post-operative adhesion formation, hydrogel barriers were formed on intraperitoneal surfaces by bulk photopolymerization of poly(ethylene glycol-co-lactic acid) diacrylate. Several examples of molecules-adhesive hydrogels able to give covalent grafting on tissue damaged are reported by Messersmith and co-workers. They developed a catechol-based modification to a PEG hydrogel implant in order to improve extrahepatic islet transplantation for managing type I diabetes mellitus[126]. The hydrogel modification, using a catechol moiety [3,4-dihydroxy- L-phenylalanine (DOPA)], is derived from the tethering chemistry that allows mussels to adhere to wet organic surfaces[127-128]. Under oxidizing conditions, DOPA rapidly forms cross-links when bound, for example, to an end-functionalized star-PEG precursor. The catechol moiety forms strong covalent interactions with nucleophiles such as thiols and imidazoles found in organic substrates (ECM). The effective immobilization of the islet-containing catechol PEG hydrogels on the surface of the liver of diabetic rats enabled revascularization with minimal inflammation and permitted effective glucose management comparable with the gold-standard intra hepatic islet delivery. In particular, in ophthalmology wounds repair, many adhesive hydrogels strategies were performed on the direct chemical reaction between activated hydrogels and tissue injuries. Margalit et al.[129] studied hydrogel adhesives made from tetrafunctional amine-terminated PEG and either PEG-succinimidyl succinate, PEG-succinimidyl propionate or thiol-terminated PEG and PEG-succinimidyl glutarate. Covalent chemical cross-linking of these hydrogels occurs by amide bond formation PEG-succinimidyl succinate and PEG-succinimidyl propionate and for SH hydrogel cross-links upon formation of thioester bonds, were made directly on cornea of guinea pig. All three hydrogels studied were able to sustain much higher loads before failure than

commercial and autologous fibrin or photocurable acrylic adhesives, but only SH hydrogels were able to sustain the largest load, most likely due to the higher polymer concentration in this adhesive formulation. *In-vivo* studies showed that hydrogels derived by thiol-terminated PEG provoked only a mild inflammatory response and caused moderate damage of corneal tissue, while hydrogels derived by PEG-succinimidyl propionate caused severe damage of corneal tissue. In a collaborative study between the Schepens Eye Research Institute at Harvard Medical School and Confluent Surgical reported in 2003, NHS-terminated 4-arm succinimidyl-glycolate PEG and amine-terminated 4-arm PEG were combined to form amide cross-linked hydrogels that polymerized in seconds and persisted for 4–6 weeks and the adhesive-sealed wounds exhibited higher pressures before leaking than the single suture-treated wounds for all wound models[130]. Sueda et al. in 2007 reported hydrogels composed of NHSterminated 4-arm glutaryl PEG and a tri-lysine peptide for in vivo cytotoxicity and fixing retinal detachment at the Schepens Eye Institute. The hydrogel adhesive was found to have a persistence time of 4–6 weeks and was found that for the adhesive-treated eyes, 2 out of 6 eyes developed posterior subcapsular cataract, 4 out of 6 eyes developed vitreous opacity, and 2 out of 6 eyes developed retinal traction, but no retinal detachments occurred[131]. In every case reported above the invasive covalent chemistry caused damages of tissue treated and also an inadequate control of biodegradability of the hydrogels. Therefore, bioadhesive features can be engineered into a hydrogel network by using linker molecules that enable covalent or non-covalent molecular interactions between the implant and its surroundings, including cell-adhesive or tissue-adhesive oligopeptides derived, for example, from fibronectin[132]. Tissue-adhesive modifications to hydrogels can further improve performance of cell-delivery scaffolds by stabilizing the in vivo location of the graft. One of the most popular oligopeptide whit covalent adhesive interaction is given by fibrin. Fibrin is a specialized ECM protein network, formed principally in spontaneous tissue

repair[133]. Fibrin forms spontaneously by polymerization of fibrinogen in the presence of thrombin; the resulting network is further cross-linked by the transglutaminase activity of factor XIIIa[134]. Fibrin has been utilized in skin repair, for example, in sutureless fixation of skin grafts[103] and keratinocyte transplantation in burn patients[135], with considerable success. Covalently attachment of fibrin on hydrogels or fibrin matrices with the character of ECM molecules or other bioactive molecules has been investigated as useful glue[136] in the genesis of wound healing. The major drawback of fibrin is that it is susceptible to rapid degradation in vivo and has difficulty maintaining structural integrity[137]. Today, example of non-covalently adhesive peptide-conjugated hydrogels able to recognize tissue in supramolecular manner, and promote tissue adhesion for wounds healing or simply with covering efficiency for tissues undergo a surgery injury, in literature are still less investigated. As well, the fixation and anchorage of engineered tissues is rarely discussed in the published literature on biomaterials used for skeletal tissue engineering. It is now understood that surgical fixation of tissues injuries is a crucial step for successful cell-based therapy.

1.6. References

1. Williams, D. F., On the nature of biomaterials. *Biomaterials* **2009,** *30* (30), 5897-5909.
2. Bellis, S. L., Advantages of RGD peptides for directing cell association with biomaterials. *Biomaterials* **2011,** *32* (18), 4205-4210.
3. Kopeček, J., Hydrogel biomaterials: a smart future? *Biomaterials* **2007,** *28* (34), 5185-5192.
4. Vandermeulen, G. W.; Klok, H. A., Peptide/protein hybrid materials: enhanced control of structure and improved performance through conjugation of biological and synthetic polymers. *Macromol Biosci* **2004,** *4* (4), 383-98.
5. Subr, V.; Duncan, R.; Kopecek, J., Release of macromolecules and daunomycin from hydrophilic gels containing enzymatically degradable bonds. *J Biomater Sci Polym Ed* **1990,** *1* (4), 261-78.
6. Ehrbar, M.; Rizzi, S. C.; Schoenmakers, R. G.; San Miguel, B.; Hubbell, J. A.; Weber, F. E.; Lutolf, M. P., Biomolecular hydrogels formed and degraded via site-specific enzymatic reactions. *Biomacromolecules* **2007,** *8* (10), 3000-3007.
7. Chen, G.; Hoffman, A. S., Graft copolymers that exhibit temperature-induced phase transitions over a wide range of pH. *Nature* **1995,** *373* (6509), 49-52.
8. Lu, Z. R.; Kopečková, P.; Kopeček, J., Antigen responsive hydrogels based on polymerizable antibody Fab′ fragment. *Macromolecular bioscience* **2003,** *3* (6), 296-300.
9. Tamerler, C.; Khatayevich, D.; Gungormus, M.; Kacar, T.; Oren, E. E.; Hnilova, M.; Sarikaya, M., Molecular biomimetics: GEPI-based biological routes to technology. *Peptide Science* **2010,** *94* (1), 78-94.
10. de la Rica, R.; Matsui, H., Applications of peptide and protein-based materials in bionanotechnology. *Chemical Society Reviews* **2010,** *39* (9), 3499-3509.
11. Davies, C.; Tournier, C., Exploring the function of the JNK (c-Jun N-terminal kinase) signalling pathway in physiological and pathological processes to design novel therapeutic strategies. *Biochemical Society Transactions* **2012,** *40* (1), 85.
12. Ye, H.; Daoud-El Baba, M.; Peng, R.-W.; Fussenegger, M., A synthetic optogenetic transcription device enhances blood-glucose homeostasis in mice. *Science* **2011,** *332* (6037), 1565-1568.
13. Mantovani, A.; Cassatella, M. A.; Costantini, C.; Jaillon, S., Neutrophils in the activation and regulation of innate and adaptive immunity. *Nature Reviews Immunology* **2011,** *11* (8), 519-531.

14. Johnson, R. M.; Harrison, S. D.; Maclean, D., Therapeutic applications of cell-penetrating peptides. In *Cell-Penetrating Peptides*, Springer: 2011; pp 535-551.
15. Stewart, K. M.; Horton, K. L.; Kelley, S. O., Cell-penetrating peptides as delivery vehicles for biology and medicine. *Org. Biomol. Chem.* **2008,** *6* (13), 2242-2255.
16. Whitney, M. A.; Crisp, J. L.; Nguyen, L. T.; Friedman, B.; Gross, L. A.; Steinbach, P.; Tsien, R. Y.; Nguyen, Q. T., Fluorescent peptides highlight peripheral nerves during surgery in mice. *Nature biotechnology* **2011,** *29* (4), 352-356.
17. Causa, F.; Battista, E.; Della Moglie, R.; Guarnieri, D.; Iannone, M.; Netti, P. A., Surface investigation on biomimetic materials to control cell adhesion: the case of RGD conjugation on PCL. *Langmuir* **2010,** *26* (12), 9875-9884.
18. Sugahara, K. N.; Teesalu, T.; Karmali, P. P.; Kotamraju, V. R.; Agemy, L.; Greenwald, D. R.; Ruoslahti, E., Coadministration of a tumor-penetrating peptide enhances the efficacy of cancer drugs. *Science* **2010,** *328* (5981), 1031-1035.
19. Ruoslahti, E., Peptides as targeting elements and tissue penetration devices for nanoparticles. *Advanced Materials* **2012,** *24* (28), 3747-3756.
20. Oyama, T.; Sykes, K. F.; Samli, K. N.; Minna, J. D.; Johnston, S. A.; Brown, K. C., Isolation of lung tumor specific peptides from a random peptide library: generation of diagnostic and cell-targeting reagents. *Cancer letters* **2003,** *202* (2), 219-230.
21. Place, E. S.; Evans, N. D.; Stevens, M. M., Complexity in biomaterials for tissue engineering. *Nature materials* **2009,** *8* (6), 457-470.
22. Ruoslahti, E., RGD and other recognition sequences for integrins. *Annual review of cell and developmental biology* **1996,** *12* (1), 697-715.
23. Langer, R.; Tirrell, D. A., Designing materials for biology and medicine. *Nature* **2004,** *428* (6982), 487-492.
24. Aota, S.-i.; Nomizu, M.; Yamada, K. M., The short amino acid sequence Pro-His-Ser-Arg-Asn in human fibronectin enhances cell-adhesive function. *Journal of Biological Chemistry* **1994,** *269* (40), 24756-24761.
25. Kim, T.-I.; Jang, J.-H.; Lee, Y.-M.; Ryu, I.-C.; Chung, C.-P.; Han, S.-B.; Choi, S.-M.; Ku, Y., Design and biological activity of synthetic oligopeptides with Pro-His-Ser-Arg-Asn (PHSRN) and Arg-Gly-Asp (RGD) motifs for human osteoblast-like cell (MG-63) adhesion. *Biotechnology letters* **2002,** *24* (24), 2029-2033.
26. Tashiro, K.; Sephel, G. C.; Weeks, B.; Sasaki, M.; Martin, G. R.; Kleinman, H. K.; Yamada, Y., A synthetic peptide containing the IKVAV sequence from the A chain of laminin mediates cell attachment, migration, and neurite outgrowth. *J Biol Chem* **1989,** *264* (27), 16174-82.
27. Sreejalekshmi, K. G.; Nair, P. D., Biomimeticity in tissue engineering scaffolds through synthetic peptide modifications—Altering chemistry for

enhanced biological response. *Journal of biomedical materials research Part A* **2011,** *96* (2), 477-491.
28. Xu, Y.; Gurusiddappa, S.; Rich, R. L.; Owens, R. T.; Keene, D. R.; Mayne, R.; Hook, A.; Hook, M., Multiple binding sites in collagen type I for the integrins alpha1beta1 and alpha2beta1. *J Biol Chem* **2000,** *275* (50), 38981-9.
29. Knight, C. G.; Morton, L. F.; Onley, D. J.; Peachey, A. R.; Messent, A. J.; Smethurst, P. A.; Tuckwell, D. S.; Farndale, R. W.; Barnes, M. J., Identification in collagen type I of an integrin alpha2 beta1-binding site containing an essential GER sequence. *J Biol Chem* **1998,** *273* (50), 33287-94.
30. Yamada, K. M.; Kennedy, D. W., Dualistic nature of adhesive protein function: fibronectin and its biologically active peptide fragments can autoinhibit fibronectin function. *J Cell Biol* **1984,** *99* (1 Pt 1), 29-36.
31. Boucaut, J. C.; Darribere, T.; Poole, T. J.; Aoyama, H.; Yamada, K. M.; Thiery, J. P., Biologically active synthetic peptides as probes of embryonic development: a competitive peptide inhibitor of fibronectin function inhibits gastrulation in amphibian embryos and neural crest cell migration in avian embryos. *J Cell Biol* **1984,** *99* (5), 1822-30.
32. Seliktar, D., Designing cell-compatible hydrogels for biomedical applications. *Science* **2012,** *336* (6085), 1124-1128.
33. Slaughter, B. V.; Khurshid, S. S.; Fisher, O. Z.; Khademhosseini, A.; Peppas, N. A., Hydrogels in regenerative medicine. *Advanced Materials* **2009,** *21* (32-33), 3307-3329.
34. Van Vlierberghe, S.; Dubruel, P.; Schacht, E., Biopolymer-based hydrogels as scaffolds for tissue engineering applications: a review. *Biomacromolecules* **2011,** *12* (5), 1387-1408.
35. Berger, J.; Reist, M.; Mayer, J.; Felt, O.; Peppas, N.; Gurny, R., Structure and interactions in covalently and ionically crosslinked chitosan hydrogels for biomedical applications. *European Journal of Pharmaceutics and Biopharmaceutics* **2004,** *57* (1), 19-34.
36. Ulijn, R. V.; Bibi, N.; Jayawarna, V.; Thornton, P. D.; Todd, S. J.; Mart, R. J.; Smith, A. M.; Gough, J. E., Bioresponsive hydrogels. *Materials Today* **2007,** *10* (4), 40-48.
37. Wu, D.-Q.; Sun, Y.-X.; Xu, X.-D.; Cheng, S.-X.; Zhang, X.-Z.; Zhuo, R.-X., Biodegradable and pH-sensitive hydrogels for cell encapsulation and controlled drug release. *Biomacromolecules* **2008,** *9* (4), 1155-1162.
38. Liu, Y.; Vrana, N.; Cahill, P.; McGuinness, G., Physically crosslinked composite hydrogels of PVA with natural macromolecules: structure, mechanical properties, and endothelial cell compatibility. *Journal of Biomedical Materials Research Part B: Applied Biomaterials* **2009,** *90* (2), 492-502.
39. Kraehenbuehl, T. P.; Zammaretti, P.; Van der Vlies, A. J.; Schoenmakers, R. G.; Lutolf, M. P.; Jaconi, M. E.; Hubbell, J. A., Three-

dimensional extracellular matrix-directed cardioprogenitor differentiation: systematic modulation of a synthetic cell-responsive PEG-hydrogel. *Biomaterials* **2008,** *29* (18), 2757-2766.
40. Jo, S.; Kim, D.; Woo, J.; Yoon, G.; Park, Y. D.; Tae, G.; Noh, I., Development and physicochemical evaluation of chondroitin sulfate-poly (ethylene oxide) hydrogel. *Macromolecular Research* **2011,** *19* (2), 147-155.
41. Tokarev, I.; Minko, S., Stimuli-responsive hydrogel thin films. *Soft Matter* **2009,** *5* (3), 511-524.
42. Schneider, U.; Rackwitz, L.; Andereya, S.; Siebenlist, S.; Fensky, F.; Reichert, J.; Löer, I.; Barthel, T.; Rudert, M.; Nöth, U., A Prospective Multicenter Study on the Outcome of Type I Collagen Hydrogel–Based Autologous Chondrocyte Implantation (CaReS) for the Repair of Articular Cartilage Defects in the Knee. *The American Journal of Sports Medicine* **2011,** *39* (12), 2558-2565.
43. Burdick, J. A.; Prestwich, G. D., Hyaluronic acid hydrogels for biomedical applications. *Advanced Materials* **2011,** *23* (12), H41-H56.
44. Madhumathi, K.; Shalumon, K.; Rani, V.; Tamura, H.; Furuike, T.; Selvamurugan, N.; Nair, S.; Jayakumar, R., Wet chemical synthesis of chitosan hydrogel–hydroxyapatite composite membranes for tissue engineering applications. *International journal of biological macromolecules* **2009,** *45* (1), 12-15.
45. Nishiyama, Y.; Nakamura, M.; Henmi, C.; Yamaguchi, K.; Mochizuki, S.; Nakagawa, H.; Takiura, K., Development of a three-dimensional bioprinter: construction of cell supporting structures using hydrogel and state-of-the-art inkjet technology. *Journal of biomechanical engineering* **2009,** *131* (3).
46. Hennink, W.; Van Nostrum, C., Novel crosslinking methods to design hydrogels. *Advanced drug delivery reviews* **2012**.
47. Miller, J. S.; Shen, C. J.; Legant, W. R.; Baranski, J. D.; Blakely, B. L.; Chen, C. S., Bioactive hydrogels made from step-growth derived PEG–peptide macromers. *Biomaterials* **2010,** *31* (13), 3736-3743.
48. Aimetti, A. A.; Machen, A. J.; Anseth, K. S., Poly(ethylene glycol) hydrogels formed by thiol-ene photopolymerization for enzyme-responsive protein delivery. *Biomaterials* **2009,** *30* (30), 6048-6054.
49. Yeom, J.; Bhang, S. H.; Kim, B.-S.; Seo, M. S.; Hwang, E. J.; Cho, I. H.; Park, J. K.; Hahn, S. K., Effect of cross-linking reagents for hyaluronic acid hydrogel dermal fillers on tissue augmentation and regeneration. *Bioconjugate chemistry* **2010,** *21* (2), 240-247.
50. Dhanasingh, A.; Groll, J., Polysaccharide based covalently linked multi-membrane hydrogels. *Soft Matter* **2012,** *8* (5), 1643-1647.
51. Alves, M. H.; Jensen, B. E.; Smith, A. A.; Zelikin, A. N., Poly (vinyl alcohol) physical hydrogels: New vista on a long serving biomaterial. *Macromolecular bioscience* **2011,** *11* (10), 1293-1313.

52. Peng, K.; Tomatsu, I.; van den Broek, B.; Cui, C.; Korobko, A. V.; van Noort, J.; Meijer, A. H.; Spaink, H. P.; Kros, A., Dextran based photodegradable hydrogels formed via a Michael addition. *Soft Matter* **2011,** *7* (10), 4881-4887.
53. Tabata, Y.; Horiguchi, I.; Lutolf, M. P.; Sakai, Y., Development of bioactive hydrogel capsules for the 3D expansion of pluripotent stem cells in bioreactors. *Biomaterials Science* **2014,** *2* (2), 176-183.
54. Moses, J. E.; Moorhouse, A. D., The growing applications of click chemistry. *Chemical Society Reviews* **2007,** *36* (8), 1249-1262.
55. Strehin, I.; Nahas, Z.; Arora, K.; Nguyen, T.; Elisseeff, J., A versatile pH sensitive chondroitin sulfate–PEG tissue adhesive and hydrogel. *Biomaterials* **2010,** *31* (10), 2788-2797.
56. Tang, D.-W.; Yu, S.-H.; Wu, W.-S.; Hsieh, H.-Y.; Tsai, Y.-C.; Mi, F.-L., Hydrogel microspheres for stabilization of an antioxidant enzyme: Effect of emulsion cross-linking of a dual polysaccharide system on the protection of enzyme activity. *Colloids and Surfaces B: Biointerfaces* **2014,** *113*, 59-68.
57. Hu, Y.; Lin, H.; Liu, L.; Dan, W. H., Study of Physical Properties of Poly (vinyl alcohol)-Collagen Hydrogels Using a Response Surface Methodology. *Advanced Materials Research* **2013,** *710*, 60-66.
58. Nguyen, M. K.; Alsberg, E., Bioactive factor delivery strategies from engineered polymer hydrogels for therapeutic medicine. *Progress in Polymer Science* **2014**.
59. Appel, E. A.; del Barrio, J.; Loh, X. J.; Scherman, O. A., Supramolecular polymeric hydrogels. *Chemical Society Reviews* **2012,** *41* (18), 6195-6214.
60. Yan, X.; Wang, F.; Zheng, B.; Huang, F., Stimuli-responsive supramolecular polymeric materials. *Chemical Society Reviews* **2012,** *41* (18), 6042-6065.
61. Leenders, C. M.; Mes, T.; Baker, M. B.; Koenigs, M. M.; Besenius, P.; Palmans, A. R.; Meijer, E., From supramolecular polymers to hydrogel materials. *Materials Horizons* **2014,** *1* (1), 116-120.
62. Lehn, J.-M., Constitutional dynamic chemistry: bridge from supramolecular chemistry to adaptive chemistry. In *Constitutional Dynamic Chemistry*, Springer: 2012; pp 1-32.
63. Huang, F.; Scherman, O. A., Supramolecular polymers. *Chemical Society Reviews* **2012,** *41* (18), 5879-5880.
64. Jin, H.; Huang, W.; Zhu, X.; Zhou, Y.; Yan, D., Biocompatible or biodegradable hyperbranched polymers: from self-assembly to cytomimetic applications. *Chemical Society Reviews* **2012,** *41* (18), 5986-5997.
65. Shin, H.; Jo, S.; Mikos, A. G., Biomimetic materials for tissue engineering. *Biomaterials* **2003,** *24* (24), 4353-4364.
66. Patterson, J.; Martino, M. M.; Hubbell, J. A., Biomimetic materials in tissue engineering. *Materials Today* **2010,** *13* (1–2), 14-22.
67. Hermanson, G. T., *Bioconjugate techniques*. Academic press: 1996.

68. Gauthier, M. A.; Klok, H.-A., Peptide/protein–polymer conjugates: synthetic strategies and design concepts. *Chemical Communications* **2008,** (23), 2591-2611.
69. Collier, J. H.; Segura, T., Evolving the use of peptides as components of biomaterials. *Biomaterials* **2011,** *32* (18), 4198-4204.
70. Lutolf, M.; Tirelli, N.; Cerritelli, S.; Cavalli, L.; Hubbell, J., Systematic modulation of Michael-type reactivity of thiols through the use of charged amino acids. *Bioconjugate chemistry* **2001,** *12* (6), 1051-1056.
71. Censi, R.; Fieten, P. J.; di Martino, P.; Hennink, W. E.; Vermonden, T., In situ forming hydrogels by tandem thermal gelling and Michael addition reaction between thermosensitive triblock copolymers and thiolated hyaluronan. *Macromolecules* **2010,** *43* (13), 5771-5778.
72. Miron, T.; Wilchek, M., A simplified method for the preparation of succinimidyl carbonate polyethylene glycol for coupling to proteins. *Bioconjugate chemistry* **1993,** *4* (6), 568-569.
73. Baroli, B., Hydrogels in Tissue Engineering. In *Cell and Tissue Engineering*, Springer: 2012; pp 197-216.
74. Bhuniya, S.; Park, S. M.; Kim, B. H., Biotin-amino acid conjugates: an approach toward self-assembled hydrogelation. *Organic letters* **2005,** *7* (9), 1741-1744.
75. Lutz, J.-F.; Zarafshani, Z., Efficient construction of therapeutics, bioconjugates, biomaterials and bioactive surfaces using azide–alkyne "click" chemistry. *Advanced drug delivery reviews* **2008,** *60* (9), 958-970.
76. Iha, R. K.; Wooley, K. L.; Nyström, A. M.; Burke, D. J.; Kade, M. J.; Hawker, C. J., Applications of orthogonal "click" chemistries in the synthesis of functional soft materials. *Chemical Reviews* **2009,** *109* (11), 5620-5686.
77. Jing, P.; Rudra, J. S.; Herr, A. B.; Collier, J. H., Self-assembling peptide-polymer hydrogels designed from the coiled coil region of fibrin. *Biomacromolecules* **2008,** *9* (9), 2438-2446.
78. Paramonov, S. E.; Gauba, V.; Hartgerink, J. D., Synthesis of collagen-like peptide polymers by native chemical ligation. *Macromolecules* **2005,** *38* (18), 7555-7561.
79. Khetan, S.; Katz, J. S.; Burdick, J. A., Sequential crosslinking to control cellular spreading in 3-dimensional hydrogels. *Soft Matter* **2009,** *5* (8), 1601-1606.
80. Uttamchandani, M.; Walsh, D. P.; Yao, S. Q.; Chang, Y.-T., Small molecule microarrays: recent advances and applications. *Current Opinion in Chemical Biology* **2005,** *9* (1), 4-13.
81. Nguyen, K. T.; West, J. L., Photopolymerizable hydrogels for tissue engineering applications. *Biomaterials* **2002,** *23* (22), 4307-4314.
82. Shin, H., Fabrication methods of an engineered microenvironment for analysis of cell–biomaterial interactions. *Biomaterials* **2007,** *28* (2), 126-133.

83. Hahn, M. S.; Taite, L. J.; Moon, J. J.; Rowland, M. C.; Ruffino, K. A.; West, J. L., Photolithographic patterning of polyethylene glycol hydrogels. *Biomaterials* **2006,** *27* (12), 2519-2524.
84. Yi, H.; Wu, L.-Q.; Bentley, W. E.; Ghodssi, R.; Rubloff, G. W.; Culver, J. N.; Payne, G. F., Biofabrication with chitosan. *Biomacromolecules* **2005,** *6* (6), 2881-2894.
85. Hahn, M. S.; Miller, J. S.; West, J. L., Three-Dimensional Biochemical and Biomechanical Patterning of Hydrogels for Guiding Cell Behavior. *Advanced Materials* **2006,** *18* (20), 2679-2684.
86. Wylie, R. G.; Ahsan, S.; Aizawa, Y.; Maxwell, K. L.; Morshead, C. M.; Shoichet, M. S., Spatially controlled simultaneous patterning of multiple growth factors in three-dimensional hydrogels. *Nature Materials* **2011,** *10* (10), 799-806.
87. Wylie, R. G.; Shoichet, M. S., Three-Dimensional Spatial Patterning of Proteins in Hydrogels. *Biomacromolecules* **2011,** *12* (10), 3789-3796.
88. Kashyap, N.; Kumar, N.; Kumar, M. R., Hydrogels for pharmaceutical and biomedical applications. *Critical Reviews™ in Therapeutic Drug Carrier Systems* **2005,** *22* (2).
89. Ratner, B. D.; Bryant, S. J., Biomaterials: where we have been and where we are going. *Annu. Rev. Biomed. Eng.* **2004,** *6*, 41-75.
90. Drury, J. L.; Mooney, D. J., Hydrogels for tissue engineering: scaffold design variables and applications. *Biomaterials* **2003,** *24* (24), 4337-4351.
91. Euliss, L. E.; DuPont, J. A.; Gratton, S.; DeSimone, J., Imparting size, shape, and composition control of materials for nanomedicine. *Chemical Society Reviews* **2006,** *35* (11), 1095-1104.
92. Pierschbacher, M. D.; Ruoslahti, E., Cell attachment activity of fibronectin can be duplicated by small synthetic fragments of the molecule. *Nature* **1984,** *309* (5963), 30-3.
93. Juliano, R., Signal transduction by cell adhesion receptors and the cytoskeleton: functions of integrins, cadherins, selectins, and immunoglobulin-superfamily members. *Annual review of pharmacology and toxicology* **2002,** *42* (1), 283-323.
94. Rezania, A.; Healy, K. E., Biomimetic Peptide Surfaces That Regulate Adhesion, Spreading, Cytoskeletal Organization, and Mineralization of the Matrix Deposited by Osteoblast-like Cells. *Biotechnology progress* **1999,** *15* (1), 19-32.
95. Schneider, G. B.; English, A.; Abraham, M.; Zaharias, R.; Stanford, C.; Keller, J., The effect of hydrogel charge density on cell attachment. *Biomaterials* **2004,** *25* (15), 3023-3028.
96. Ulman, A., Formation and structure of self-assembled monolayers. *Chemical Reviews* **1996,** *96* (4), 1533-1554.
97. Furth, M. E.; Atala, A.; Van Dyke, M. E., Smart biomaterials design for tissue engineering and regenerative medicine. *Biomaterials* **2007,** *28* (34), 5068-5073.

98. Boudreau, N.; Jones, P., Extracellular matrix and integrin signalling: the shape of things to come. *Biochem. J* **1999,** *339*, 481-488.
99. Juliano, R.; Haskill, S., Signal transduction from the extracellular matrix. *Journal of Cell Biology* **1993,** *120*, 577-577.
100. Reid, L.; Morrow, B.; Jubinsky, P.; Schwartz, E.; Gatmaitan, Z., REGULATION OF GROWTH AND DIFFERENTIATION OF EPITHELIAL CELLS BY HORMONES, GROWTH FACTORS, AND SUBSTRATES OF EXTRACELLULAR MATRIX*. *Annals of the New York Academy of Sciences* **1981,** *372* (1), 354-370.
101. Birkedal-Hansen, H., Proteolytic remodeling of extracellular matrix. *Current opinion in cell biology* **1995,** *7* (5), 728-735.
102. Yannas, I. V.; Lee, E.; Orgill, D. P.; Skrabut, E. M.; Murphy, G. F., Synthesis and characterization of a model extracellular matrix that induces partial regeneration of adult skin. *Proc Natl Acad Sci U S A* **1989,** *86* (3), 933-7.
103. Currie, L. J.; Sharpe, J. R.; Martin, R., The use of fibrin glue in skin grafts and tissue-engineered skin replacements: a review. *Plast Reconstr Surg* **2001,** *108* (6), 1713-26.
104. Lutolf, M. P.; Gilbert, P. M.; Blau, H. M., Designing materials to direct stem-cell fate. *Nature* **2009,** *462* (7272), 433-441.
105. Rosso, F.; Marino, G.; Giordano, A.; Barbarisi, M.; Parmeggiani, D.; Barbarisi, A., Smart materials as scaffolds for tissue engineering. *Journal of cellular physiology* **2005,** *203* (3), 465-470.
106. Lutolf, M.; Hubbell, J., Synthetic biomaterials as instructive extracellular microenvironments for morphogenesis in tissue engineering. *Nature biotechnology* **2005,** *23* (1), 47-55.
107. Sittinger, M.; Hutmacher, D. W.; Risbud, M. V., Current strategies for cell delivery in cartilage and bone regeneration. *Current opinion in biotechnology* **2004,** *15* (5), 411-418.
108. Luo, Y.; Shoichet, M. S., A photolabile hydrogel for guided three-dimensional cell growth and migration. *Nat Mater* **2004,** *3* (4), 249-253.
109. Dong, L.; Agarwal, A. K.; Beebe, D. J.; Jiang, H., Adaptive liquid microlenses activated by stimuli-responsive hydrogels. *Nature* **2006,** *442* (7102), 551-4.
110. Lloyd, A. W.; Faragher, R. G.; Denyer, S. P., Ocular biomaterials and implants. *Biomaterials* **2001,** *22* (8), 769-85.
111. Hubbell, J. A., Hydrogel systems for barriers and local drug delivery in the control of wound healing. *Journal of Controlled Release* **1996,** *39* (2), 305-313.
112. Hoffman, A. S., Hydrogels for biomedical applications. *Ann N Y Acad Sci* **2001,** *944*, 62-73.
113. Oelker, A. M.; Grinstaff, M. W., Ophthalmic adhesives: a materials chemistry perspective. *Journal of Materials Chemistry* **2008,** *18* (22), 2521-2536.

114. Kirker, K. R.; Luo, Y.; Nielson, J. H.; Shelby, J.; Prestwich, G. D., Glycosaminoglycan hydrogel films as bio-interactive dressings for wound healing. *Biomaterials* **2002,** *23* (17), 3661-71.
115. Miki, D.; Dastgheib, K.; Kim, T.; Pfister-Serres, A.; Smeds, K. A.; Inoue, M.; Hatchell, D. L.; Grinstaff, M. W., A photopolymerized sealant for corneal lacerations. *Cornea* **2002,** *21* (4), 393-9.
116. Gilbert, M. E.; Kirker, K. R.; Gray, S. D.; Ward, P. D.; Szakacs, J. G.; Prestwich, G. D.; Orlandi, R. R., Chondroitin sulfate hydrogel and wound healing in rabbit maxillary sinus mucosa. *Laryngoscope* **2004,** *114* (8), 1406-9.
117. Li, Q.; Williams, C. G.; Sun, D. D.; Wang, J.; Leong, K.; Elisseeff, J. H., Photocrosslinkable polysaccharides based on chondroitin sulfate. *J Biomed Mater Res A* **2004,** *68* (1), 28-33.
118. Pirouzmanesh, A.; Herretes, S.; Reyes, J. M.; Suwan-apichon, O.; Chuck, R. S.; Wang, D. A.; Elisseeff, J. H.; Stark, W. J.; Behrens, A., Modified microkeratome-assisted posterior lamellar keratoplasty using a tissue adhesive. *Arch Ophthalmol* **2006,** *124* (2), 210-4.
119. Luo, Y.; Kirker, K. R.; Prestwich, G. D., Cross-linked hyaluronic acid hydrogel films: new biomaterials for drug delivery. *J Control Release* **2000,** *69* (1), 169-84.
120. Wichterle, O.; Lim, D., Hydrophilic gels for biological use. **1960**.
121. Peppas, N.; Huang, Y.; Torres-Lugo, M.; Ward, J.; Zhang, J., Physicochemical foundations and structural design of hydrogels in medicine and biology. *Annual Review of Biomedical Engineering* **2000,** *2* (1), 9-29.
122. Heng, B. C.; Cao, T.; Stanton, L. W.; Robson, P.; Olsen, B., Strategies for directing the differentiation of stem cells into the osteogenic lineage in vitro. *Journal of Bone and Mineral Research* **2004,** *19* (9), 1379-1394.
123. Kuroda, Y.; Kitada, M.; Wakao, S.; Dezawa, M., Mesenchymal stem cells and umbilical cord as sources for Schwann cell differentiation: their potential in peripheral nerve repair. *Open Tissue Engineering and Regenerative Medicine Journal* **2011,** *4*, 54-63.
124. West, J. L.; Hubbell, J. A., Separation of the arterial wall from blood contact using hydrogel barriers reduces intimal thickening after balloon injury in the rat: the roles of medial and luminal factors in arterial healing. *Proceedings of the National Academy of Sciences* **1996,** *93* (23), 13188-13193.
125. Hill-West, J. L.; Dunn, R. C.; Hubbell, J. A., Local release of fibrinolytic agents for adhesion prevention. *J Surg Res* **1995,** *59* (6), 759-63.
126. Brubaker, C. E.; Kissler, H.; Wang, L.-J.; Kaufman, D. B.; Messersmith, P. B., Biological performance of mussel-inspired adhesive in extrahepatic islet transplantation. *Biomaterials* **2010,** *31* (3), 420-427.
127. Ryu, J. H.; Lee, Y.; Kong, W. H.; Kim, T. G.; Park, T. G.; Lee, H., Catechol-functionalized chitosan/pluronic hydrogels for tissue adhesives and hemostatic materials. *Biomacromolecules* **2011,** *12* (7), 2653-2659.

128. Lee, H.; Lee, B. P.; Messersmith, P. B., A reversible wet/dry adhesive inspired by mussels and geckos. *Nature* **2007,** *448* (7151), 338-341.
129. Margalit, E.; Fujii, G. Y.; Lai, J. C.; Gupta, P.; Chen, S. J.; Shyu, J. S.; Piyathaisere, D. V.; Weiland, J. D.; De Juan, E., Jr.; Humayun, M. S., Bioadhesives for intraocular use. *Retina* **2000,** *20* (5), 469-77.
130. Kalayci, D.; Fukuchi, T.; Edelman, P. G.; Sawhney, A. S.; Mehta, M. C.; Hirose, T., Hydrogel tissue adhesive for sealing corneal incisions. *Ophthalmic Res* **2003,** *35* (3), 173-6.
131. Sueda, J.; Fukuchi, T.; Usumoto, N.; Okuno, T.; Arai, M.; Hirose, T., Intraocular use of hydrogel tissue adhesive in rabbit eyes. *Jpn J Ophthalmol* **2007,** *51* (2), 89-95.
132. Martino, M. M.; Mochizuki, M.; Rothenfluh, D. A.; Rempel, S. A.; Hubbell, J. A.; Barker, T. H., Controlling integrin specificity and stem cell differentiation in 2D and 3D environments through regulation of fibronectin domain stability. *Biomaterials* **2009,** *30* (6), 1089-1097.
133. Hubbell, J. A., Materials as morphogenetic guides in tissue engineering. *Current opinion in biotechnology* **2003,** *14* (5), 551-558.
134. Lorand, L.; Graham, R. M., Transglutaminases: crosslinking enzymes with pleiotropic functions. *Nat Rev Mol Cell Biol* **2003,** *4* (2), 140-56.
135. Horch, R. E.; Bannasch, H.; Stark, G. B., Transplantation of cultured autologous keratinocytes in fibrin sealant biomatrix to resurface chronic wounds. *Transplant Proc* **2001,** *33* (1-2), 642-4.
136. Brennan, M., Fibrin glue. *Blood reviews* **1991,** *5* (4), 240-244.
137. Huang, S.; Fu, X., Naturally derived materials-based cell and drug delivery systems in skin regeneration. *Journal of Controlled Release* **2010,** *142* (2), 149-159.

2. PhD project: focusing the aims

In scientific literature still today, example of non-covalent adhesive interactions between peptide-conjugated hydrogels surfaces and biological tissues are not well discussed. In particular peptide-conjugated hydrogels are able to recognize tissues in order that to promote wound dressing and tissue injury covering, as post-damage protective device are still rarely investigated. Despite in scientific literature are reported many examples of hydrogel designs on biological rationale and therapeutic demands as molecular platforms for interactions at the cell/material interface like artificial ECM that find use in regenerative medicine and tissue engineering. Hydrogels, even if represent one of the materials more studied for biomedical applications, are in many cases only used as barriers or replenishment post surgical tissues explants or as wound dressing agents that are *in vivo* produced by mean covalent bounds directly on damaged tissue using invasive chemical reactions. These reactions often originate further more grave post-clinical complications. Furthermore, in literature are abundantly investigated peptide properties useful to improve biological properties of the hybrid materials.

In the first part of my PhD project, the purpose is been investigate the properties of peptide-conjugated hydrogels to recognize in specific and selective manner tissues containing collagen type I, in order to improve supplemental scientific knowledge on the behaviour of novel supramolecular recognitions of rational designed biomaterials at wound interface. Peptides could be used as molecular glues for hydrogels wound dressing or in other hand in tissue injury covering as post-damage as novel biotechnological device. The starting idea was to take advantages from natural peptide abilities to recognize and adhere on specific tissue site-binding and using the total amounts of these interactions, to firmly holding engineered artificial micro hydrogels on tissue injury. In this way is been possible to favourite wound dressing actions avoiding direct formation of covalent bounds by mean *in*

vivo chemical reactions. In addition, opportune peptides conjugated to hydrogels can mediate not only for protection and maintenance of tissue injury but they can also favourite cell-guidance process for tissue regeneration. As described in Chapter 1 ("*Novel smart HA-based hydrogels with non-covalent adhesive properties for tissues healing applications*"), tissues as human derma and cornea of the eye undergone to surgical or accidental trauma were used as tissue model to investigate the covering abilities of micro hydrogels conjugated with peptides capable of recognize and bound collagen type I in selective and specific manner. Was understood that effectively the micro hydrogels surprisingly shown adhesion capabilities until to forming a continuous covering layer on anywhere was provoked the injuries. So, in smart manner, those peptide-conjugated hydrogels can adhere on tissue and operate like temporary tissues substitutes.

In the last years an intriguing class of hydrogel defined supramolecular polymer hydrogels have raised great scientific interest. Supramolecular hydrogels have several advantages respects to crosslinked hydrogels, because an appropriate design allows efficient control over the assembled structure. Therefore a response on the molecular level can directly cause a physical or chemical change on the macroscopic level and represented a valid alternative to cross-linked hydrogels for molecules encapsulation and controlled release. However, the scientific community looks at supramolecular hydrogels as versatile toolbox for the design and fine-tuning of novel biomaterials, even if supramolecular hydrogels still remains a challenge.

In the second part of this PhD project, adopting several feedbacks from scientific community, the purpose was investigated the abilities of chemically modified PEI polymer branched to form supramolecular hydrogels. In particular, self-assembly of amphiphilic branched polymers are a newly emerging class of materials and their precise hierarchical structures are biological like ECMs. As described in chapter 2 (*"Novel supramolecular*

PEI-based hydrogels for plasmid DNA controlled release") several novel supramolecular hydrogels material based on the chemical modification of branched PEI with methacrylic groups, were synthesized and characterized. The properties of the PEI hydrogel in terms of swelling and porosity were controlled during synthesis by the amount of functional methacrylic groups, these supramolecular hydrogels swell with a large extent in water and show exceptional binding properties with plasmid DNA. In addition, as described in chapter 3 (*"A supramolecular two-photon-active hydrogel from polyethyleneimine for photo-conjugation at near-infrared wavelengths")*, these PEI hydrogels are also easily activated by multi-photon laser irradiation and show interesting three-dimensional patterning capabilities in presence of peptide as RGD and biomolecules with free carboxylic acid or hydroxyl groups without use of adjunctive photo-initiators or activators. PEI hydrogels activated for photo-conjugation can be indispensable to the spatial distribution control of bioactive signal, which represents an important factor for cell recognition and cell-guidance behaviour in tissue genesis and regeneration. This project is today the first study on the supramolecular hydrogels activated for photo-conjugation chemistry, and can represent a novel cell-instructive platform that can be selectively encoded with active signals, with relevant applications in biotechnology and medicine.

3. CHAPTER 1

Novel smart HA-based hydrogels with non-covalent adhesive properties for tissues healing applications*

3.1. Abstract

Wound dressing after surgical and traumatic tissue injuries has been always one the most interesting research field, overall due to its impact in clinical trials. Hydrogels are good candidates in this related application because they own scaffolding properties and can be easy tuned. Selected peptide for tissue recognition can also be considered biomolecular glues able to adhere on particular tissue target. Here, collagen type I binding fragment conjugated to microbeads of hyaluronic acid have shown non-covalent adhesive interactions on human derma and cornea of eye, after mechanical or photo-removal of epithelial tissues. Were evaluated microbeads adhesive properties on human derma and cornea of the eye, and was observed that they formed a *continuous covering layer* from indiscriminately biological provenience of the collagen type I. For unfunctionalized microbeads surface we did not observe adhesive recognition. Was also found that adhesive recognition was more predominant in human cornea, where the non-covalent estimated layer was of *34 μm in thickness*. Was also proved that the hydrogel microspheres can deform, changing their initial shape, when were upon peptides interaction forces and this behaviour was also recorded. Finally, this novel instructed biomaterial show abilities to cover damaged tissue only where was provoked the injury, as well as the final layer was originated by deformation of many micro-entities capable to arrange itself until to completely dress the injury regions.

---

*The work in this chapter has been submitted for publication by A. Paciello and P. A. Netti

---

3.2. Introduction

Tissue engineering has been an active ground of scientific research as a fundamental tool in regenerative medicine in the last decades[1], and in particular wound repair after traumatic or surgical injuries has always engendered particular attention as such significant clinical and research importance[2-3]. Today, research in the field of the ophthalmology represents one of the most interesting scientific sectors, where many researchers are making many efforts to develop new relief for the corneal and stromal repair after treatment of surgical and trauma induced ocular wounds[4]. Corneal wounds are often caused by laceration, perforation, corneal transplants, laser or mechanical removal of epithelium tissue, or incision in the care of cataract and in many others cases in oculist pathology[5]. In particular, several million of patients are exposed to photorefractive keratectomy, as PRK procedure for the cure of disease of vision as well as many patients resaved accidental damages of corneal epithelium. Fundamentally, these techniques entailed photoablation of the corneal epithelium by excimer laser, exposing out the corneal collagen fibres without thermal damage to deeper cells[6-7]. After removal of epithelial tissue and after revision of damage, collagen is often covered with artificial therapeutic lens to defend the exposed collagen and to soothe the pain felt by the patient[8]. Lens application however are not indicated for all corneal disease, as example in chronic dry eye and in particular they can originate, below them, oxygen partial pressure decreasing[9-10]. In the last decades, several adhesive biomaterials have been developed for tissue repair including cornea disease, but their translation into clinical practice has been slow in part due to their invasive use, and in part due to materials not yet believed safes for human use[11]. Glues cyanoacrylate-based have been useful for corneal perforations treatment[12]. They are directly applied to wound site and the reaction undergoes as free radical polymerization to form a covalent covering film and its degradation products,

including formaldehyde, are toxic. Furthermore, several post-operative complications caused by cyanoacrylate adhesives have been described, including granulomatous keratitis, cataract formation, retinal toxicity, and glaucoma[4]. Therefore, has been interested of the biomaterials scientists to change direction towards tissue regeneration heavily reliant by man-made micro and nanodevices[13]. Today, hydrogel-based molecules adhesives are the other materials under investigation for ocular wound repair. They can be used as artificial corneas, intraocular or contacts lenses and vitreous humor substitutes[14]. Hydrogels show desirable optical properties and these properties can also be tuned[15]. Hydrogels can show refractive index values from 1.33 to 1.43, light transmission from 0 to greater than 90%, can have good transport of oxygen and nutrients to facilitate wound healing and good mechanical properties for structural sustainability for tissues injuries[4]. In the last decades, several *in situ* forming hydrogels are been investigated, but still their applications remain a challenge. Margalit et al. developed three different PEG-based hydrogels obtained directly via crosslinking on interest sites. Those hydrogels were able to sustain much higher loads before failure than commercial and autologous fibrin or photocurable acrylic adhesives[16]. In every case, they provoked only a inflammatory response and caused damage of cornea tissue. Hirose et al. have evaluated the behaviour of PEG-based hydrogel obtained using NHS-terminated 4-arm succinimidyl-glycolate PEG and amine-terminated 4-arm PEG to form amide groups. This hydrogel polymerize in a few seconds and persist for 4–6 weeks[17]. Sueda et al. reported hydrogels formulated with NHS terminated 4-arm glutaryl PEG and a tri-lysine peptide for in vivo cytotoxicity[18]. For this hydrogel was found after application a develop eyes posterior subcapsular cataract and vitreous opacity but no retinal detachments occurred. In every case reported above the invasive covalent chemistry caused a damage of tissue treated and also an inadequate control of biodegradability of the hydrogels. Grinstaff et al. performed an dendron cross-linked PEG hydrogels as corneal adhesive that

showed to have adhesiveness, biodegradability and swelling behaviour dependence by chemical composition[19]. In addition, several examples of molecules-adhesive hydrogels able to give covalent grafting on tissue damaged are reported by Messersmith and co-workers[20]. The star-PEG based hydrogel modification with catechol moiety [3,4-dihydroxy- L-phenylalanine (DOPA)][21-22], under oxidizing conditions rapidly forms cross-links on tissue injury. Hyaluronic acid (HA) and chondroidin sulphate are the most biological derived polysaccharides to be used in wound repair[23]. The structure of HA consists of repeating disaccharide units of D-glucuronic acid and (1-β-3) *N*-acetyl-D-glucosamine and it is an important constituent of extracellular matrices, synovial fluid and the vitreous humor in the eyes[24]. HA modified with dihydrazide and methacrylated groups, can form hydrogels by chemical or photo crosslinking, or HA can be also auto-crosslinked using divinyl sulphone (DVS) as reaction activator[25] in basic solution. Grinstaff et al. developed an adhesive HA-based hydrogel, where the starting biomaterial was modified with methacrylated groups. HA modified was directly crosslinked on corneas injury and after several days were observed lack in inflammation and infection but only mild corneal scarring remained[26]. Another example of tissue adhesive material is given by crosslinking in situ by star-PEG and engineered protein having repeated blocks of an elastin domain. The star-PEG polymer, modified with succinimidyl glutarate, form covalent linkage with primary amines of protein ECM-derived until to form a film directly on cornea injury[27]. In every cases reported above, the mechanism of adhesion of those materials were provided by chemical bonding[28] which can procure additional strain to ocular tissues. In scientific literature, example of peptide-conjugated hydrogels with non-covalent adhesive properties capable to recognize tissue site-binding, and promote tissue adhesion for wound healing, dressing or tissue injury covering are still rarely investigated. Peptides and their non-covalent abilities to adhere on biological tissues can also be used as organic molecular glues able to

recognize, in specific and selective manner, their molecular determinants into components of biological tissues. So, in smart manner, these peptides can recognize tissues and the hydrogels can provide for wound dressing like temporary tissues substitutes. Therefore, opportune peptides conjugated hydrogels can mediate for protection and maintenance of tissue injury and furthermore they can favourite cell-guidance process for tissue regeneration. One the most popular oligopeptides with covalent adhesive interaction is fibrin. Fibrin is a specialized ECM protein network, formed principally in spontaneous tissue repair[29] by polymerization of fibrinogen in the presence of thrombin[30]. Fibrin has been utilized in skin repair, for example, in sutureless fixation of skin grafts[31] and keratinocyte transplantation in burn patients[32], with considerable success. Fibrin covalently attached to hydrogels or as fibrin matrices has been investigated as useful glue[33] in the genesis of wound healing. The major drawbacks of fibrin is that it is susceptible to rapid degradation in vivo and has difficulty maintaining structural integrity[34], difficult applications, cost and potential transmitting of viral infection[35].

Collagen is a major conservative protein of the extracellular matrix of connective tissues and to providing mechanical integrity, it can also affect cell behaviour and gene expression through interactions with other matrix proteins and cellular receptors. In addition the bulk of the corneal stroma is comprised of a layered network of fibrillar collagen[36]. Integrins domains α1β2 and α2β1 are two major collagen receptors on the surface of eukaryotic cells[37]. These cell-integrin receptors are able to recognize on collagen specific targets for molecular recognition and cell-attachment. Adopting techniques based on screening of peptide recombinant fragment, is been possible to isolate collagen binding fragment able to recognize some molecular determinants on collagen type I in specific and selective way[38-40]. One of the sequences isolated, Gly-Cys-Glu-Asp-Ser-Glu-Thr-Arg-Thr-Phe-Tyr (CIBF), in particular way, showed high binding affinity with collagen

type I receptors. Thus, in this way, peptides can also be utilized in molecular recognition of collagen tissue showing absence of cytotoxicity[41].

In this work we investigated peptide-conjugated hydrogel for tissue injury recognition as potential applications of novel medical post surgery devices. Here, DVS-crosslinked micro-hydrogels hyaluronic acid-based were decorated on their surfaces with CIBF peptide. Effectively, were been effectively understood that those micro-hydrogels showed adhesion capability when were applied on tissue and, in anywhere was provoked the injury, until to form a continuous covering layer. Tissue recognition experiments were performed on fibrillated porcine collagen type I, histological slices of human derma and porcine derma[42], as well as on human cornea of eye explanted and for only research use. We observed that in every case, indiscriminately from the collagen provenience, the peptide conjugated hydrogel microbeads formed a continuous covering layer. Despite, for unmodified surface hydrogel did not observed anything adhesive recognition. The microbeads adhesive phenomena was observed and characterized by several techniques including laser scanner confocal microscopy (LSCM), Optical Coherence Tomography (OCT) e corneal topography (CT).

This pioneering work could open a new point of view in order to improve scientific knowledge on the behaviour of novel supramolecular recognitions of rational designed biomaterials at wound interface.

3.3. Materials and methods

3.3.1. Chemicals and general materials

Sodium Hyaluronate (MW~900 kDa) was purchased from Novozymes, China. NH_2-GCQDSETRTFY-biotin (CIBF-biotin) and COOH-GCQDSETRTFY-(Mini PEG-Mini PEG)-NH_2 (CIBF) were synthesized and purchased from Proteogenix, France. Divinyl sulfone (DVS), isopropyl

meristate, trichloromethane, 1-butanol, acetone, *n*-exane, hydrochloric acid, *N*-(3-Dimethylaminopropyl)-*N*′-ethylcarbodiimide hydrochloride (EDAC), *N*-Hydroxysuccinimide (NHS), sodium hydroxide, sodium chloride, potassium chloride, glycine, ditiotreitiol (DTT) and 5,5′-ditiobis-(2-nitrobenzoic acid) solution were purchased from Sigma-Aldrich. Triethylamine (TEA), dry *N,N*-Dimethylformamide (DMF) were purchased from Romil. ABIL EM 90 (cetyl PEG/PPG – 10/1 dimethicone) was purchased from Evonik Industries. ATTO 647N free amine group and ATTO 647N strepdavidin were purchased from ATTO TECH GmbH, Deutschland. Porcine collagen type I was purchased from YoProteins, Sweden. Mica sheets were purchased from Asheville-Schoonmaker Mica, USA. Strepdavidin coated microspheres (480, 520) Dragon Green were purchased from Bangs Laboratories Inc, USA. Human corneas have been gave by Fondazione Banca degli Occhi del Veneto, Italy. Spectra/Por® Dialysis membrane MWCO:. 12-14,000 was purchased from Spectrum Laboratories. Reagent and solvent were used without further purification unless otherwise specified.

3.3.2. General methods

Microbeads HA-based were prepared by single emulsion technique using Ultra turrax Heidolph R2R 2102 Control. Microbeads ATR characterizations was performed by NICOLET 6700 Thermo Scientific. Fluorescence and transmission bright-field imaging was performed by Laser Scanning Confocal Microscopy (LSCM) Leica TCS SP5. Morphological analysis was performed by Ultra plus field Emission Scanning Electron Microscopy (ESEM), Zeiss Instruments. Microbead diameter measurements were performed by Mastersizer 2000 Malvern Instruments. Superior corneal imaging was performed by Optic Coherent Tomography (OCT) Optovue, Alfa Intes. Corneal topography mapping was performed by Corneal Topography (CT) Precisio, Ligi Italy. Simulation of photorefractive

keratectomy on cornea was performed by excimer laser iRES, Ligi Tecnologie Medicali srl, Italy.

3.3.3. Microbeads prepared by DVS-crosslinked HA with simultaneous fluorescent probe incorporation (fcMB)

HA microspheres were prepared using water-in-oil emulsion system according to the previously procedure reported in elsewhere[43] with some modifications. DVS-crosslinked HA microbeads were prepared at different crosslinking ratio (fcMB350 and fcMB420). For the preparation of the emulsion, dispersed phase was prepared at 2.5% (w/w) solving 0.25 g of HA 900 kDa in 9.75 g of 0.2 M NaOH solution with a further adding 25 mg of NaCl. HA solution was made uniform under ultrasound sonication (40 Hz) for 5 minutes at room temperature. The dispersion medium was prepared mixing 24.6 ml of isopropyl meristate and 2.45 ml (about 2.18 g) of cetyl PEG/PPG – 10/1 dimethicone (10:1 ratio), under stirring for 20 minutes at room temperature. DVS (350µl and 420µl) and 2 mg of ATTO 647N amine free groups were added to 10 ml of HA alkaline solution and mixed vigorously for 2 minutes. The aqueous phase was added to oil phase drop to drop, and when emulsion appeared, it was kept under stirring at 480 rpm for 40 minutes at room temperature. The alkaline emulsion was neutralized adding 460 µl of 4 M HCl leaving again under stirring for further 40 minutes at room temperature. Next, emulsion was broken by dropping of 50 ml of acetone under vigorous stirring. Finally crosslinked HA microbeads were recovered for gravity. Organic residues were removed by several rinsing with a mixture of trichloromethane / *n*-butanol (1: 1 ratio) then followed further several rinsing with *n*-exane. After balancing with acetone, the microbeads were dialyzed in deionised water for 72 hours. Next the dialysis the microbeads were dehydrated adding drop to drop acetone. In this way the slow dehydration avoided a probable damage of obtained soft micro-hydrogel. Finally, the microbeads were exsiccated under critical point drying,

passed throughput sieves at different pore cat off and stored in dry conditions at 4 ˚C.

3.3.4. Microbeads characterization and morphological analysis

Starting HA polymer, fcMB350 and fcMB420 were chemically characterized by Fourier transform infrared (FTIR) spectroscopy. FTIR were performed on a Nicolet 6700 spectrometer (Thermo Scientific) equipped with a single-reflection attenuated total reflectance accessory (Smart iTR) under ambient conditions. ATR spectra were acquired at 18 °C on dried simples. ATR correction (germanium crystal) and baseline correction were applied to the data before analysis. Spectra were collected in the range 600-4000 cm^{-1} with a resolution of 4 cm^{-1} and averaging over 128 scans. Morphological analysis of hydrated fcMB350 and fcMB420 were performed by an inverted Leica TCS SP5 laser scanning confocal microscope (LSCM). Experiments were conducted at 20 °C. ATTO 647N stained microbeads, that had been completely swollen in physiological solution, were transferred in fluorodishes (World Precision Instruments, Inc.) and imaged by a HeNe 633 excitation laser, detecting 650-750 nm emission band and using a Leica HCX IRAPO L 25×/0.95 W water immersion objective. Transmitted ligth brightfield images were simultaneously acquired as well. Morphological analysis of dried microbeads was performed by ultra plus field emission scanning electron microscope (ESEM), Zeiss Instruments. Microbeads in a small amount were sprinkled on the metallic stubs and were coated with gold palladium until 10 nm under controlled argon atmosphere using Cressington Sputter Coater 208HR. The simples were observed at 10.00 KV and 937X in magnification.

3.3.5. fcMB swelling studies

Swelling studies on fcMB350 and fcMB420 were evaluated on five single emulsion prepared at different stirring velocity (275, 350, 450, 500 and 600 Ncm). The microbeads were prepared, purified and dehydrated using the same method and conditions as reported above. 50 mg of each dried samples were dispersed in absolute ethanol. In the same way, were weighted 50 mg of each simple and were swelled and dispersed in physiological solution. For each simple, three aliquots of dispersed microbeads were analyzed using Mastersizer 2000 Malvern Instruments to misure diameter. For this analysis, was used refractive index of 1.36 at 20 ˚C for the simples in ethanol and 1.33 at 20 ˚C for the simples in physiological solution. The diameters were assumed at maximum of Gaussian distribution and considering the Mass Median Diameter, which is the size in microns where the 50% of the microbeads is smaller and 50% is larger. The collected data for every sets were plotted with Origin lab software and were calculated the linear equations, a) and b), which were matched to obtain the swelling equation c). The swelling equations were related to diameter of swelled microbeads, when they were dispersed in two different solvents.

$$\textbf{a)}\ S(s) = a1(rpm) + b1 \qquad \textbf{b)}\ S(d) = a2(rpm) + b2$$

$$a1(rpm) = a2(rpm)$$

$$\textbf{c)}\ S(s) = S(d) + (b1 + b2)$$

S(h) and S(d), a1(rpm) and a2(rpm), b1 and b2 are respectively diameter, stirring velocity and constant calculated for swelled and dried fcMB350 and fcMB420, respectively.

3.3.6. cMB420-CIBF-biotin synthesis

DVS-crosslinked HA microbeads (cMP420) were prepared using the same condition reported above but without adding of ATTO 647N free amine group. 50 mg of cMB420, previously dried under vacuum oven at 30 C, were introduced into round-bottom flask and kept under nitrogen flow for 20 minutes, after 1 ml of dry DMF was added under stirring at room temperature. 15 mg of NHS and 15 mg of EDAC ($1.3*10^{-4}$ and $7.8*10^{-5}$ mol) dissolved in 1 ml of dry DMF were added to microbeads. Next, 3 mg of CIBF-biotin ($1.7*10^{-6}$ mol, MW = 1762.62 Da) and 15 µl of TEA dissolved in 1 ml of dry DMF were added to solution. The mixture was kept under stirring for 4 hours, in dry conditions at room temperature. The microbeads were rinsed with acetone three times, recovered for gravity and finally were dialysed in deionised water for 48 hours. Subsequently cMB420-CIBF-biotin were dehydrated adding drop to drop acetone, recovered for precipitation, further exsiccated with critical point drying and stored at 4 ˚C. Conjugation of peptides was verified using biotin-strepadavidin assay. 10 mg of cMB420 and cMB420-CIBF-biotin were treated with 500 µl of a solution 100 µg/ml ATTO 647N-strepdavidin and were kept in stirring under orbital shaker for 15 minutes at room temperature. Microbeads were recovered via precipitation washed five times for 10 minutes each one, and finally imaged using fluorescence confocal microscope.

3.3.7. fcMB-CIBF synthesis

fcMB420-CIBF and fcMB350-CIBF were prepared at different fuctionalization degree using three different CIBF amount. 50 mg of fcMB420 and 50 mg of fcMB350, previously dried under vacuum oven at 30 ˚C, were introduced into round-bottom flasks and kept under nitrogen flow for 20 minutes, after 1 ml of dry DMF was added to each simple, under stirring at room temperature. 15 mg of NHS and 15 mg of EDAC ($1.3*10^{-4}$

and $7.8*10^{-5}$ mol) dissolved in 1 ml of dry DMF was added to microbeads. After, CIBF (1.5, 2.5 and 3.1 mg, $9.2*10^{-7}$, $1.6*10^{-6}$ and $1.94*10^{-6}$ mol respectively, MW = 1596.62 Da) and 15 µl of TEA dissolved in 1 ml of dry DMF were added to the microbeads dispersion and further kept under stirring for 4 hours, in dry conditions at room temperature. The microbeads were rinsed three times with acetone, recovered for gravity and finally dialysed in deionised water for 48 hours. Subsequently fcMB420-CIBF and fcMB420-CIBF were dehydrated adding drop to drop acetone, recovered for precipitation and further exsiccated on critical point drying and stored at 4 ˚C. Peptide-conjugation was qualitatively verified by ATR-FTIR and also using Ellman reactive assay. 2 mg of microbeads prepared were completely swelled in 500 µl of water treated with ditiotreitiol (DTT), after with an excess of 0.5 mM 5,5′-ditiobis-(2-nitrobenzoic acid) solution. Morphological analysis to verify the microbeads integrity after reaction was evaluated by LSCM.

3.3.8. Preparation of collagen substrates for CIBF binding assay

CIBF were tested on biological collagen substrates to verify their adhesive abilities after tissues recognition. CIBF binding assay were evaluated on fibrillated porcine collagen type I, histological slices of porcine and human derma, and human cornea as well. Fibrillated collagen solution was prepared mixing 0.1 mg/ml of porcine collagen type I and 27 µl of restored buffer. Buffer restored solution was prepared solving 373 mg of KCl (0.05 mol) and 94 mg of glycine (1.25*10-3 mol) in 25 ml of water biological grade. The final solution was adjusted with NaOH until pH was about 9.2. Subsequently, collagen solution was deposited on mica sheets and incubated for 6 hours at 37 ˚C. Next, it was washed in physiological solution and imaged by mean of transmitted light brightfield using LSCM. Histological slices of human and

porcine derma, included in resin water soluble, were deposed on glass slides, next, washed to remove hydro-soluble resin excess and imaged in transmission breight-field on LSCM. Corneal epithelium was mechanically removed by mean surgical scalpel to bring out the cornel collagen and washed in physiological solution to completely removal epithelium residues. The biological simples were treated with 300 µl of 25 µg/ml of CIBF-biotin in physiological solution each one, and then were incubated for 40 minutes in orbital shaker at room temperature. After that simples were washed for 15 minutes each one and for three times to remove CIBF-biotin unbind. Biotin was revealed by molecular recognition with ATTO 647N streptavidin. The simples were treated with 300 µl of 10 µg/ml ATTO 647N streptavidin in physiological solution each one, were incubated for 40 minutes at room temperature, then were washed to remove ATTO 647N streptavidin unbind for 15 minutes each one. Negative control of the same simples were only treated with 300 µl of 10 µg/ml ATTO 647N streptavidin in physiological solution each one, anyway, were incubated for 40 minutes at room temperature, then were washed to remove ATTO 647N streptavidin unbind for 15 minutes each one. In the last, the simples were imaged in fluorescence on LSCM.

3.3.9 Preparation of biological simples for wound dressing experiments

fcMB420-CIBF prepared at different molar ratio of CIBF were used to estimate their collagen covering abilities in supramolecular manner. 8 mg of each simple were swollen in physiological solution and from the top were instilled on collagen fibrillated on mica. After 5 minutes of incubation at 37 °C, the simples were washed with physiological solution to remove unbind microbeads. Covering parameter was estimated by fluorescence microscopy to also evaluate more suitable peptide fuctionalization degree. Adhesive non-covalent interactions on biological tissues as porcine fibrillated collagen type I, human derma and cornea, were investigated. Histological slices of human

derma were previously washed several times to remove hydro-soluble resin, while was removed epithelium tissue from cornea for 100-110 µm per 9 mm in diameter by *in vitro* surgical photorefractive keratectomy simulation, using excimer laser at 193 nm. fcMB420-CIBF and fcMB350-CIBF with functional degree of 3 mg of CIBF per 50 mg of dry microbeads, were swelled in physiological solution for 5 minutes at room temperature. Next, microbeads suspension was instilled on biological simples and the instillations were accomplished from the previous one, after 1 minute for three times at room temperature. After, the substrates were washed with physiological solution to remove microbeads unbind. The images were collected in fluorescence and transmission bright-field using LSCM. Corneal mapping was performed by CT and thickness of microbeads layer adhered on cornea was estimated by OCT equipped with advanced low-power fibres-optic interferometers coupled in mid-IR region (1,320 nm).

3.4. Result and discussion

The purpose of this work is been to design a novel rational instructive biomaterials for specific recognition of collagen when the biological tissues are been damaged by surgical or accidental trauma. This novel smart material has wound dressing properties and is capable to cover damaged tissue in non-invasive manner. The design of this biomaterial was inspired by molecular recognition between two biological entities as the interaction among proteins. In particular, the use of peptide for the development of new medical devices is today looked with strong interest. The interactive peptide ability can be considered as authentic molecular glue by using as adhesive force for surface materials interaction. The natural material used in the work is the most popular hyaluronic acid, not only used for its biocompatibility and biodegradability properties, but also for its ease manipulation. Sodium salt of

hyaluronic acid can be obtained by recombinant technology using a fermentation process with Bacillus Subtilis. This microorganism, during biosynthesis do not produce endo or eso-toxins, helping to reduce the risk of contamination and thus offering greater security than those of animal origin. Typically, the hyaluronic acid has elastic, plastics, lubricants and filling properties and when it is crosslinked is able to retain a large amount of water up 98%. Crosslinked HA hydrogel can be obtained in the form of disk or lenses as well as microspheres. The first, having a predetermined geometry and dimension, do not adapt easily to the various shapes and sizes of damage regions, despite the second, used in aqueous suspension, offer the advantage to cover tissue damage of any shape and size, in adaptive way. Further, we also demonstrated that for microbeads HA-based, with a diameter of around 80 µm, have a good transparency properties. Transparency parameter was calculated as refractive index and the measurement was performed by refractometer Abbemat 300/350, assuming the sodium wavelength at 589.3 nm. The measurement of refractive index was carried out on monolayer of microbeads and was ranged between 98 - 99% in reference to that of pure water at 25 ° C. Adhesive events mediated by fibronectin and other extracellular attachment proteins provide experimental systems for analyzing polypeptide domains that mediate binding and adhesive functions. In the literature are reported several conserved peptides isolated from fibronectin in the collagen binding region, that containing the sequence Cys-GIn-Asp-Ser-Glu-Thr-Arg-Thr-Phe-Tyr, Ser-Pro-Ala-Ser-Ser-Lys-Pro and Gly-Arg-Gly-Asp-Ser-Pro-Cys. These peptides showed good abilities for recognition sites in extracellular proteins as collagen type I and can have a crucial rule in several biomolecular process[40]. As showed in elsewhere[39], peptide binding activity is related to asparagine, serine and arginine interactions on specific site-binding on collagen type I. In this work, we suggest a complementary approach to the purpose of these bioactive peptides: the use of a synthetic peptide that competitively bind specific molecular target useful for

collagenous tissues recognition. In this work the peptide (Cys-GIn-Asp-Ser-Glu-Thr-Arg-Thr-Phe-Tyr, GenBank code: AAI43755.1), briefly denominated CIBF, was used as pioneering molecular glue, where the contribution of every single peptide interaction at biomaterial interfaces represent the full amount for the final adhesive force. This peptide was opportunely modified with biotin at *C*-terminal region in order to introduce a secondary recognition site for labelled streptavidin. In this way, was verified synthetic peptide ability to recognize a specific target region on collagen type I from *in-vivo* fibrillated collagen, porcine and human derma as well as on human cornea of eye. As showed in Figure 3.1., CIBF-biotin was able to interaction with the biological substrates, without any limitations due to the conservative biological properties of the collagen type I. Fluorescence images, after binding assay, (as in Figure 3.1. c, f, i and n) showed substantial difference among a substrate to another one. In effect, the used tissues exhibited different morphological organization of the collagen fibres. Even if, the collagen fibres in the corneal stroma are the same nature of collagen in other connectives tissues, the fibrils in lamellae arrangement are not crosslinked and proteoglycans are easily extracted with salt solutions[44]. Therefore, appeared evident that CIBF-biotin interactions with corneal collagen (Figure 3.1.i) were supported to major spatially and hindrance assessment.

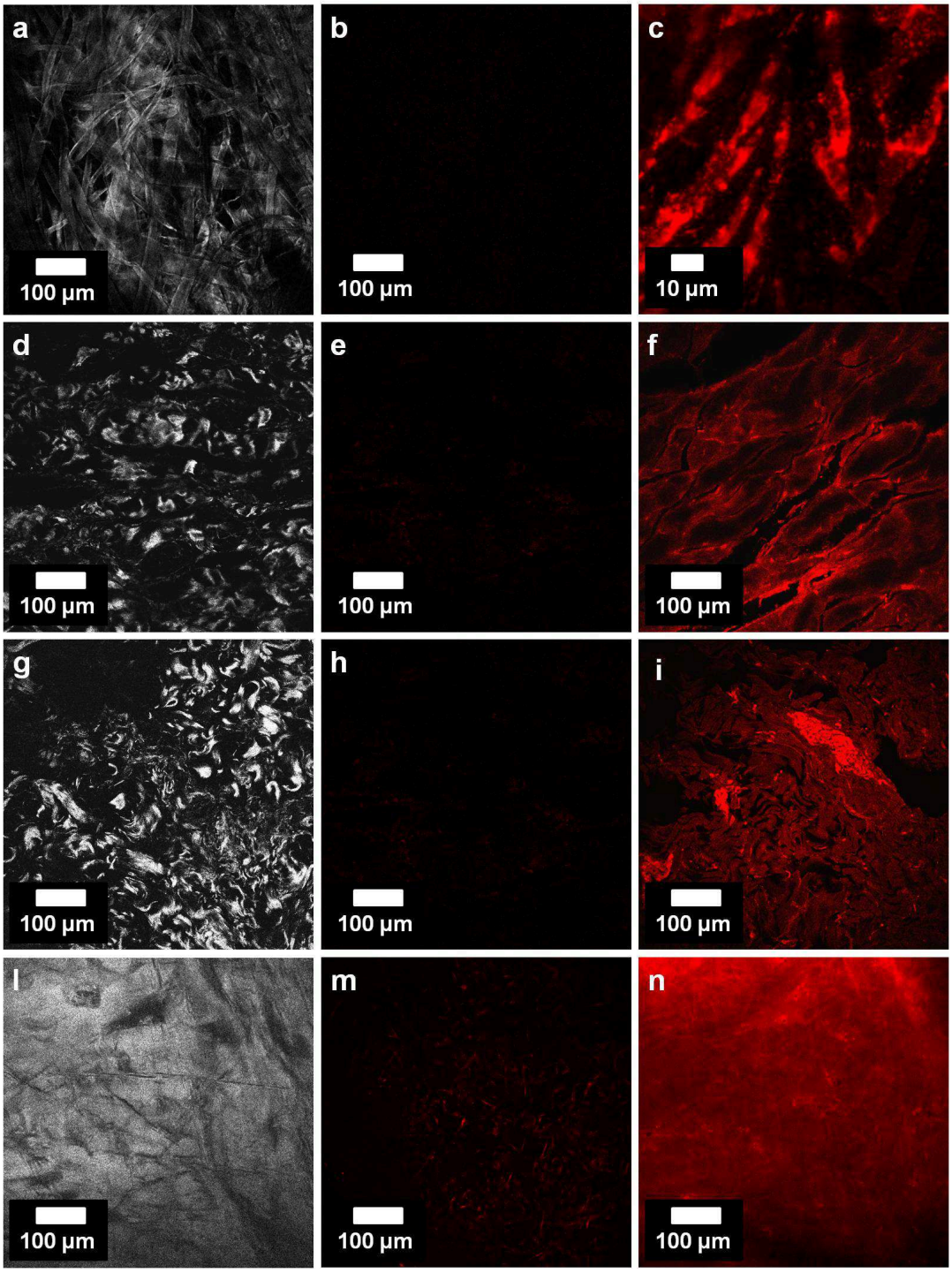

Figure 3.1. – Collagen Binding Fragment assay of CIBF-biotin after detection with streptavidin stained with ATTO 647 N dye: a) white light transmission and b, c) fluorescence images of CIBF binding on collagen type I fibrillated on mica; d) white light transmission and e, f) fluorescence images of CIBF binding on porcine derma; f) white light transmission and (g, h) fluorescence images of CIBF binding on human derma; i) white light transmission and l, m) fluorescence images of CIBF binding on human cornea.

3.4.1. Preparation of fcMA-CIBF and general synthetic scheme

fcMB were prepared using sodium hyaluronate (fig. 1a) and DVS such as crosslinking agent. The reaction was performed in 0.2 M NaOH because a high pH values favourite the formation of sulfonyl bis-ethyl linkages between the hydroxyl groups of HA to form consequently ether bonds. NaCl was added at reaction mixture to increase the crosslinking degree. fcMB was labelled using ATTO 647N free amine groups fluorescent probe. This fluorescent probe was statistically and simultaneously conjugated to hydrogel network, taking advantage by Michael addition reaction and from sulfonyl bis-ethyl linkages formation between HA hydroxyl group and primary amine group of fluorescent probe. fcMB were prepared using *water in oil* single emulsion technique, which allowed to combine simultaneously microbeads preparation method and crosslinking chemistry strategy. Was used AbilEM as surfactant, which allow a better dispersion of the microspheres being formed in order to reduce the probability of particle aggregation upon hardening conditions. Furthermore this technique allowed collecting fcMB in quantitative yield in weight, after every purifications and dehydrations step. Primary hydroxyl group of starting hyaluronic acid was required in the DVS-crosslinking reaction in order to leave unmodified carboxylic functions. CIBF peptide, previously, was further modified at *N*-terminal region using PEG spacer at low molecular weight for modulate the peptide structure conformation to be properly spatial arranged in order to favourite cooperative interactions, which are essential mechanism for molecular recognition. Next, CIBF peptides were conjugated to dried microbeads surface (Figure 3.2.b) to form amide bound between carboxylic group of hyaluronic acid and amine groups of mini-PEG spacer (Figure 3.2.c). Coupling reaction was performed in dry condition, using DMF[25] as solvent and the most popular EDC/NHS chemistry with added of TEA as basic activator. These microbeads are designed to recognize collagen on tissue surface (Figure 3.2.d) executing tissue wound dressing, and can be deformed upon peptide interactions until to

form a continuous layer (Figure 3.3.e). In Figure 3.2.f, instead, is reported an illustrative particular of interaction at nanometer level.

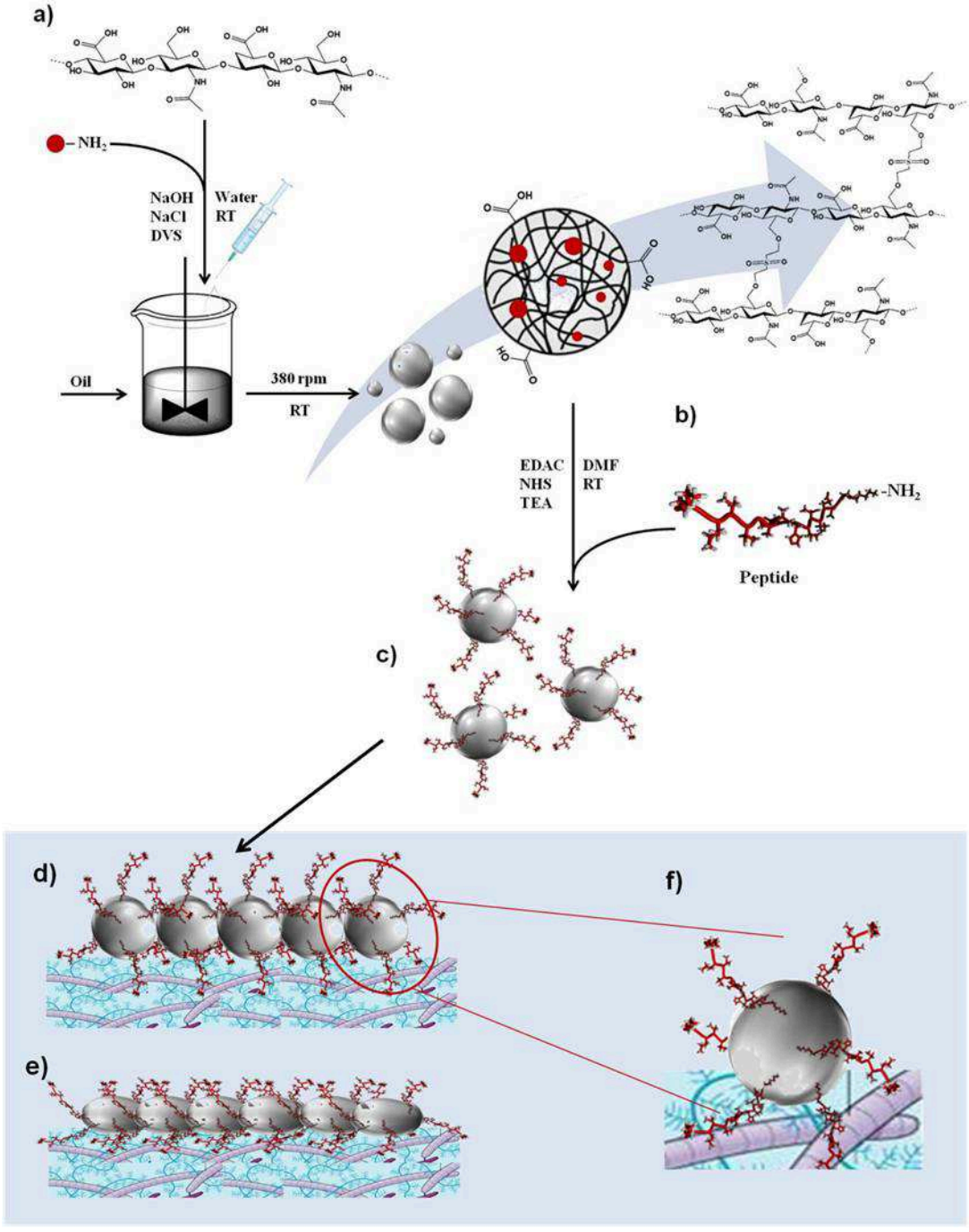

Figure 3.2.– Synthetic scheme and action mechanism of DVS-crosslinked microbeads HA-based: a) preparation of fcMB by single emulsion technique; b) amide group formation between MB-COOH and peptide-NH_2; c) final microbeads (fcMB-CIBF) specialized for specific and selective recognition of collagen type I in eukaryotic tissue; d) tissue covering mediated by fcMB-CIBF; e) microbeads deformation upon peptide interaction forces and HA layer formation; e) representative molecular binding between peptide and site-binding on collagen.

3.4.2. FTIR and SEM characterization of fcMB

The successful crosslinking formation for fcMB350 and fcMB420 was demonstrated by ATR-FTIR. Picks attribution are been made with helping of HA FTIR analysis as reported elsewhere[45-46]. By HA spectra was found for HA a sharp band at 1655 cm^{-1} due to the C=O carboxyl amide I group, the pick at 1108 cm^{-1} due to the C-O-C, C-O and C-O-H stretching, at 2924 cm^{-1} due to the CH stretching and the large pick at 3424 cm^{-1} due to the NH and OH stretch mode. DVS-crosslinked hyaluronic acid in fcMB, for both microbeads crosslinking degrees prepared, was confirmed by ATR analysis. In fcMB was found a weak picks at 1031 cm^{-1} due to S-O and S-C stretching frequencies coming from DVS, around 1230 and 1121 cm^{-1} which are coming both from C-O stretch modes involved in the HA-DVS bonding and at 1131 cm^{-1} due to the S=O stretching mode of DVS. Furthermore, ATR analysis also shown that crosslinking conditions did not provoke chemical degradation of HA, and any modification of the –COOH pick around 1640 cm^{-1} was further confirm that the main reaction between HA and DVS was between the hydroxyl groups. From the ratio between pick intensity at 1131 cm^{-1} of S=O stretching and pick intensity at 1655 cm^{-1} of C=O carboxyl amide I relate to uncrosslinked HA was also calculated the crosslinking degree percentage. For fcMB350 and fcMB420 they were approximately estimated of 0.6% and 0.8% respectively. Single emulsion techniques, however, have one limitation related to the size of the produced microspheres, because they are obtained with substantial dispersion range, therefore the size of interest may be restricted using sieves. The size of particles produced with our preparation condition was ranged between 1 and 150 µm. In this work the size of microbeads play a fundamental rule, because they have got to be used in order to form a monolayer over collagenous tissue. Were selected microbeads ranged from 25 to 30 µm with a final yield of 59%. LSCM morphological analysis of swollen microbeads, as showed in Figures 3.3.a and 3.3.b, highlighted presence of pores on fcMBs surfaces

probably due to a rapid swelling when they were immersed in physiological solution, but also by dehydrated processes and critical point drying purification step. The high rate of evaporation adopted for hardening exsiccation of microbeads provoked the formation of pores on and within the polymeric network. This contributes to reduce the density and stiffness of the particles. Moreover, the medium porosity observed increases the unevenness of the surface with a positive effect on desiderate prominent deformability properties indispensable for continuous layer formation on collagenous tissue. Furthermore, the sizes of swelled microbeads were found to be from 60 to 90 µm in diameter. By SEM morphological analysis of dried fcMB, as showed in Figure 2c, microbeads presented a proper morphology of spherical shapes and closing structure, the size was ranged from 21 to 32 µm in diameter and without any pores evaluation.

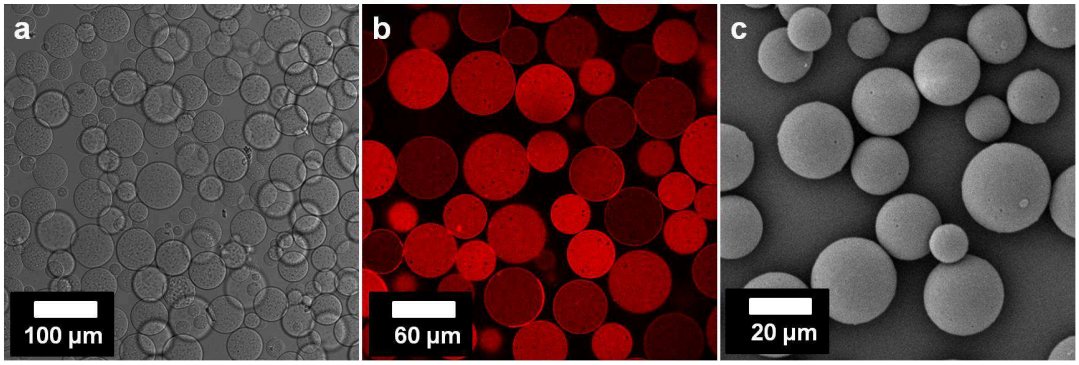

Figure 3.3. – DVS-crosslinked microbeads HA-based stained with ATTO 647N dye, morphological characterization: LSCM: a) white light transmission and b) fluorescence images. SEM: c) microphotographs of loaded fcMB (Magnification 937X and EHT = 10.00 KV

3.4.3. Swelling studies of microbeads

DVS-crosslinked HA micro-hydrogels swell with a large extent of water and appear clear and uncoloured. When the microbeads are dispersed in ethanol they do not swell and their diameters remain the same of that ones in the starting dried microbeads. Hydrodynamic radius measurement of dried and swollen fcMB350 and fcMB420 was performed by Dynamic Light Scattering

(Mastersizer-DLS). As reported in method, were prepared five emulsions for which was only changed the velocity of stirring. In this way, the size of microspheres population distribution is shifted towards formation of microspheres with smaller size. In single emulsion technique the size distribution is inversely proportional to velocity of stirring. Therefore, the average diameter of the main population was assumed at maximum of Gaussian distribution for all swollen and dried simples. Effectively, the measured diameters resulted to be decreased when was increased the velocity of stirring. After purification and drying step, were prepared five microbeads dispersion in absolute ethanol and five simples of microbeads swollen in water, for each prepared microspheres simple and in triplicate. The average diameters values were plotted using Excel Windows Microsoft. In the start were obtained the linear equations relative to value sets for each series of simple. The average diameter estimated for dispersed microbeads in ethanol was used as dried microbeads diameter. As reported in Figure 3.4., from the linear matching of the pair equations relative to fcMB350 and fcMB420 was obtained the swelling equations. These equations put in correlation the size of swollen and dried microspheres. Swelling equations of dried/swollen fcMB350 (Equation1) and dried/swollen fcMB420 (Equation 2) are following reported:

$$\textbf{\textit{Equation 1 -}}\quad S(s) = 3\,S(d) - 5.3$$

$$\textbf{\textit{Equation 2 -}}\quad S(s) = 2.7\,S(d) + 2.6$$

S(d) and S(h) are dried and swollen fcMB diameter for both pair correlated measurement. By these equations were studied the swelling behaviour, and the swelling factor was calculated as slope of the lines, which approximately, coincides with 3.0 for fcMB350 and 2.7 for fcMB420. Swelling factors result to be in according with the crosslinking degree percentage estimated with FTIR analysis. In fact, the total amount of water adsorbed depending on crosslinking number in the network. The swelling percentages resulted to be

between 98 and 96% by weight for fcMB350 and fcMB420 respectively. In addition, this swelling behaviour also suggests that the crosslinking reactions take place in isotropic manner when the network is being formed.

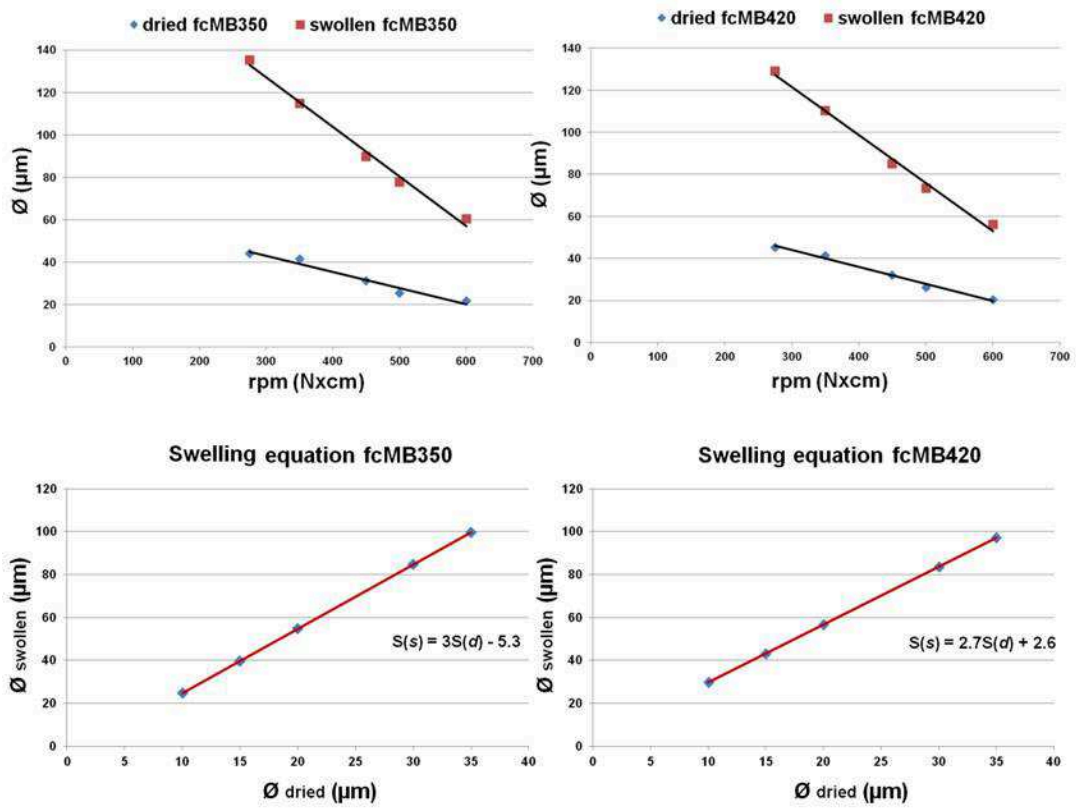

Figure 3.4. – Swelling behaviour of microbeads: Top) the relationship between diameter versus velocity of stirring is reported for both different crosslinked swollen and dried microbeads; bottom) swelling equations of fcMB350 and fcMB420 are respectively reported, assuming that the slope of the line coincides with the swelling factor.

3.4.4. Synthesis of fcMB-CIBF-biotin and tissue covering assay

Preliminarily, synthesis of fcMB-CIBF-biotin was designed in order to demonstrate and characterize the formation of amide bound between carboxylic groups on microbeads surface and amine groups of biotinylated peptides. The bioconjugation reaction was made using EDC/NHS as chemistry strategy. After several purification steps the fcMB and fcMB-CIBF-biotin were equilibrated in physiological solution and treated with

ATTO 647N labelled streptavidin. The unfunctionalized microbeads, (Figures 3.5.d and 3.5.e) fluorescence images shown homogeny absorption of labelled streptavidin. This is probably due to the diffusion of streptavidin through the crosslinked network, also highlighting, that the micro-hydrogels can operate like biomolecular sponge. Fluorescent image of functionalized microbeads (Figure 3.5.f), instead, did not show any streptavidin adsorption, but show an evident formation of fluorescent crown. In this case, the biotin interacting with streptavidin prevented the diffusion of execs of this one into hydrogel network. At the same way, as further confirmation of collagen site-binding recognition, CIBF-biotin was detected using Strepdavidin coated polystyrene microspheres (480, 520) Dragon Green with diameter of 1µm, using the same binding condition reported above, and as substrate was used *de-novo* fibrillated collagen. With this method, was found that the microbeads were firmly maintained on collagen surface after several washing (Figure 3.6.c). After these interesting results, was investigate the covering ability of fcMB-CIBF, testing functionalized microbeads at different conjugation degree. Since the size of HA microbeads used were surely greater then polystyrene one, the peptide was modified at N-terminal region with a spacer in order to improve peptide spatial control and mobility for collagen site-binding recognition. Surprisingly, fcMB-CIBF were able to recognize collagen and to be maintained firmly to it, even if several washed followed. As showed in Figure 3.7. the covering was evaluated to be highly dependent on substantial interactions number. In particular in Figure 3.7.c, corresponding to collagen treated with fcMB-CIBF with a conjugation degree of 3.1 mg of peptide per 50 mg of dried HA microspheres, show a complete covering in anywhere the collagen was deposed.

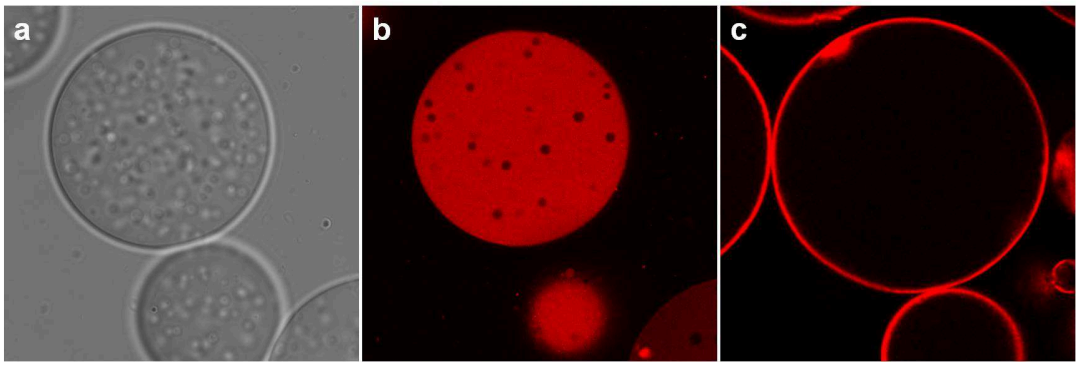

Figure 3.5. – fcMB-CIBF-biotin, ATTO 647 N labelled streptavidin binding assay: white light transmission and fluorescence images of a, b) fcMB unfunctionalized show adsorption of fluorescent streptavidin; c) shows a fluorescent crown formation due to molecular recognition between biotin and streptavidin.

.

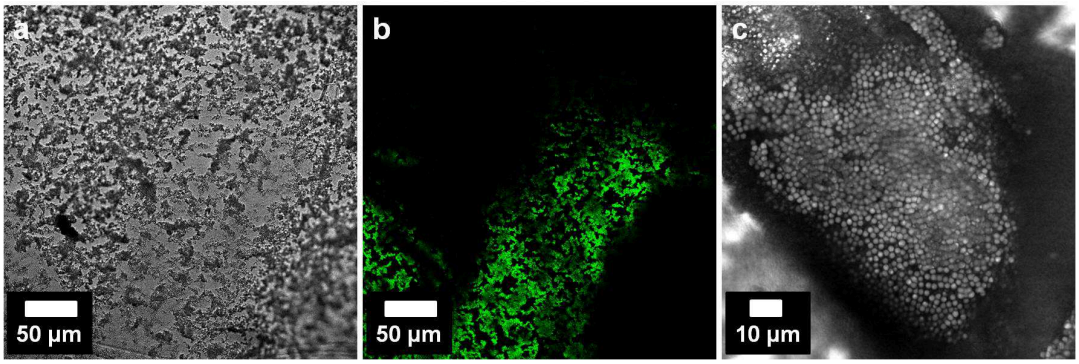

Figure 3.6. – LSCM analisys: a) bright-field, b) fluorescence and c) white light transmission images of CIBF-biotin and collagen recognition as well as biotin and Strepdavidin coated microspheres (480, 520) Dragon Green.

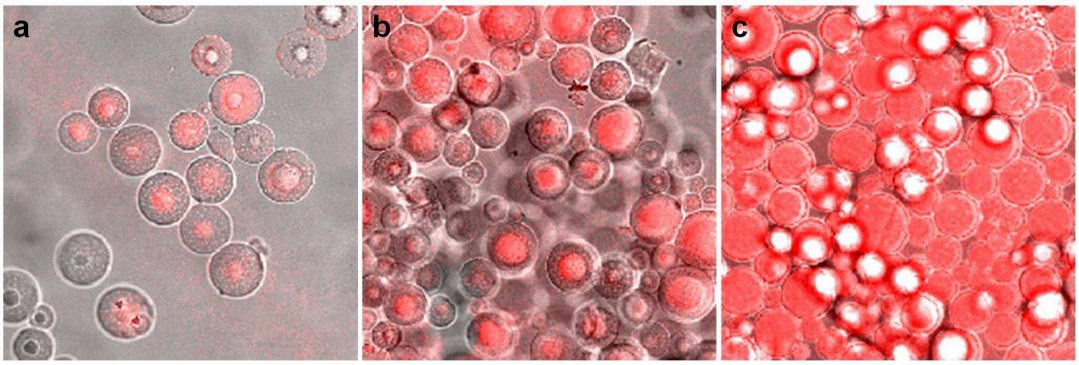

Figure 3.7. – Collagen covering ability of fcMB-CIBF with different conjugation degree. Overlapping of white light transmission and fluorescence images: fcMB420-CIBF prepared using 50 mg of fcMB420 and a) 1.5, b) 2.5 and c) 3.1 mg of CIBF.

3.4.5. Wound dressing properties of microbeads prepared with different crosslinking degree

Covering experiment, mentioned above, suggested that the covering was highly dependent by conjugation degree of the prepared fcMB-CIBF. The same experiments were also performed on biological tissue, where collagen fibres organization is arranged on different complexes scale. In this experiment we also verified that the crosslinking degree of microbeads play a fundamental rule when the HA layer was being formed. Microbeads being hydrogels are able to absorb water, and in this case up 98 and 96% for cfMB350-CIBF and cfMB420-CIBF respectively. The total amount of fragment between two distinct crosslinking points is related to swelling factor but also to deformability of reticulate structure and these obligations determinate the stiffness of hydrogels. We found that the microbeads, after adhesion were able to form a HA layer and the thickness was function of crosslinking degree, assuming for each one the same peptide conjugated degree. As demonstration of this, human derma and cornea of the eye were treated with fcMB350-CIBF and fcMB420-CIBF suspension, using them like collyrium. In effect, fcMB420-CIBF and fcMB350-CIBF showed different covering properties not only due to different collagen fibres organization but also to the microbeads deformation. Beside, microbead deformation allowed a major surface exposure, which favourite an enhancement of peptide interactions on collagen fibres and for single microbead. As showed in Figure 3.8., the instillation of fcMB420-CIBF and fcMB350-CIBF on the tissues surface, after several washed, showed different arrangement of the fluorescence on collagen due to the different deformability properties and consecutively thickness of the layer formed. Microbeads with different crosslinking degree on fibrillated collagen showed that fcMB420-CIBF (Fig. 3.8.b) was able to interaction with collagen surface and covering disposition was dependent by the peptide interaction number. The fcMB350-CIBF (Fig. 3.8.c) showed means a major biaxial deformation related to covering

disposition due to more high deformability of microbeads. The same microbeads were tasted on human derma and were observed that for fcMB420-CIBF (Fig. 3.8.e) promoted a covering disposition more regular than that one on fibrillated collagen, while for fcMB350-CIBF (Fig. 3.8.f) looked like a continuous films. In this case we assumed that, after interactions between peptide and collagen, the microbeads deformation causing high microbeads surfaces exposure, in this way was increased in number the peptide interactions. The same experiments performed on human cornea showed that both microbeads (Fig. 3.8.h and 3.8.i) were able to give films. In these cases, means, we supposed that the intrinsic deformation related to only microbead began secondary effect. As previously reported, the difference between the collagen fibres organization in human cornea respect to that one of derma, is the absence of natural crosslink. This property may increases the number of collagen binding domains available for the bioactive peptide sequence on microbeads surface and simplifying potential interactions. Probably the deformation effect was extended by the enhanced number of interaction with final holding forces more prominent at molecular level.

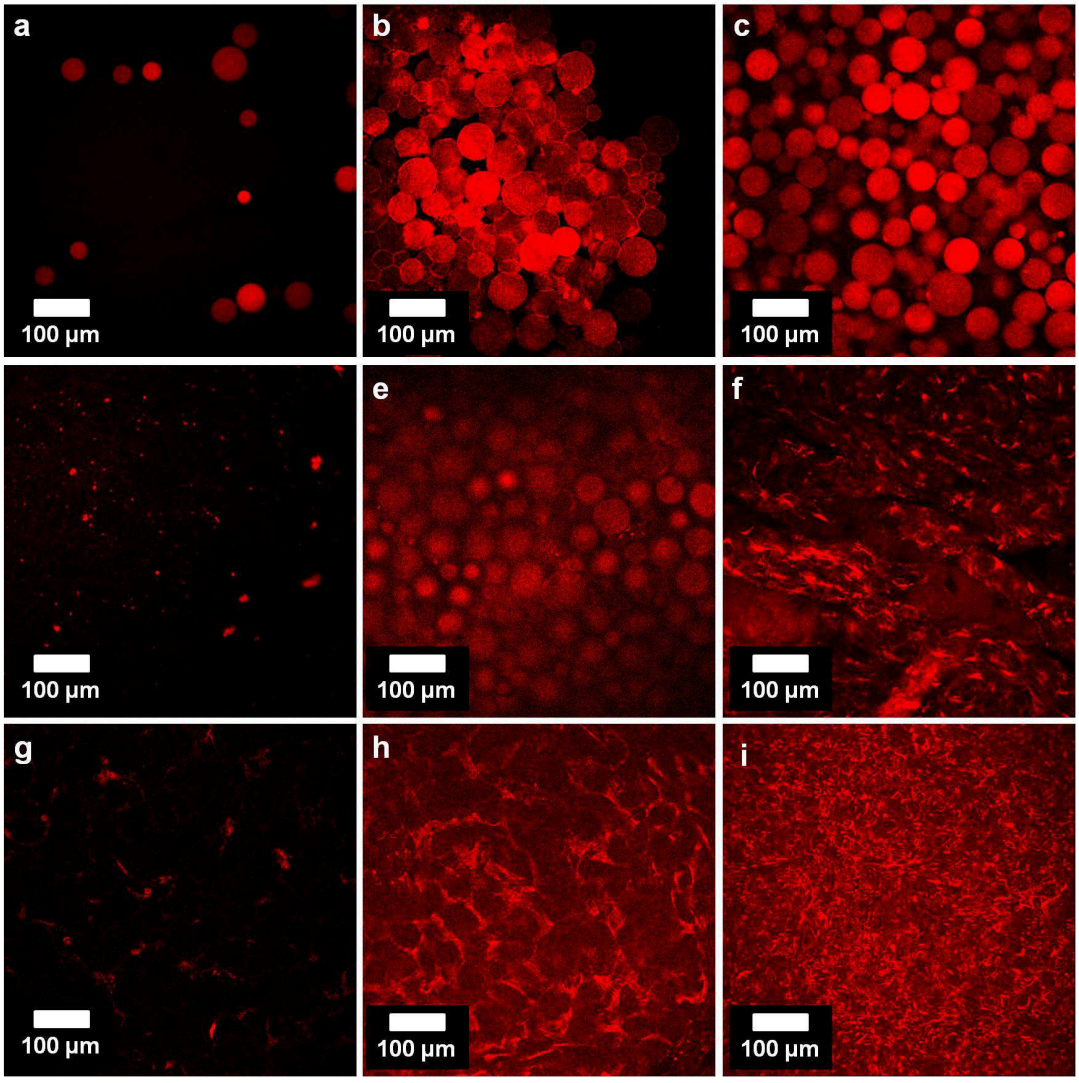

Figure 3.8. - LSCM characterization of fcMB-CIFB abilities to cover human derma and cornea of the eye: fluorescence images show a, d, g) non-adhesive capability of unfunctionalised fcMB; adhesive abilities of fcMB420-CIBF and fcMB350-CIBF on b, c) fibrillated collagen, e, f) human derma and h, i).human cornea

3.4.6. Thickness evaluation of hydrogel layer

The thickness of formed HA layer was investigate using LSCM, OCT and CT. Human cornea was exposed to oculist surgical laser in order to bring out the first layer of corneal collagen. Later, the photoablated cornea was washed with physiological solution to completely removal epithelium tissue residues, dried with ophthalmic lance and treated with a few drops of microbeads suspension. After five minutes from microbeads application, the cornea was

vigorous washed several times. Cornea surfaces appeared birefringence and reflective as well as hydrated. By fluorescence analysis, as reported in Figures 3.9.a and b, showed a diffuse fluorescence in deepness over 75 µm along z-axis. The overlapping of the photo-frames along z-axis highlighted the fluorescent HA continuous layer for both different microbeads prepared at different crosslinking degree. The thickness measured for fcMB420-CIBF (Figure 3.9.a) was of 34 µm and for fcMB350-CIBF (Figure 3.9.b) was of 24 µm. Even if the conjugated degree for both microspheres was the same, the different layers thickness is correlated to the deformability of the microbeads. Being fcMB350-CIMB less stiff of fcMB420-CIBF the consequence was for the first one, an enhanced predisposition to recline around collagen fibres. Additional validation of the layering capability of the microbeads was carried out by OCT and CT analysis. The OCT is one technique that allows obtaining corneal and retinal scan in very precise way and allows analysing the eye morphology such as epithelium, anterior and posterior segment and central region of the retina, as well as the stroma. After fcMB420-CIBF application on the photoablated cornea, the OCT exam shown the presence of a hexogen layer (Figure 3.9.d, black layer) of hyaluronic acid, even if followed several washed. The average thickness measured was of 35 µm, despite cornea treated with unfunctionalized microbeads did not show any formed HA layer (Fig. 3.9.c) after washing. In adding, CT exam simply confirmed the presence of HA layer by mean to the light scattering on treated cornea surface, as showed in Figure 3.9.e and f. The scattering was caused by the water evaporation from HA hydrogel. We deduced that this layer formation was ascribed by several cooperative effects. The thickness measured is related to crosslinking degree of microbeads, because the higher network opening allows a major exposure of the recognition signals on microbeads surface and the absence of crosslinks among the collagen fibres allows a major exposure of the collagen epitope to facilitate peptide molecular recognitions.

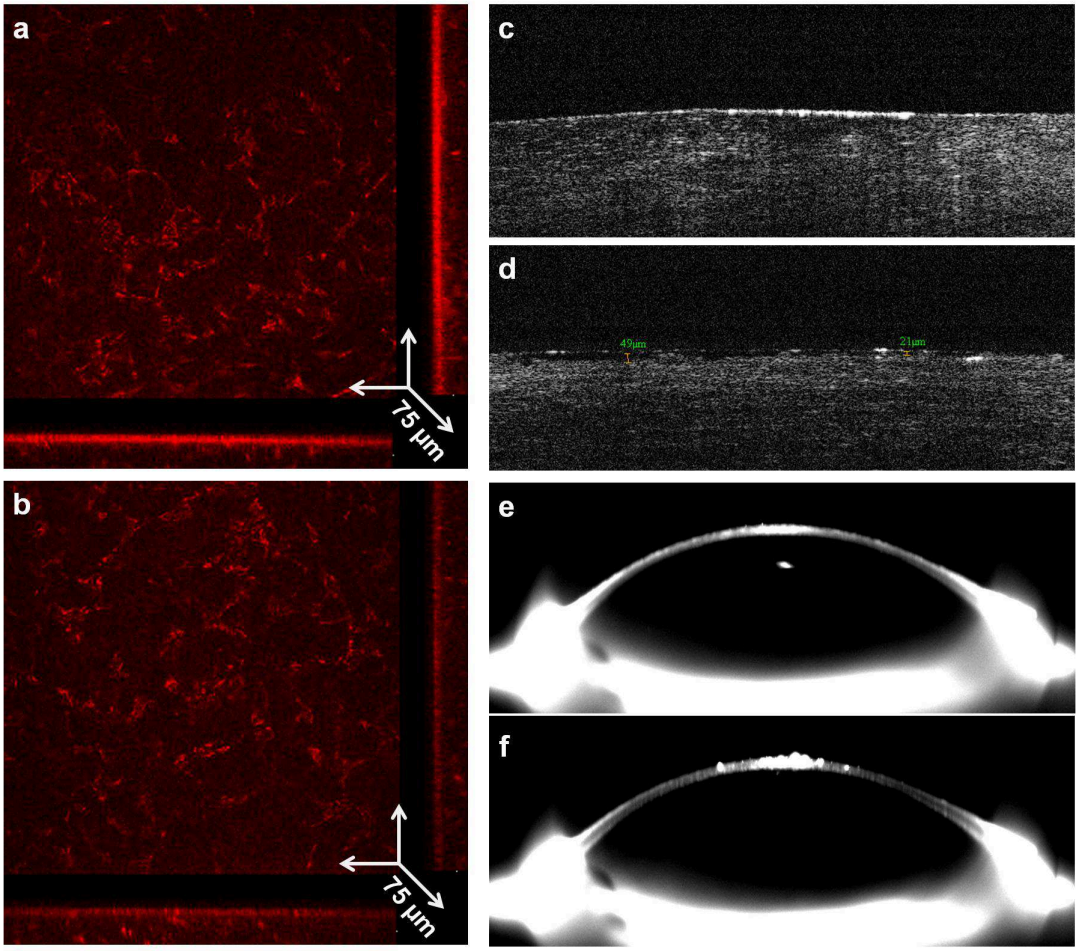

Figure 3.9. – LSCM fluorescent images: a) and b) show the photo-frame overlapping on overall z-stuck of 75 µm of human cornea treated with fcMB420-CIBF and fcMB350-CIBF: both microbeads show abilities to form a layer of about 34 and 20 µm respectively. OCT analysis of untreated c) and treated d) human cornea with fcMB420-CIBF: in according to fluorescence analysis, OCT images show the formation of the layer with a thickness of about 34 µm. CT analysis for untreated e) and treated human f) cornea show the light scattering relative to a slow water evaporation from formed HA layer.

3.4.7. Proposed Mechanism of the HA layering mediated by non-covalent adhesion of fcMB420-CIBF

Experimental studies to evaluate the covering mechanism, with which fcMB420-CIBF can adhere on human derma, were carried out by an optic system made at home. This optic microscope, as in Figure 3.12., was equipped with a white light source, light filter Techspec, objective Newport M-20X 0.40 and camera uEye. The experiments were carried out arranged one derma histological slice on the border of a glass slide and this one was

willed in horizontal alignment with objective and camera so that taking advantages from the scattering of the light across the glass. Basically, 1 drop of 2 mg/ml fcMB420-CIBF physiological solution dispersion was instilled from the top and coincidently with glass slide border, when the sample was focused. Non-covalent adhesion phenomena and deformation mechanism of fcMB420-CIBF were observed and recoded (Figure 3.10. and 3.13.). We observed that when fcMB420-CIBF dispersion was dropped along glass slide border the microbeads immediately stitched to collagen fibres and before a few minutes appeared not only adhered on collagen (Figure 3.10.b) but also they arranged as agree with fluorescence image in Figure 3.7.e. Extraordinarily we were able to film an isolate microbead on collagen (Figure 3.10.a) and observed the deformation was agreed with our assumptions. This observation probably suggested that the contribution of adhesive force was much higher than the cohesive one, providing an additional stretching effect on the microbeads (Figure 3.11.). This result was most important because helped us to understand that the amount of cooperative interaction forces established between peptide and collagen were able to firmly hold the microbeads. Those interactions were also responsible of the film formation on the human cornea collagen and in particular we demonstrated that the film formation was closely related to crosslinking degree and the stretching effect was due to the binding interactions involved to give adhesion between microbeads and collagen surface.

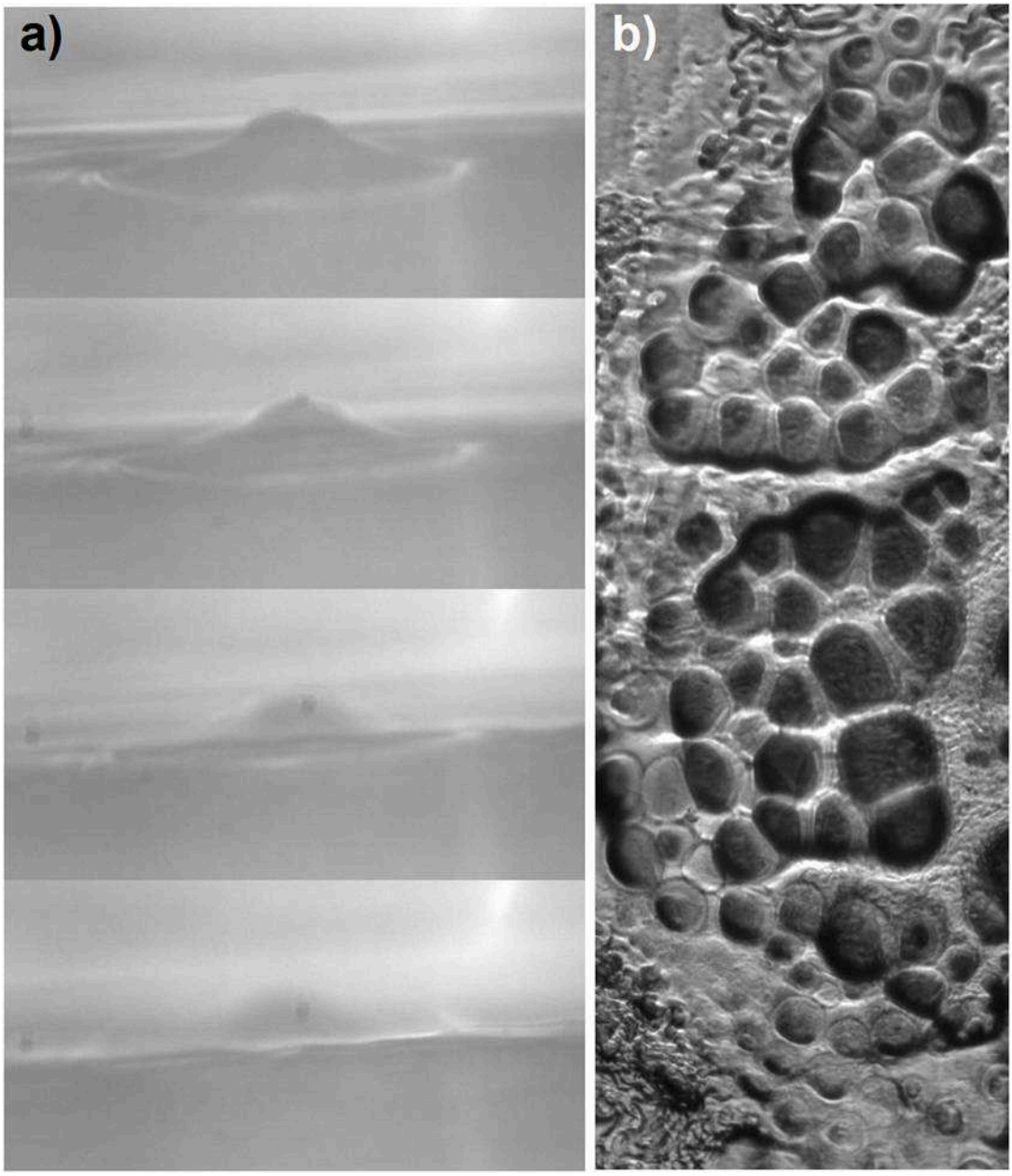

Figure 3.10. - Images acquired by optical microscope show: b) single microbead deformation (magnification 10X) with frontal observation and four different focuses; c) microbeads deformations (magnification 20X) in axial observation.

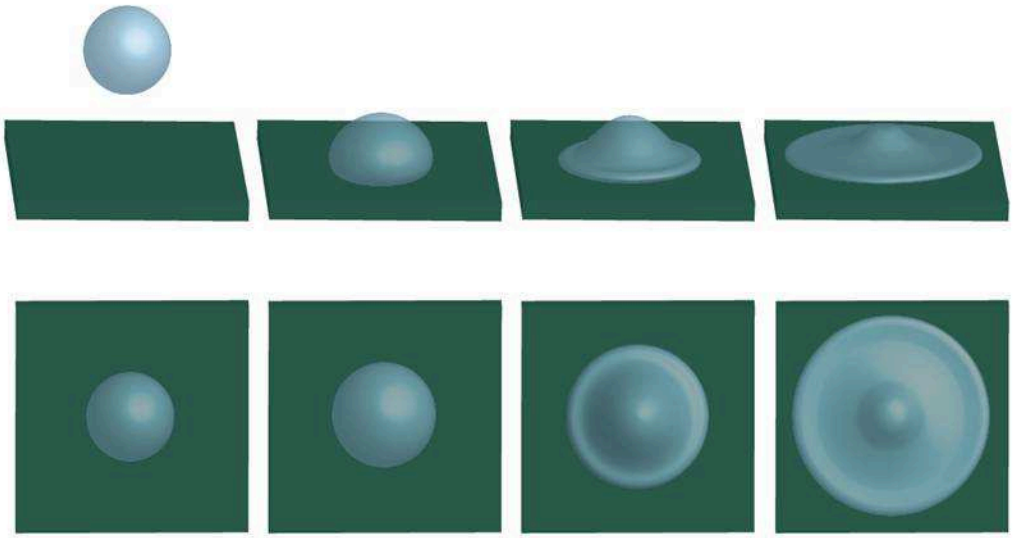

Figure 3.11. - Illustrative picture of supposed microbeads deformation mechanism: top) view of deformation along x-axis; bottom) view of deformation along z-axis.

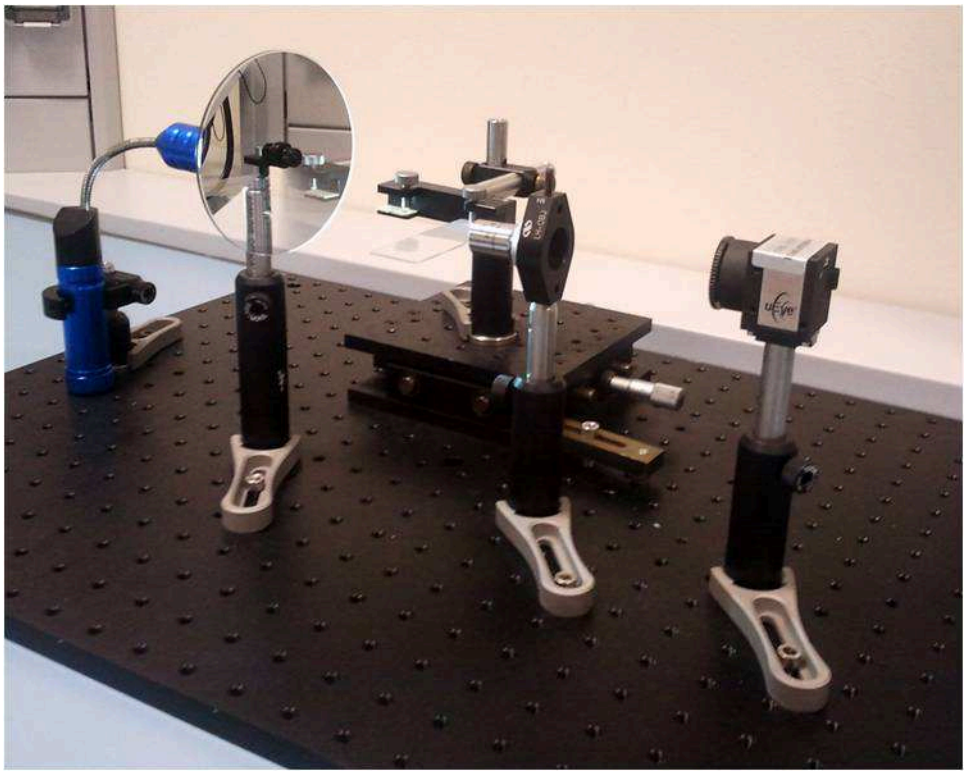

Figure 3.12. - Optic microscope picture. From the right to the left: camera, objective, simple, light filter and visible light source.

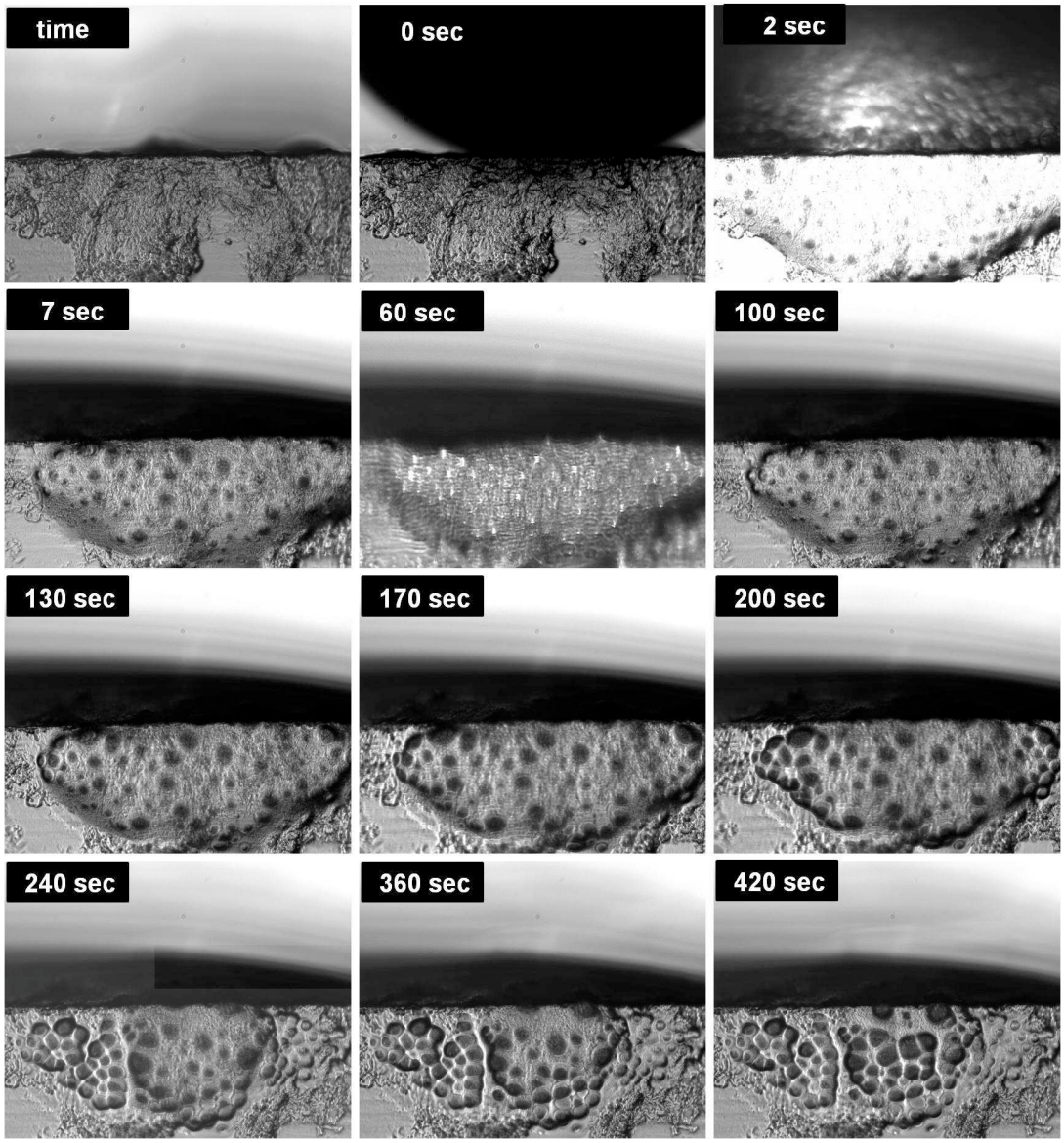

Figure 3.13. - Recognition, adhesion and HA layer formation of fcMB420-CIBF loaded on human derma. Photo-frame images were collected using a homemade optical microscope. The layer formation was completed after 420 seconds.

3.5. Conclusion

In this work are been investigate the collagen type I site-binding recognition properties of CIBF-conjugated HA microbeads hydrogel. This novel rational designed biomaterial shows unexpected abilities to recognize biological tissues containing collagen type I, until to generate HA continuous layer on

it. Obviously, this biomaterials can be also instructive in different manner, in order to extend their use in a wide range of biomedical application, simply using others biochemical signals *ad-hoc* selected to obtain novel specialized tissue recognition systems. Furthermore, is been understood that the microbeads deformation mechanism is strictly related to crosslinking degree of hydrogel network and conjugation degree on microspheres surface. Therefore, we have supposed that HA layer is been formed by simultaneous interaction among peptides and collagen surface as well as the total amount of peptide interactions inducing a further stretching contribute for the microbeads deformation. In other hand, the final layer is originated by deformable of many micro-entities capable to arrange itself until to form a continuous layer, which is firmly maintained on tissue surface by peptide interactions. So, this novel instructive biomaterial can find useful biomedical application for tissue wound dressing. In particular it finds easy applicability in ophthalmic field as temporary substitute of epithelium after surgical or accidental removal of natural one, because it is able to completely cover damaged collagen. In the end, this novel device could open a new feature for rational design of instructive biomaterials and could be used as new interesting approach to study supramolecular interaction at biomaterials interfaces.

3.6. References

1. Khang, D.; Carpenter, J.; Chun, Y. W.; Pareta, R.; Webster, T. J., Nanotechnology for regenerative medicine. *Biomedical microdevices* **2010,** *12* (4), 575-587.
2. Gurtner, G. C.; Werner, S.; Barrandon, Y.; Longaker, M. T., Wound repair and regeneration. *Nature* **2008,** *453* (7193), 314-321.
3. Stappenbeck, T. S.; Miyoshi, H., The role of stromal stem cells in tissue regeneration and wound repair. *Science* **2009,** *324* (5935), 1666-1669.

4. Oelker, A. M.; Grinstaff, M. W., Ophthalmic adhesives: a materials chemistry perspective. *Journal of Materials Chemistry* **2008,** *18* (22), 2521-2536.
5. Dawson, D. G.; Grossniklaus, H. E.; McCarey, B. E.; Edelhauser, H. F., Biomechanical and wound healing characteristics of corneas after excimer laser keratorefractive surgery: is there a difference between advanced surface ablation and sub-Bowman's keratomileusis? *Journal of refractive surgery (Thorofare, NJ: 1995)* **2008,** *24* (1), S90.
6. Shanyfelt, L. M. ArF Excimer Laser Corneal Ablation: Effects of Laser Repetition Rate and Fundamental Laser-tissue Coupling. University of Florida, 2008.
7. Reynolds, A.; Moore, J. E.; Naroo, S. A.; Moore, C.; Shah, S., Excimer laser surface ablation–a review. *Clinical & experimental ophthalmology* **2010,** *38* (2), 168-182.
8. Mann, A.; Tighe, B., Wound healing studies and interfacial phenomena: use and relevance of the corneal model. Woodhead Publishing, Oxford, UK: 2011; pp 284-320.
9. Evans, M. D. M.; Prakasam, R. K.; Vaddavalli, P. K.; Hughes, T. C.; Knower, W.; Wilkie, J. S.; McLean, K. M.; Johnson, G.; McFarland, G. A.; Xie, R. Z.; Sweeney, D. F., A perfluoropolyether corneal inlay for the correction of refractive error. *Biomaterials* **2011,** *32* (12), 3158-3165.
10. Thissen, H.; Gengenbach, T.; du Toit, R.; Sweeney, D. F.; Kingshott, P.; Griesser, H. J.; Meagher, L., Clinical observations of biofouling on PEO coated silicone hydrogel contact lenses. *Biomaterials* **2010,** *31* (21), 5510-5519.
11. Grinstaff, M. W., Designing hydrogel adhesives for corneal wound repair. *Biomaterials* **2007,** *28* (35), 5205-5214.
12. Bhatia, S. S., Ocular surface sealants and adhesives. *The Ocular Surface* **2006,** *4* (3), 146-154.
13. Furth, M. E.; Atala, A.; Van Dyke, M. E., Smart biomaterials design for tissue engineering and regenerative medicine. *Biomaterials* **2007,** *28* (34), 5068-5073.
14. Peppas, N.; Huang, Y.; Torres-Lugo, M.; Ward, J.; Zhang, J., Physicochemical foundations and structural design of hydrogels in medicine and biology. *Annual Review of Biomedical Engineering* **2000,** *2* (1), 9-29.
15. Stuart, M. A. C.; Huck, W. T.; Genzer, J.; Müller, M.; Ober, C.; Stamm, M.; Sukhorukov, G. B.; Szleifer, I.; Tsukruk, V. V.; Urban, M., Emerging applications of stimuli-responsive polymer materials. *Nature materials* **2010,** *9* (2), 101-113.
16. Margalit, E.; Fujii, G. Y.; Lai, J. C.; Gupta, P.; Chen, S. J.; Shyu, J. S.; Piyathaisere, D. V.; Weiland, J. D.; De Juan, E., Jr.; Humayun, M. S., Bioadhesives for intraocular use. *Retina* **2000,** *20* (5), 469-77.

17. Kalayci, D.; Fukuchi, T.; Edelman, P. G.; Sawhney, A. S.; Mehta, M. C.; Hirose, T., Hydrogel tissue adhesive for sealing corneal incisions. *Ophthalmic Res* **2003,** *35* (3), 173-6.
18. Sueda, J.; Fukuchi, T.; Usumoto, N.; Okuno, T.; Arai, M.; Hirose, T., Intraocular use of hydrogel tissue adhesive in rabbit eyes. *Jpn J Ophthalmol* **2007,** *51* (2), 89-95.
19. Oelker, A. M.; Berlin, J. A.; Wathier, M.; Grinstaff, M. W., Synthesis and characterization of dendron cross-linked PEG hydrogels as corneal adhesives. *Biomacromolecules* **2011,** *12* (5), 1658-1665.
20. Brubaker, C. E.; Kissler, H.; Wang, L.-J.; Kaufman, D. B.; Messersmith, P. B., Biological performance of mussel-inspired adhesive in extrahepatic islet transplantation. *Biomaterials* **2010,** *31* (3), 420-427.
21. Ryu, J. H.; Lee, Y.; Kong, W. H.; Kim, T. G.; Park, T. G.; Lee, H., Catechol-functionalized chitosan/pluronic hydrogels for tissue adhesives and hemostatic materials. *Biomacromolecules* **2011,** *12* (7), 2653-2659.
22. Lee, H.; Lee, B. P.; Messersmith, P. B., A reversible wet/dry adhesive inspired by mussels and geckos. *Nature* **2007,** *448* (7151), 338-341.
23. Burdick, J. A.; Prestwich, G. D., Hyaluronic acid hydrogels for biomedical applications. *Advanced Materials* **2011,** *23* (12), H41-H56.
24. Van Vlierberghe, S.; Dubruel, P.; Schacht, E., Biopolymer-based hydrogels as scaffolds for tissue engineering applications: a review. *Biomacromolecules* **2011,** *12* (5), 1387-1408.
25. Schanté, C. E.; Zuber, G.; Herlin, C.; Vandamme, T. F., Chemical modifications of hyaluronic acid for the synthesis of derivatives for a broad range of biomedical applications. *Carbohydrate Polymers* **2011,** *85* (3), 469-489.
26. Miki, D.; Dastgheib, K.; Kim, T.; Pfister-Serres, A.; Smeds, K. A.; Inoue, M.; Hatchell, D. L.; Grinstaff, M. W., A photopolymerized sealant for corneal lacerations. *Cornea* **2002,** *21* (4), 393-9.
27. Wang, M.; Mattson, M. S.; Tirrell, D. A.; Kornfield, J. A., Tissue Adhesive Using Engineered Proteins. Google Patents: 2010.
28. Mehdizadeh, M.; Weng, H.; Gyawali, D.; Tang, L.; Yang, J., Injectable citrate-based mussel-inspired tissue bioadhesives with high wet strength for sutureless wound closure. *Biomaterials* **2012,** *33* (32), 7972-7983.
29. Hubbell, J. A., Materials as morphogenetic guides in tissue engineering. *Current opinion in biotechnology* **2003,** *14* (5), 551-558.
30. Lorand, L.; Graham, R. M., Transglutaminases: crosslinking enzymes with pleiotropic functions. *Nat Rev Mol Cell Biol* **2003,** *4* (2), 140-56.
31. Currie, L. J.; Sharpe, J. R.; Martin, R., The use of fibrin glue in skin grafts and tissue-engineered skin replacements: a review. *Plast Reconstr Surg* **2001,** *108* (6), 1713-26.

32. Horch, R. E.; Bannasch, H.; Stark, G. B., Transplantation of cultured autologous keratinocytes in fibrin sealant biomatrix to resurface chronic wounds. *Transplant Proc* **2001,** *33* (1-2), 642-4.
33. Brennan, M., Fibrin glue. *Blood reviews* **1991,** *5* (4), 240-244.
34. Huang, S.; Fu, X., Naturally derived materials-based cell and drug delivery systems in skin regeneration. *Journal of Controlled Release* **2010,** *142* (2), 149-159.
35. Anderson, N. J.; Hardten, D. R., Fibrin glue for the prevention of epithelial ingrowth after laser in situ keratomileusis. *J Cataract Refract Surg* **2003,** *29* (7), 1425-9.
36. Meek, K. M.; Boote, C., The use of X-ray scattering techniques to quantify the orientation and distribution of collagen in the corneal stroma. *Progress in retinal and eye research* **2009,** *28* (5), 369-392.
37. Xu, Y.; Gurusiddappa, S.; Rich, R. L.; Owens, R. T.; Keene, D. R.; Mayne, R.; Hook, A.; Hook, M., Multiple binding sites in collagen type I for the integrins alpha1beta1 and alpha2beta1. *J Biol Chem* **2000,** *275* (50), 38981-9.
38. Knight, C. G.; Morton, L. F.; Onley, D. J.; Peachey, A. R.; Messent, A. J.; Smethurst, P. A.; Tuckwell, D. S.; Farndale, R. W.; Barnes, M. J., Identification in collagen type I of an integrin alpha2 beta1-binding site containing an essential GER sequence. *J Biol Chem* **1998,** *273* (50), 33287-94.
39. Yamada, K. M.; Kennedy, D. W., Dualistic nature of adhesive protein function: fibronectin and its biologically active peptide fragments can autoinhibit fibronectin function. *J Cell Biol* **1984,** *99* (1 Pt 1), 29-36.
40. Boucaut, J. C.; Darribere, T.; Poole, T. J.; Aoyama, H.; Yamada, K. M.; Thiery, J. P., Biologically active synthetic peptides as probes of embryonic development: a competitive peptide inhibitor of fibronectin function inhibits gastrulation in amphibian embryos and neural crest cell migration in avian embryos. *J Cell Biol* **1984,** *99* (5), 1822-30.
41. Yamada, K. M.; Kennedy, D. W., Dualistic nature of adhesive protein function: fibronectin and its biologically active peptide fragments can autoinhibit fibronectin function. *The Journal of cell biology* **1984,** *99* (1), 29-36.
42. Imparato, G.; Urciuolo, F.; Casale, C.; Netti, P. A., The role of microscaffold properties in controlling the collagen assembly in 3D dermis equivalent using modular tissue engineering. *Biomaterials* **2013,** *34* (32), 7851-7861.
43. Malle, B. M., Crosslinked-hyaluronic acid in emulsion. Google Patents: 2008.
44. Meek, K. M.; Boote, C., The organization of collagen in the corneal stroma. *Experimental Eye Research* **2004,** *78* (3), 503-512.
45. Alkrad, J. A.; Mrestani, Y.; Stroehl, D.; Wartewig, S.; Neubert, R., Characterization of enzymatically digested hyaluronic acid using NMR,

Raman, IR, and UV–vis spectroscopies. *Journal of pharmaceutical and biomedical analysis* **2003,** *31* (3), 545-550.
46. Ekici, S.; Ilgin, P.; Butun, S.; Sahiner, N., Hyaluronic acid hydrogel particles with tunable charges as potential drug delivery devices. *Carbohydrate Polymers* **2011,** *84* (4), 1306-1313.

4. CHAPTER 2

Novel supramolecular PEI-based hydrogels for plasmid DNA controlled release*

4.1. Abstract

In recent years bioactive hydrogels of natural and synthetic branched polymers are being widely explored as media for tissue engineering and drug delivery, due to their structural similarity to the macromolecular components in the body. Polycations, such as poly(ethylenimine) (PEI), have been used as non-viral gene carriers because they form stable complexes with nucleic acids by electrostatic interactions, and their binding and release properties have been investigated. Yet there are no reports in the literature on pH-responsive PEI-based hydrogels that are able to release DNA and its derivates in a controlled manner. Here we present the preparation of a novel supramolecular hydrogel material based on the chemical modification of branched PEI with methacrylate groups. These supramolecular hydrogels swell to a large extent in water and show exceptional binding properties with plasmid DNA. PEI hydrogels are able to entrap and release biomolecules such as DNA upon variations of pH in a controlled manner, and show different morphological structures at different temperatures. The properties of the PEI hydrogel in terms of swelling and porosity can be controlled during synthesis by the amount of functional methacrylate groups. The hydrogel microstructure was characterized by several techniques including small-angle X-ray scattering (SAXS) and fluorescence microscopy to visualize the gel

---

* *The work in this chapter has been submitted for publication by A. Paciello, A. M. Cusano and M. G. Santonicola.*

---

porous network. The DNA entrapment and release kinetics were studied by UV spectroscopy at 260 nm, whereas the different hydrogel microstructures induced by temperature variations were characterized with confocal fluorescence microscopy. The novel PEI-based hydrogels represent a sophisticated potential platform where the function, activity and mobility of biomolecules can be manipulated for significant advances in bio-nanotechnology and nanomedicine.

3.2. Introduction

Supramolecular hydrogels are a fascinating class of *smart materials*[1-2] because of the various and often intriguing physical and chemical phenomena that they can display when subjected to a variety of external stimuli[3] such as change in solvent composition[4], ionic strength[5], electric fields[6], light, pH and temperature[7]. Those hydrogels have been utilised as useful tools in a wide spectrum of applications in which a hydrogel can effectively serve like controlled drug delivery, sensors, energy-transducing devices[8] and biomedical applications[9]. Opportune modifications on materials can stabilize reversible and strong unidirectional non-covalent interactions to give self-assembled structures in supramolecular hydrogels preparation[10-12]. Modified polymers may give fundamentally two types of structures for the hydrogels depending on the mechanism of their formation: "random-coil supramolecular polymers" formed without internal order, and "ordered supramolecular polymers" when the nanostructure is persistent with a high level of internal order[13]. One of the major advantages of supramolecular materials is that appropriate design allows efficient control over the assembled structure and its fuction[14] and, in some cases, a response on the molecular level can directly cause a physical or chemical change on the macroscopic level[15-16]. Supramolecular hydrogels should not only have conventional cross-linked hydrogels properties but also additional properties

such as processability, recycling and self-healing[17]. Therefore, the use of cross-linked hydrogels for molecules encapsulation and controlled release applications is limited. In contrast, supramolecular hydrogels are for the most part smart and adaptive hydrogels that respond[18] to external stimuli, therefore a tunable form of soft matter, and they can be potentially useful in a wide range of applications in medicine, nanobiotechnology and environmental sustainability[19-20].

Polyethyleneimine (PEI) is a linear or branched polymer which has been extensively used in the gene delivery field[21] because of its high buffering capacity and DNA condensation ability, and it is frequently utilized as a coating material in biosensor applications[22]. The high concentration of amine functional groups in PEI makes it an ideal polymeric ligand for complexing heavy metal ions[23], as well as zwitterionic and anionic biomolecules[24-25]. Compared with other cationic gene delivery polymers such as poly(2-dimethylaminoethyl methacrylate) (pDMAEMA), and poly-L-lysine (pLL), PEI has a high buffer capacity over a broad range of pH values[26-27], which makes it a buffering agent to weak acids and a powerful proton sponge[28]. One of the considerable characteristics of this polymer is the significantly high concentration of positively charged nitrogen atoms that can effectively bind with negatively charged groups of linear and plasmid DNA[29]. In particular, branched PEI presents in its backbone a high density of primary, secondary, and tertiary amines, of which only 15–20% are protonated at physiological pH[30] (primary amine pKa ~ 9.0, secondary amine pKa ~ 8.0, and tertiary amine pKa ~ 6–7). The protonation capacity of PEI is an essential requisite for its success as an anionic species delivery vector[16]. In particular, PEI has a much higher protonation ratio of amine groups at low pH than at high pH[31]. Today, examples of sorbents as pH-responsive supramolecular hydrogels based on branched PEI for complex formation or biomacromolecules absorption, such as linear or plasmid DNA, are not yet not reported in the literature.Some examples available in the literature consist in hydrogels

obtained by crosslinking of branched PEI with disulfide bonds formation through Michael addition between amine groups and carbon–carbon double bonds of N,N′-bis(acryloyl)cystamine[32]. In the same way, some polymer modifications reported in the literature are represented by acylation reactions of amino groups of PEI using acetic anhydride[33-34] as cationic charge modulation. DNA can be physically entrapped into the hydrogel network[35] through electrostatic interactions, and it can be subsequently eluted using basic or salt solution at fixed pH. Plasmids such as pUC19 and pUC18 are commonly used cloning vectors in *E.coli*. These molecules are a small double-stranded circle of 2686 and 2850 base pairs in length[36]. Examples of DNA adsorption capacity are shown by physical hydrogels based on chitosan and grafted with poly(*p*-chloromethylstyrene) or with poly(*N*,*N*-dimethylacrylamide). This two different modifications of chitosan hydrogels are able to entrapping 2.90 and 4.62 µg of DNA per 1 mg of dry hydrogels respectively[37]. Another example ofstrong anion-exchange hydrogel in the form of small membranes is able to immobilize 227µg/cm^2 of pUC19 plasmid DNA per 12.4 mg/ml of hydrogel[38].

We discovered that a branched PEI modified with methacrylic groups self-assembles to form a supramolecular hydrogel pH-responsive[39] and capable of entrapping and releasing plasmid DNA in a controlled manner, where the amine groups in its backbone absorb incoming hydrogen ions like a ‘‘proton-sponge”. These novel PEI-based hydrogel is capable of loading plasmid pUC18 up to 14 µg per 1 mg of dry hydrogel, equivalent to324.64 µg of plasmid DNA per 1 ml of hydrated gel, and release it almost quantitatively. Purification of nucleic acids from biological sources or post enzymatic reactions is frequently a primary step in molecular biology studies and diagnostic tests. Many techniques have been developed to isolate DNA and RNA, for example, phenol extraction, alcohol precipitation, density gradients, dialysis, ion exchange, electroelution, silica binding, membrane filtration and column filtration. The supramolecular PEI hydrogel is a

potential new material for applications in molecular biology such as alternative size exclusion and ionic exchange chromatography to isolate DNA at different molecular weight and N/P ratio. The preparation of these novel supramolecular hydrogels based on the chemical modification of branched PEI with methacrylate (MA) groups introduced utilizing metacrylic anhydride. Such covalent modifications make branched PEI-MA more hydrophobic then the unmodified polymer. In fact, the hydrogel supramolecular network is obtained from a fine balance between the hydrophobic and the hydrophilic structural contribute. The hydrogels were characterized by FTIR in ATR mode and ^{1}H-NMR. These supramolecular hydrogels swell to a large extent in water and show high swelling factor. The properties of the PEI-MA hydrogel in terms of swelling and porosity were controlled during synthesis by the amount of functional methacrylate groups and its microstructure was studied by several techniques including small-angle X-ray scattering and fluorescence microscopy to visualize the gel porous network. The buffering capacities were studied through titration and pH-responsive properties, structural changes by fluorescence microscopy. Finally, the hydrogel exceptional capacity to load plasmid DNA (pUC18) and to release it in basic solution without DNA denaturation was studied. The PEI-MA hydrogels presented in this work are a sophisticated platform where the function, activity and mobility of biomolecules can be manipulated by external stimuli for significant advances in bio-nanotechnology and nanomedicine.

4.3. Material and methods

4.3.1. Materials

Branched polyethylenimine (MW~25,000 Da, average Mn~10,000 by GPC), methacrylic anhydride 94% (d=1.035 g/cm^{3}) and ethanol absolute were

purchased from Sigma-Aldrich. Dichloromethane (DCM) stabilized with amilene extra dry, triethylamine (TEA) and ultrapure water SpS (Super purity Solvent) were purchased from Romil Pure Chemistry. Deuterium oxide (100 atom% D) was purchased from ARMAR Chemicals Switzerland. Sodium hydroxide anhydrous pellet (NaOH) was purchased from Carlo Erba. Sodium chloride crystal (NaCl) was purchased from J.T. Baker. Hydrochloric acid (HCl), standard volumetric solution 1 M and agarose low EO were purchased from Applichem. Standard solutions with pH of 4.01, 7.01 and 10.01 were purchased from Hanna Instruments. Alexa Fluor®350 carboxylic acid succinimidyl ester and pUC18-100 supercoiled plasmid modified form (2800 bp) were purchased from Invitrogen Life Technology. 1X TAE buffer and bidistilled water used to hydrate, wash and prepare the DNA solution were purchased from Applichem GmbH (Darmstadt, GERMANY). Reagents and solvents were used without further purification unless otherwise specified. Spectra/Por® Dialysis membrane MWCO:12-14,000 was purchased from Spectrum Laboratories, Inc.

4.3.2. Hydrogels synthesis and characterization

Several PEI-MA hydrogels were prepared at different molar ratio of branched PEI and methacrylic anhydride to obtain five methacrylated PEI gels with different properties. Five round-bottom flasks containing branched PEI (1 g, 4.0×10^{-5} mol) were first dried under vacuum and then 3 mL of dichloromethane was added to each flask under argon flow. After 30 min, triethylamine (10 µL, 7.2×10^{-5} mol) was added to each of the five samples, the mixtures were stirred for 5 min, so that primary and secondary amine groups were activated in basic conditions to favourite amide groups formation. In the end , methacrylic anhydride (PEI-MA2: 71.5 µL, 4.80 x 10^{-4} mol; PEI-MA3: 110 µL, 7.39 x 10^{-4} mol; PEI-MA4: 148 µL, 9.94 x 10^{-4} mol; PEI-MA5: 185 µL, 1.24 x 10^{-3} mol; PEI-MA7: 218 µL, 1.46 x 10^{-3} mol)

was added to each of the five flasks under argon flow and the reactions was allowed to proceed under stirring for 18 h at room temperature. After synthesis, the modified polymer material was dried under vacuum for 12 h to remove excess dichloromethane. Next, the hydrogels were dialyzed for one week against ultrapure water and ethanol in several cycles using Spectra/Por® Dialysis membrane to remove unreacted methacrylic anhydride and triethylamine. After purification, the PEI hydrogels were dried under vacuum at room temperature and stored at -20 °C until further use. ^{1}H NMR and ^{13}C-NMR spectra were recorded using a Varian Unity INOVA 700-MHz spectrometer. Spectra were acquired at 25 °C using D_2O as solvent. PEI and methacrylated PEI samples were first dried in vacuum for 24 h and then dissolved in D_2O and kept before spectra acquisition for 3 days. The extent of methacrylation of PEI was determined by peak integration following the procedure reported by Forrest et al.[40] Fourier transform infrared (FTIR) spectroscopy of dried methacrylated PEI was performed on a Nicolet 6700 spectrometer (Thermo Scientific) equipped with a single-reflection attenuated total reflectance accessory (Smart iTR) under ambient conditions. ATR spectra were acquired at 18 °C on dried samples. ATR correction (germanium crystal) and baseline correction were applied to the data before analysis. Spectra were collected in the range 600-4000 cm^{-1} with a resolution of 4 cm^{-1} and averaging over 128 scans.

4.3.3. Hydrogels swelling studies

For analyzing the hydrogel swelling in water, methacrylated PEI samples were dried in vacuum and dry weights (W_d) were measured in glass vials. The hydrogels samples were prepared in quintuplicate. Next, the samples were incubated in ultrapure water at ambient temperature for five days to reach the equilibrium swelling state. Excess water was removed from the vials and the swollen hydrogel sample weights (W_s) were measured. The

swelling ratio was calculated as W_s/W_d averaging the weights of five different samples.

4.3.4. Hydrogels structural studies

Experimental studies to evaluate the intra- and inter- molecular distances between supramolecular hydrogels structures were carried out by small-angle X-ray scattering (SAXS) on a NanoSTAR instrument (Bruker AXS) equipped with a 2D position sensitive detector (Vantec 2000, Bruker AXS). PEI-MA 2, 3, 4, 5 and 7 hydrogel samples were weighted (200 mg) and swollen in 15 ml of ultrapure water (biological grade) for 7 days at room temperature until swelling equilibrium was reached. The five hydrogels samples were measured at a sample to detector distance of 107.5 cm (SAXS configuration). The hydrogels were measured in Mylar cells, the measuring times were 7200 seconds and samples transmission was measured using a "Glassy Carbon" secondary standard. The scattering signal from an empty cell (kapton) was used for background correction. Scattering data were analyzed and plotted with software SAXS for Windows™ NT, Origin and Sigmaplot. The hydrogel morphology, microscopic structures and pore network dimension were investigated by confocal laser scanning microscopy using an inverted Leica TCS SP5 confocal and multiphoton microscope (Leica Microsystems) equipped with a HeNe/Argon/MP laser source for fluorescence images and differential interference contrast optics for transmission images. Dry PEI-MA 3, 4 and 5 were weighted (40 mg, 41 mg and 40.6 mg respectively) and swollen until complete equilibrium at room temperature for 48 hours. After that the water in excess was removed, the hydrogels samples were immersed in 1 ml of Alexa Fluor®350 carboxylic acid succinimidyl ester (λ_{abs} = 346 nm and λ_{fl} = 442 nm) solution (1.4 mg/ml) at room temperature overnight to favour the adsorption of the fluorescent probe. Next, the samples were washed several times to remove excess

fluorescent probe, and then transferred to fluorodishes for microscopy observation using a two-photon laser source at 700 nm and a water immersion objective Leica HCX IRAPO L 25×/0.95 W. Z-stacks of 300 µm-thick sections were collected.

4.3.5. pH dependence and buffering capacity of hydrogels

The hydrogels buffering capacity of branched PEI and its modifications (PEI-MA 3, 4 and 5) was estimated from pH titrations. pH measurements of branched PEI in basic solution to which HCl was added were performed by Mettler Toledo SevenLab pHmeter (0.01 pH unit sensitivity) with an InLab®Flex-Micro electrode. Branched PEI (100.1 mg) was dissolved in 50 ml of a 10 mM NaCl solution and the pH was adjusted to 12.40 using 2 ml of 1M NaOH. The solution was titrated with 0.1 M HCl until the pH was 1.99. The final volume of HCl solution needed to complete the titration was of 44 ml. The titration of the swollen hydrogels was estimated in a different way with respect to the titration of branched PEI. The protons variation inside the hydrogels structures were estimated by measuring the external pH of the solutions where they were immersed. Dry PEI-MA 3, 4 and 5 polymers (100.6 mg, 100.2 mg and 100.2 mg respectively) were inserted in dialysis membrane with a MW 12-14,000 Da cut-off, and immersed in 50 ml of 10 mM NaCl solution for 4 days at room temperature. The pH of external solutions of the swollen hydrogels samples, after reaching swelling equilibrium at room temperature, were adjusted with 1 M NaOH (2.55 ml, 2.60 ml and 2.55 ml respectively) until the equilibrium pH was 12.43, 12.33 and 12.46, respectively, after 48 hours. The solutions prepared were titrated with 500 µl additions of 0.1 M HCl every 24 hours until the external solutions pH was 2.04, 2.38 and 2.13, respectively. The final volume of HCl needed to complete the titration was 36.0 ml for PEI-MA3, 43.9 ml for PEI-MA4 and 34.8 ml for PEI-MA5. Titration data were plotted with Origin Lab

software. The buffering capacity for the three hydrogels was calculated as reported by Forrest et al.[40] The deprotonation kinetics of PEI-MA 3, 4 and 5 hydrogels were estimated by mean titrations and were performed by Mettler Toledo SevenLab pHmeter (0.01 pH unit sensitivity) with a InLAB®Viscous pro pH electrode. Dry PEI-MA 3, 4 and 5 hydrogels (41.7 mg, 41.2 mg and 41.8 mg respectively) were inserted in dialysis membrane with a thickness of 12 mm and a MW 12-14,000 Da cut-off, and then immersed in 4.0 ml of 10 mM NaCl solution for 4 days at room temperature. The electrode was directly inserted in the dialysis membrane and immersed into the swollen hydrogels. The initial pH value of the inner part of the hydrogels was measured as 8.99, 8.72 and 9.03, respectively. The titrations inside the hydrogels consisted in immersing the systems, composed by electrode, hydrogel material and dialysis membrane, directly into 3.47 ml, 3.43 ml and 3.47 ml respectively of a solution prepared by mixing 50 ml of 10 mM NaCl and 2.55 ml of 1 M NaOH with final pH value of 12.14 (the volume of solution useful for the titration was calculated with respect to the dry hydrogels weight). The internal pH of the hydrogels was measured every 5 min, since the first immersion, for a total time of 220 min. After 220 min the measured pH of the inner part of the hydrogels was 11.79 for PEI-MA3, 11.88 for PEI-MA4 and 11.88 for PEI-MA5, and the pH of the external solution was 12.14, 11.88 and 11.88, respectively. Titration data were plotted with Origin Lab software. The hydrogel pH-depending properties were studied to evaluate the variations of the hydrogel microstructure, in terms of interconnecting pores and channels, with pH. 1.7 mg/ml Alexa Fluor®350 solution was adjusted with 0.5 M HCl and NaOH until to obtain five solutions at different pH. Five solutions were also prepared without adding of fluorescent dye at the same pH values. The hydrogels were equilibrated at the selected pH values for 48 hours at room temperature with frequent changes of the solutions. After several rinses with the respective solutions, the hydrogels

were transferred to fluorodishes and were observed under laser scanning confocal microscopy (LSCM).

4.3.6. Plasmid DNA entrapment and releasing assay

DNA entrapment and elution experiments were performed with 6 mg of PEI-MA 3, 4 and 5 hydrogels. The DNA used for the experiment was a pUC18 modified plasmid. The DNA mixture for the entrapping experiment was prepared at 0.230 µg/µl starting concentration by dissolving 115 µg of DNA in molecular biology grade water. Each hydrogel sample was incubated in the DNA mixture at 25°C in static and the entrapping kinetic were monitored by measuring the DNA concentration in the supernatant using the absorbance at 260 nm on a Nanodrop spectrophotometer (Thermo Scientific) at different times ranging from 0 to 360 min. Gel incubated in pure water was used as a control. After the entrapping, each gel was washed five times in water. The elution experiment was performed by incubating the gel in 500 µl of 50 mM NaOH, 10 mM NaCl pH 12.5 buffer in static at 25°C. The elution kinetics were monitored by measuring the DNA concentration in the supernatant at different times ranging from 0 to 105 min. All the experiments were performed in triplicate for each hydrogel type. The integrity of the DNA during the entrapping and elution experiments was evaluated by agarose gel electrophoresis (1% agarose). 5 µl of plasmid released solution was collected from each sample at different times during the entrapment kinetics experiment and after the elution step and loaded on agarose gel. The agarose electrophoresis was performed in 1X TAE buffer by applying a voltage of 100 V for 50 minutes. The electrophoretic mobility of the DNA bands was visualised at Gel Doc XR (Biorad).

4.4. Result and Discussion

4.4.1 Synthesis of PEI supramolecular hydrogels

Supramolecular hydrogels were prepared taking advantages of the branched PEI properties and of the intrinsic capabilities to self-assemble when the starting PEI material was modified with methacrylic groups. To start from the experimental observation related to PEI-MA2 hydrogel formation, we prepared several hydrogels from branched PEI with different molar ratio between the amine groups and the methacrylic anhydride and we obtained five methacrylated PEI gels, which effectively showed new and different properties among them. The synthetic strategies for the PEI-based hydrogels were aimed to produce novel soft materials able to complex biomolecules and releasing them in a controlled manner. The synthesis of the methacrylated branched PEI is illustrated in Figure 4.1., where a generic methacrylation process is reported. The primary and secondary amine groups of PEI attacked the carbonyl carbon of the methacrylic anhydride to form an amide bond. TEA was added as a Lewis base catalyst to enhance the nucleophilicity of the amine groups. Methacrylic acid was formed as a by-product and was easily removed from the hydrogels through dialysis against ultrapure water and ethanol in several cycles for one week. After 18 hours of reaction, we observed that all samples in the round-bottom flasks were spontaneously assembled in DCM, and they appeared in volume reduced with respect to the starting material and amber in colour. After that the excess of DCM was removed under vacuum and at the end of the purification step the swollen materials appeared like glass with different consistence and completely transparent (Figure 4.1a, 4.1b and 4.1c). We assume that the introduction of hydrophobic moieties along the polymers backbone modified the amphiphilic properties of branched PEI in a balanced equilibrium of weak

interactions, which drives a spontaneous self-assembly according to solvent interactions. Thus, when the PEI-MA macromolecules are solved in DCM the gel network formed is dependent on hydrogen bonds and electrostatic charges between the hydrophilic portions, whereas when they are immersed in water the network depends on the hydrophobic portions and the hydrogen bonds with the solvent.

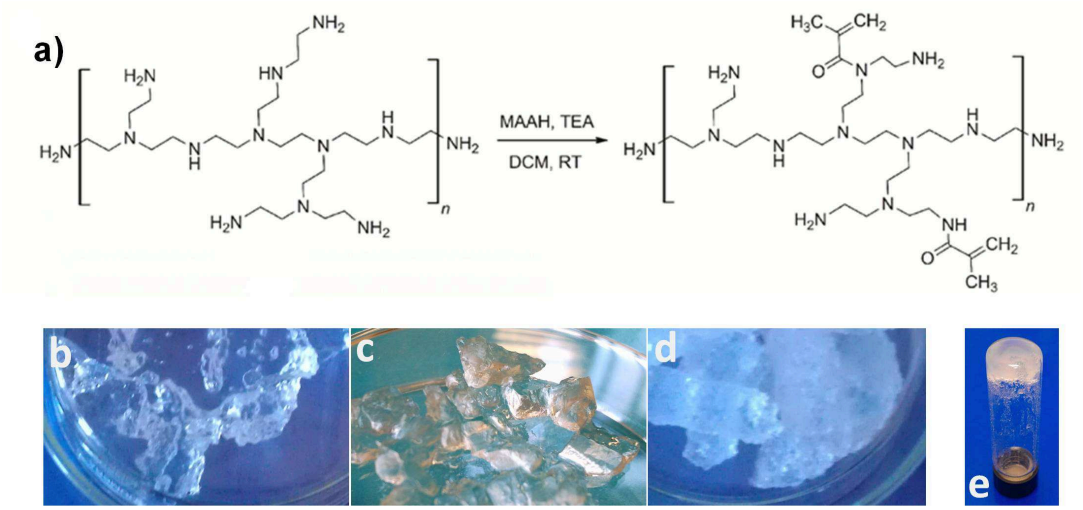

Figure 4.1. – a) General synthetic scheme of supramolecular hydrogels by methacrylation of branched PEI: **a)** indicative reaction scheme of branched PEI (M_w ~ 25 kDa) with methacrylic anhydride and triethylamine in dichloromethane; photograph of hydrogel after swelling in water **b)** PEI-MA 3; **c-e)** PEI-MA 4 and **d**) PEI-MA 5.

4.4.2 Hydrogels characterization by FTIR and NMR

The successful incorporation of the methacrylated group into branched PEI was demonstrated by ATR-FTIR and ^{1}H NMR spectroscopy, which were used to investigate and quantify the modified PEI at the level of the amine groups. In ATR-FTIR spectroscopy, the spectrum of unmodified branched PEI in the fingerprint region (Figure 4.2.) shows typical absorbance bands at 1123 cm^{-1} for C–N stretching vibrations of secondary amines, at 1298 cm^{-1} for C–N stretching vibrations of primary amines and CH bending vibrations, at 1458 cm^{-1} for N–H bending of secondary amines and CH_2 scissoring

vibrations, and at 1585 cm^{-1} for N–H bending vibrations of primary amines[41]. After reaction with methacrylic anhydride, for every one of the five dried hydrogels, the appearance of strong absorption bands in the region 1600–1700 cm^{-1} and at 1542 cm^{-1} indicated the formation of amide groups. The peak at 1652 cm^{-1} and 1615 cm^{-1} can be assigned to the C=O stretching vibration of the amide groups (amide I band), whereas the peak at 1542 cm^{-1} is related to the C–N stretching vibration (amide II band). FTIR measurements also show a decrease of the absorption bands at ~1300 cm^{-1} and at ~1100 cm^{-1} after reaction, which confirms that methacrylation, occurs at both primary and secondary amines of PEI. Next, we investigated the extent of the PEI amines methacrylation using NMR spectroscopy (Figure 4.3.). The relative ratio of the different amine functional groups in the commercial PEI starting material follows the ratio of 31% primary, 39% secondary and 30% tertiary amines, as determined from ^{13}C NMR analysis previously reported in the literature.[42] This ratio corresponds to a branching factor (% secondary / % tertiary amines) of 1.30, meaning that nearly every second nitrogen forms a branch. After chemical modification of PEI with methacrylic anhydride, we determined the extent of secondary and tertiary amide formation by ^{1}H NMR analysis using a procedure adapted from the literature,[40] in particular by analysis of δ 1.70-1.75 peaks corresponding to methacrylated secondary amines [–NH–$COC(CH_2)CH_3$] and δ 2.0-2.1 peaks corresponding to methacrylated tertiary amines [>N– $COC(CH_2)CH_3$]. From this analysis, we determined that the overall methacrylation extent of branched PEI amines amount to 19.8% for PEI-MA2, 31.1% for PEI-MA3, 23.5% for PEI-MA4, 31.0% for PEI-MA5 and 29.2% for PEI-MA7 as reported in Table 4.1. The methacrylation reactions were greatly influenced by the large number and different chemistry reactivity of the terminal functional amine groups, moreover they were also influenced by the amphiphilic property of branched PEI. The percentages of methacrylated

tertiary amines [>N–COC(CH_2)CH_3] (ex secondary amines) and secondary amines [–NH–COC(CH_2)CH_3] (ex primary amines) after methacrylation were calculated by ^{1}H-NMR analysis from the areas of the peaks related to methyl and methylene signals. As showed in the Table 4.1, it was evident that for our reaction conditions the secondary amines were more reactive then primary ones because the percentages of tertiary amines [>N–COC(CH_2)CH_3] after methacrylation for each hydrogel were higher than the percentages of secondary amines [–NH–COC(CH_2)CH_3]. Surprisingly, ^{1}H-NMR analysis highlighted some periodic properties of the PEI-MA hydrogels. As showed in Figure 4.4., the PEI-MA 3 and 5 hydrogels presented methacrylated tertiary amines percentages higher than those estimated in PEI-MA 2, 4 and 7, as well as percentages of methacrylated secondary amines in PEI-MA 3 and 5 higher than those estimated in PEI-MA 2 and 4. The percentage of methacrylated secondary amines for PEI-MA 7 was not following the trend as other hydrogels amines percentage. This anomaly can be explained referring to the reaction conditions. In fact, for the preparation of the PEI-MA7 hydrogel an excess of anhydride methacrylic was used, which probably increased the coupling reactions of the primary amines in the starting material. We concluded that at the reaction condition used the secondary amines of branched PEI resulted more reactive than those primary ones. In fact, the branched PEI is a complex amphiphilic polymer, which can give a wide number of intramolecular weak interactions, like the hydrogen bonds between primary amines, when it is solved in DCM, and the van der Waals forces between secondary amines and solvent molecules, being they more hydrophobic than primary amines. The distribution of these interactions enhanced the availability of the secondary amines for coupling reactions, probably because the spatial distributions of polymer chains contributed less to the steric hindrance. This asymmetry in the reactivity of PEI amines was a relevant feature for the self-assembly of the modified PEI-MA macromolecules into an hydrogel network, as the hydrogen bonding

interactions at the level of methacrylated secondary amines [–NH–COC(CH_2)CH_3] contributes to sustain the hydrogel structure in water.

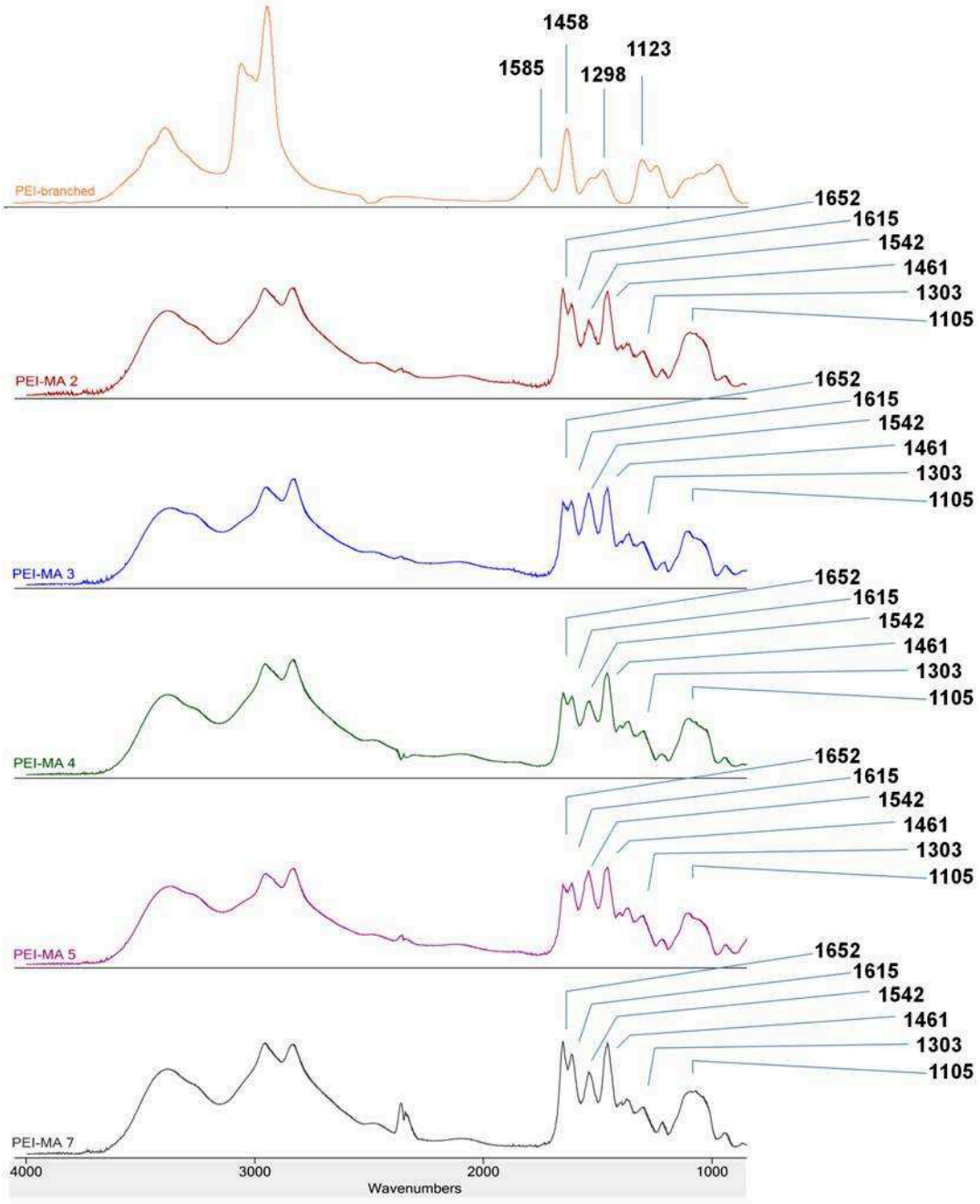

Figure 4.2. - ATR-FTIR absorbance spectra of dried branched PEI and methacrylated PEI hydrogels (PEI-MA) collected under ambient conditions.

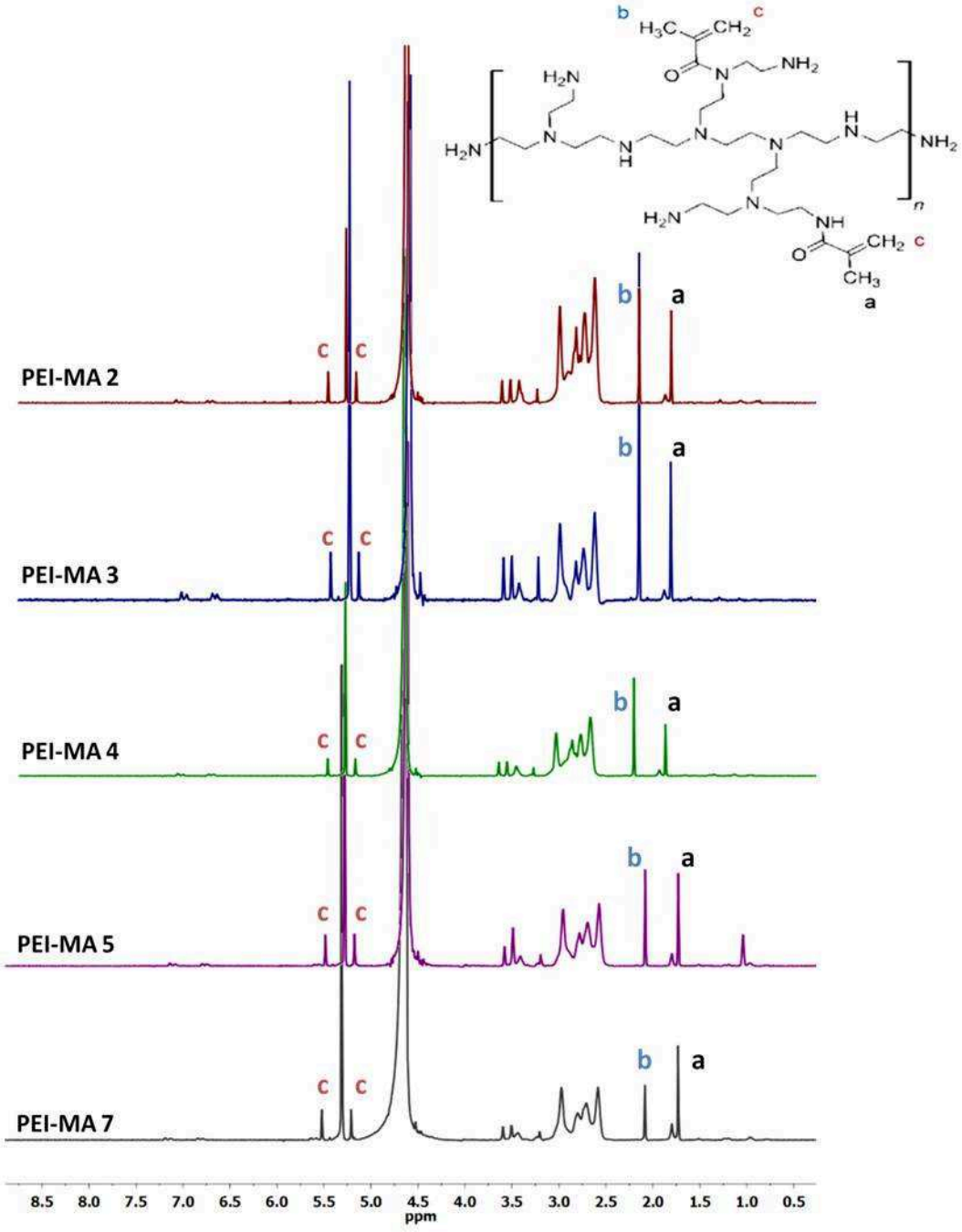

Figure 4.3. - ^{1}H NMR spectra at 700 MHz of methacrylated branched PEI hydrogels in D_2O at 25 °C. The peaks at 2.5-3.0 ppm were assigned to protons of PEI backbone, the characteristic peak at 1.70-1.75 ppm (a) to methacrylated secondary amines [−NH−COC(CH_2)CH_3] and the peak at 2.0-2.1 ppm (b) to methacrylated tertiary amines [>N− COC(CH_2)CH_3].

Table 4.1. - *Properties of the methacrylated PEI derivatives: percentages of methacrylation as determined from ^{1}H-NMR; percentages of primary and secondary amines reacted calculated with respect to amines of starting branched PEI from ^{1}H-NMR; methacrylation yields in percentage for PEI-MA hydrogels.*

	%NH - methacrylated	%N - methacrylated	% -NH_2 reacted	% >NH reacted	methacrylation yield (%)
PEI branched	-	-			
PEI-MA 2	22.5	32.9	7.0	12.8	19.8
PEI-MA 3	33.8	52.7	10.5	20.6	31.1
PEI-MA 4	26.3	39.5	8.1	15.4	23.5
PEI-MA 5	37.6	49.4	11.7	19.3	31.0
PEI-MA 7	48.8	36.2	15.1	14.1	29.2

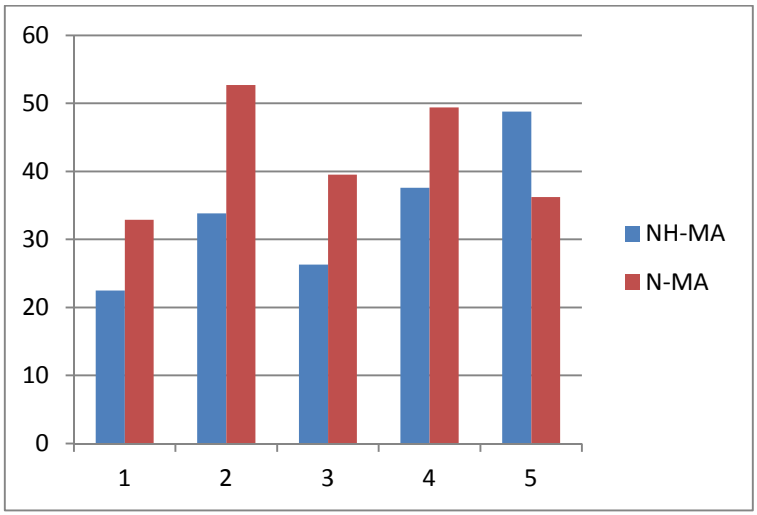

Figure 4.4. – Histogram of percentage of secondary (in blue) and tertiary (in red) methacrylated amines via H^1-NMR calculated: evidence of secondary amines of starting branched PEI more reactive of primary amines and periodic characteristics of methacrylation reactions varying only methacrylic anhydride molar ratio with respect to total amount of amines.

4.4.3. Supramolecular nature of PEI-MA hydrogels

The supramolecular nature of the PEI-MA hydrogels was verified through ^{1}H-NMR analysis from to absence of the characteristics peaks of the eventual crosslink evidences and also by conformational changes of the hydrogel network structures upon temperature variation. For PEI-MA 4 the conformational changes of the building block assemblies were evaluated

using the inverted Leica TCS SP5 laser scanning confocal microscope (LSCM). Experiments were conducted at 4 °C and 40 °C. Hydrogels stained with ATTO 647N fluorescent dye, after been completely swollen in water, were transferred to fluorodishes (World Precision Instruments, Inc.) and imaged by LSCM equipped with a HeNe excitation laser at 633 nm, detecting 650-750 nm emission band, and using a Leica HCX IRAPO L 25×/0.95 W water immersion objective. Transmitted-ligth brightfield images were simultaneously acquired as well. Z-stacks of 300 µm-thick sections were collected. In Figure 4.5. the conformational changes of the PEI-MA 4 hydrogel as dependent on temperature are shown. The network at 4 °C appears as a closed structure arranged in overlapping layers, whereas at 40 °C the structure appears open and organized to form a more complex conformation of the network. This behaviour is consistent with the temperature responsiveness of supramolecular hydrogels. The different molecular network arrangement is depending on the different molecular spatial distribution so that the interactions established are mediated by the conformational changes of the building blocks.

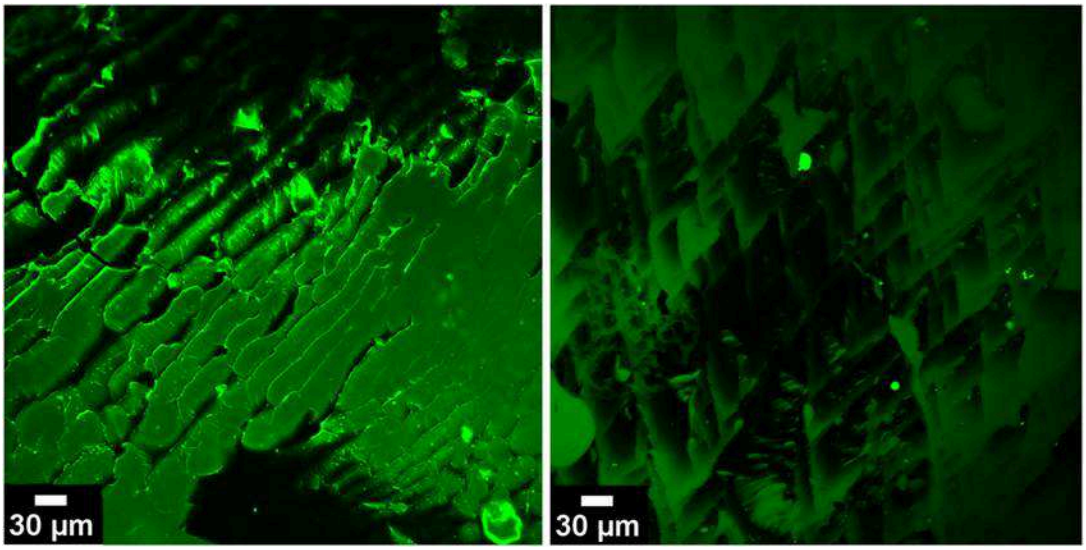

Figure 4.5. - Confocal fluorescence microscopy images of PEI-MA 4 stained with ATTO 657N imaged by a HeNe excitation laser at 633 nm, detecting 650-750 nm emission band: images show the

conformational arrangement of PEI-MA 4 hydrogel at 4 ˚C (left) and 40 ˚C (right), that are typical for supramolecular hydrogels.

4.4.4. Swelling studies of PEI-MA hydrogels

The PEI-MA hydrogels swell in water to a large extent and the networks are capable of absorbing a large volume of water, and appear clear as compared to the yellow coloured gel formed after swelling in DCM. The degree of swelling of the hydrogels was dependent on the pore size of the polymer networks and the interaction between the polymers and the solvent molecules. Hydrogels showed periodic properties also regarding the swelling properties in water. As reported in Table 4.2., the PEI-MA 4 swelling is higher with respect to other hydrogels: this behaviour finds explanation considering the different amounts of methacrylated secondary and tertiary amines assembled in the hydrogels structures. As reported in Table 4.2., the ratio between tertiary and secondary methacrylated amines in PEI-MA hydrogels confirmed the changes of the properties between different hydrogels prepared varying the molar ratio of nitrogen and methacrylic anhydride. The ratio of tertiary amines over secondary amines followed the periodic properties of the hydrogels, and this that an effective explanation regarding the composition in secondary and tertiary amines as showed in figure 4.4., because they played a fundamental role for the assembly of the methacrylated PEI polymer to give the supramolecular hydrogels. In fact, the swelling factors were also related to methacrylation yields percentage. For PEI-MA 4 with methacrylation yield of 23.5% the swelling factor was higher than other hydrogels: the fine balance between hydrophobic and hydrophilic amines after methacrylation created a structuring such to enhance the absorption of water molecules. We observed that for PEI-MA 4 the ratio between primary and secondary ammines, which became secondary and tertiary amines after methacrylation, went from about 8 to 15, before and after methacrylation reaction. In fact, PEI-MA 3 and PEI-MA 5 showed to have almost identical swelling factors and percentage of methacrylation

yields. Similarly, PEI-MA 2 and PEI-MA 7 showed similar swelling factors but different percentage of methacrylation yields. However, in every case the ratio between primary and secondary amines went from 8 to 15, before and after methacrylation reaction. We concluded that the maximum swelling ratio could be reached when it was established the ratio above reported: the composition in terms of secondary and tertiary amines played a fundamental role to sustain the structures of the swollen hydrogels in water, as to give the spatial distribution of modified PEI polymers when they assembled to form the supramolecular network. In the end, the amount of water that hydrogels were able to absorb was related to the adopted supramolecular structure and, consequently, also to the pores size of the networks formed.

Table 4.2. - *The swelling ratio was calculated by W_s/W_d averaging the weights of five different PEI-MA hydrogels obtained varying the methacrylic anhydride molar ratio; percentage ratio between tertiary and secondary methacrylated amines as indicative of the methacrylation ratio; methacrylation percentage yields for PEI-MA hydrogels.*

	Swelling ratio (W_s/W_d)	% >N-methacrylated / % -NH-methacrylated	methacrylation yield (%)
PEI-MA 2	17.3	1.5	19.8
PEI-MA 3	15.5	1.6	31.1
PEI-MA 4	20.6	1.5	23.5
PEI-MA 5	15.3	1.3	31.0
PEI-MA 7	15.5	0.8	29.2

4.4.5. Morphological analysis of PEI-MA hydrogels

Small-angle X-ray scattering (SAXS), where the scattering intensity of a molecule as a function of spatial frequency (SAXS profile) is determined, is normally used to elucidate the structures of supramolecular gels. In spite of all these investigations, several aspects of the process by which gelators aggregate to form gels are poorly understood and the process of gel formation

remains an area of intense interest. For the hydrogels in our investigation (PEI-MA 2, 3, 4, 5, and 7), the spectra in the region of the scattering vector q between 0.1 and 0.3 $Å^{-1}$ were fitted according to the relation $I(q) \sim q^{-\alpha}$, where the value of the slope α can be used as a measure of the network density of the hydrogel structure[43]. The values of the slope are reported in Figure 4.6. and were in the range from -1.5 to -1.9 for all hydrogel samples, which corresponds to mass fractal values for rigid rod to lamellae/linear swollen branched polymers. None of the hydrogels have compact structures with well-defined interfaces, with thePEI-MA 4 hydrogel (smallest slope value of -1.52) with the more loosely connected network. For all hydrogels, we observed a broad peak in the scattering profiles at $q \sim 0.7$ nm^{-1}, which according to Bragg's law corresponds to a structure with dimensions of around 9 nm. This result indicate that the hydrogel might have a well-ordered lamellar structure with a characteristic period of approximately 9 nm, in agreement with previously reported hydrogels obtained from PEI modified with octadecanoic acid[44].

Fluorescence microscopy was found to be useful for determining the microstructure and to reveal the inner morphology of the swollen hydrogels. From the observation of the fluorescent images it was possible to have an indication on the microstructures of the hydrogels and to visualize the pore connections in the hydrogels network. Confocal laser scanning microscopy images of the gel stained with Alexa Fluor®350 carboxylic acid succinimidyl ester are reported in Figure 4.7. PEI-MA 3, 4 and 5 swollen hydrogels were first treated with a water solution of Alexa Fluor®350 dye, then after several rinses they were transferred to fluorodishes and observed under microscope at room temperature. In Figure 4.7.d the PEI-MA4 3D network structure is showed, revealing the presence of many irregular interconnecting pores and relatively open hydrogel structure. In Figure 4.7.a and e the PEI-MA 3 and 5 3D network structures are reported, and, in those cases, the fluorescent imaging showed relatively absence of pores but networks of interconnected

channels with different thickness and a relatively lower opening of the hydrogels structures. These finding are supported by the swelling factors estimated for three hydrogels, and are in agreement with the SAXS analysis of the network structure. In fact PEI-MA4 showed a maximum swelling factor due to mostly open structure and presence of many pores shapes which allowed the hydrogel to trap more water. The structuring of the hydrogels as reported above depended also on the methacrylated amines compositions, and the analysis of the microstructures confirmed that the different arrangement of the modified polymers was related to the interactions established when the hydrogels self-assembled in supramolecular structures.

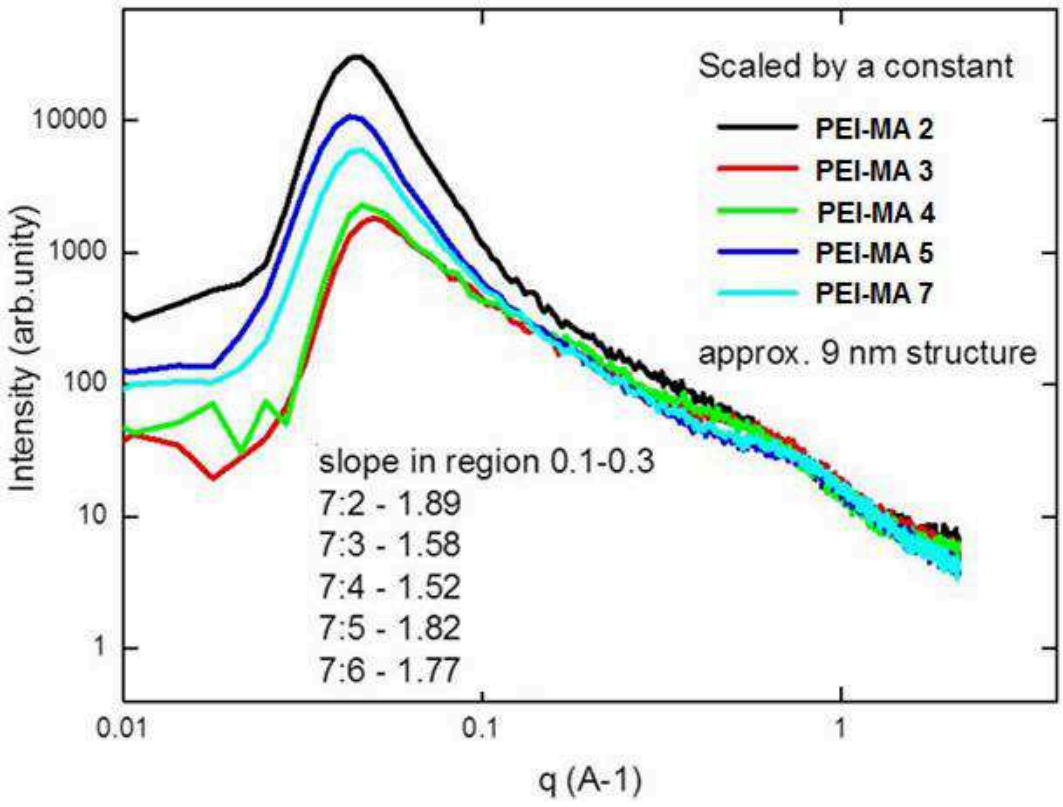

Figure 4.6.- SAXS data/analysis, spectra in the region of the scattering vector q between 0.1 and 0.3 $Å^{-1}$. PEI hydrogels show structure with dimensions of around 9 nm, assumed as lamellae organization.

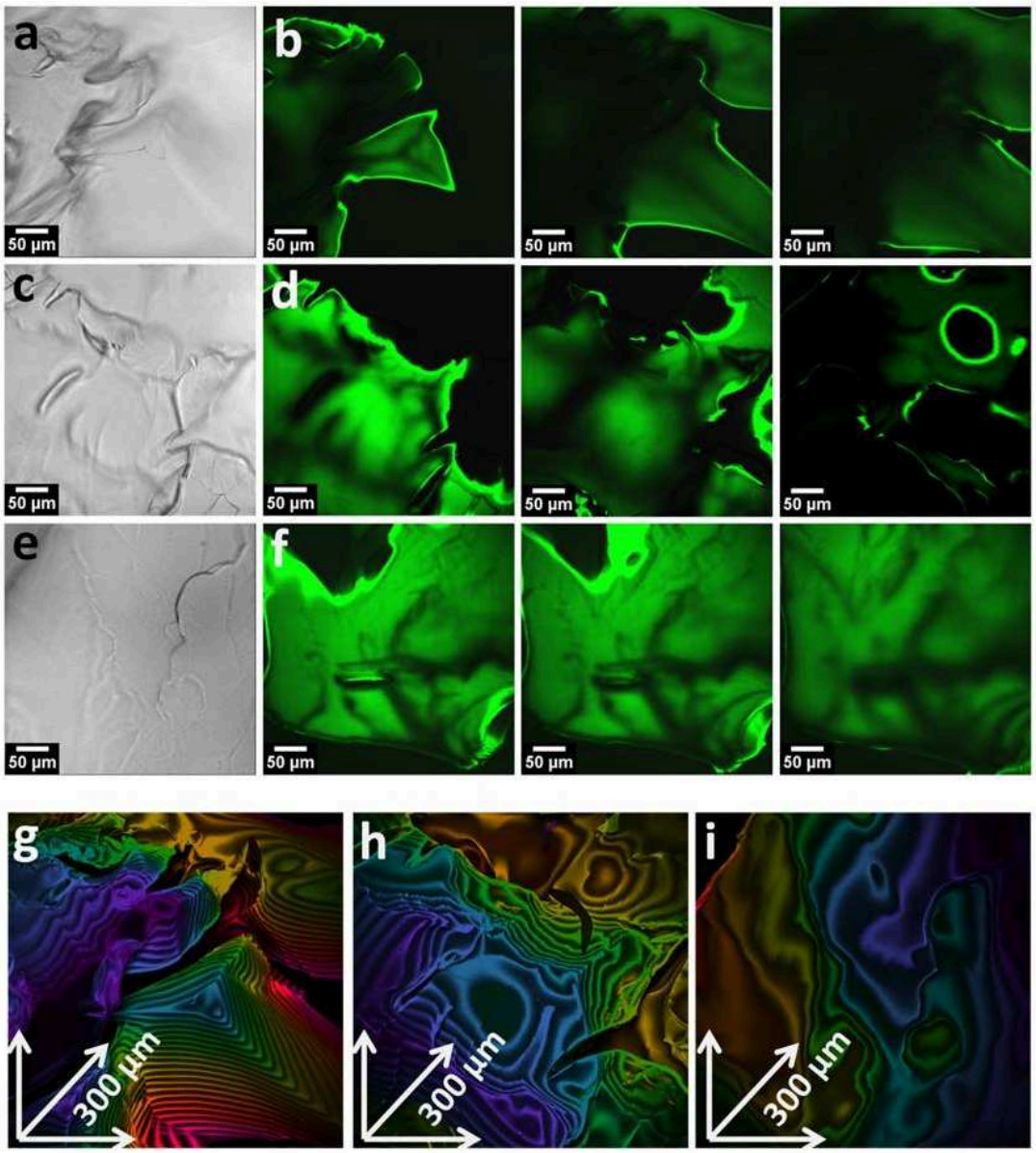

Figure 4.7. - Confocal fluorescence microscopy imaged sequences (b-d-f) show a z-stack of 10-µm-thick sections across 50 µm of PEI-MA 3, 4 and 5 respectively and white light transmission images (a-c-e) showing the porous microstructure of the supramolecular PEI-MA hydrogels labeled with Alexa Fluor® 350 dye. g-h-i) overlapping sequences shows a z-stack of 300-µm-thick sections across of hydrogels samples. All scale bars are 50 µm.

4.4.6. Buffering capacity

The responsive properties of PEI-MA hydrogels depending on pH were studied by means of acid-base titrations. Being branched PEI a polyamines it has in its backbone a large number of amine groups and the buffering

properties are influenced by the different protonation equilibriums of the amine pairs according to Lewis theory. Therefore we characterized the acid-base activities of the branched PEI used in this work by collecting HCl titration curves to estimate the pK_b constants at the different protonated amines ratio. We found in the starting PEI polymer, three distinct inflection points along the profile curve reported in Figure 4.8. (red curve). For the inflection points the pK_b values were estimated, and they were for primary amine pK_{b1} in the range 4-5, for secondary amine the pK_{b2} in the range 6-7, and for tertiary amine the pK_{b3} in the range 9-10. These values correspond to three different protonation equilibriums due to usual protonation scales of primary, secondary and tertiary amines of the unmodified PEI polymer. In particular PEI presented a much higher protonation ratio of amine groups at low pH than at high pH. As reported in Figure 4.8., the methacrylic groups conjugated to primary and secondary amines influencing strongly the protonation equilibrium of the hydrogels. In fact, the conversion of primary amines to secondary amides and secondary amines to tertiary amides shifted the average protonation constant of the PEI polymer, which became more acidic for PEI-MA 3 and 5 hydrogels (Figure 4.8., blue and green curves) and more basic for PEI-MA 4 hydrogels (Figure 4.8., black curve). The buffering capacity as showed in Table 4.3. was calculated for each sample considering the ratio between proton moles to the total amine moles (primary, secondary and tertiary). PEI branched exhibits a buffering capacity, defined as the change in protonation per amine between pH 8.6 and 5.6, of 0.257 mol H^+/mol N, while for the PEI-MA 4 hydrogels the buffering capacity resulted enhanced to 0.650 with a pronounced plateau around a pH value of 8.3, where a complete crossing of the titration profile of the PEI branched was noted. These results are again in agreement with ^{1}H-NMR analysis and again as reported in Table 4.1., the percentage of secondary and tertiary amides formed in PEI-MA 3, and 5 hydrogels presented similar values of methacrylation on starting primary and secondary amines of PEI. In PEI-MA

4 hydrogels we noted that the new modified conditions shifted the final protonation equilibrium to highest value of buffering capacity. We concluded that the variation of the ratio between free amines and methacrylated amines of the hydrogels altered the protonation properties of unmodified branched PEI because the proton balances between pairs of amines were altered. In addition, the hydrophobic interactions between methacrylated groups might modify the normal proton exchanges due to steric hindrance when the hydrogels completely reached the swelling equilibrium and minimized their free energy.

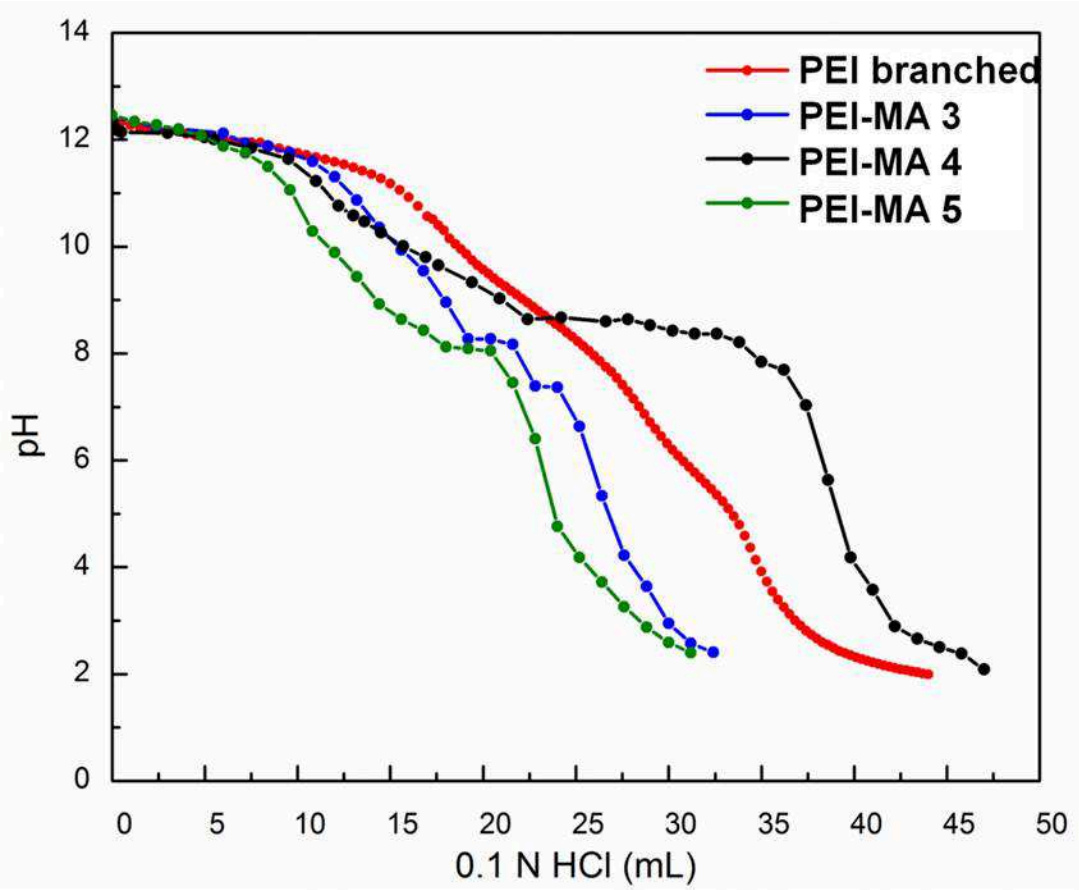

Figure 4.8. – Titration curves by 0.1 N HCl for the branched PEI (red line), PEI-MA 3 (blue line), PEI-MA 4 (black line) and PEI-MA 5 (green line).

Table 4.3. - *Physiological buffering capacity defined as the change in protonation per amine between pH 8.6 and 5.6 and expressed in mol H^+/mol N. V HCl is the volume of 0.1 N HCl added to equilibrate the hydrogels at pH 8.6 and 5.6.*

	V HCl (L) at pH=8.6	V HCl (L) at pH=5.6	Buffering capacity
PEI branched	**0.0236**	**0.0317**	**0.257**
PEI-MA 3	**0.0185**	**0.0264**	**0.163**
PEI-MA 4	**0.0224**	**0.0386**	**0.650**
PEI-MA 5	**0.0156**	**0.0215**	**0.145**

4.4.7. Morphological analysis at different pH values of PEI-MA 4

Due to the nature of the PEI-MA hydrogels, we supposed that the pH variations influenced the assemblies of modified macromolecules to give microstructural changes. In particular, we studied the pH depending properties of the PEI-MA 4 hydrogel. Confocal laser scanning microscopy images of the gel stained with Alexa Fluor®350 carboxylic acid succinimidyl ester are reported in Figure 4.9., and show the structural changes of the interconnecting pores and channels systems when the pH of the external solution, in which the hydrogels previously swollen in water were immersed, was varied. We observed that from pH=2 to pH>12, the gel structure becomes much more dense and the large pores (Figure 4.9a) changed to channels until to reach a compact structure (Figure 4.9e). The results showed that the effect of altering the hydrogen bonds network by pH changes determined a different arrangement of the empty spaces inside the hydrogels. This behaviour highlighted the pH-responsive character of the supramolecular PEI-MA hydrogel.

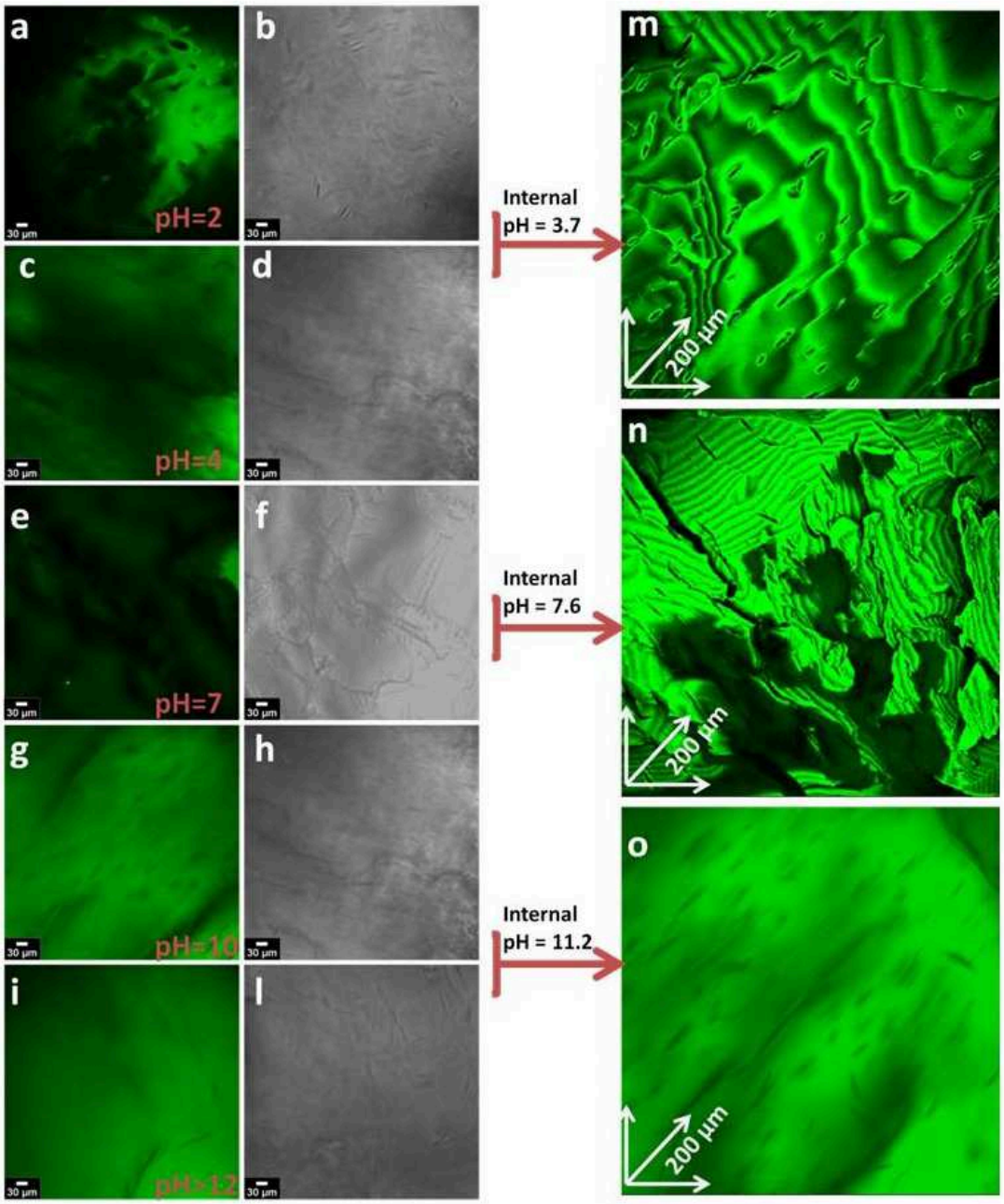

Figure 4.9. - Confocal fluorescence microscopy imaged sequences (left) and white light transmission images (bottom) showing the porous microstructure of the supramolecular PEI-MA 4 hydrogel labeled with ATTO 647 N dye; different pores size and distribution at varying pH values were observed: from open structure in image a) to close structure in image i) with increasing pH value. All scale bars are 30 µm. Fluorescence images (m-n-o) showing overlapping sequences with a z-stack of 10-µm-thick sections across 300 µm. All scale bars are 50 µm.

3.4.8. Entrapping and release kinetics of plasmid DNA

PEI polymers, being polycations, have been widely used as non-viral gene carriers because they form stable complexes with nucleic acids by electrostatic interactions, and their binding and release properties have been studied. We evaluated the entrapping and releasing kinetics of plasmid pUC18 for PEI 3, 4 and 5 hydrogels, and as reported in Figure 4.10, they showed exceptional binding properties with respect to plasmid DNA. As for the polyplex formation, reported in literature, electrostatic interactions were responsible for DNA complexation, and so in PEI-based hydrogels as well the plasmid adsorption into the hydrogel network was driven by those type of interactions. Being the hydrogels formed by solid networks, the adsorption also depended on the size of the supercoiled plasmid and on the shapes of pores and channels formed during the assembly of the methacrylated PEI polymers. The entrapping kinetic data, reported in Table 4.4., were in agreement with the microstructural characterization of the gels network. Where the hydrogel network showed a more openstructure, as for PEI-MA 4, the plasmid was adsorbed with higher capacity and more rapidly than in PEI-MA 3 and 5 hydrogels, which showed a more closed network structure. On the other hand, the releasing kinetics did not show a similar behaviour because the DNA was released in the same manner for all hydrogels. Since the elution of plasmid was induced by a basic solution at pH=12.57, we supposed that plasmid release was influenced more by microstructural changes due to a network closure at high pH values, which altered the protonation equilibrium of the amines pairs. Regarding the amount of entrapped DNA, we believe that the driving forces played a fundamental role. As a consequence, the number of the electrostatic interactions between PEI and DNA were depending on the methacrylated amines ratio and on the effective positive charge number of the three different hydrogel networks. Regarding the DNA release, instead, we think that the protons variations induced the break of gel-DNA complexes and the pH-mediated

microstructural changes enhanced the diffusion process allowing release of the plasmid. In addition, we verified the integrity of the DNA plasmids during the entrapping procedure and upon the elution steps. The plasmid integrity was evaluated electrophoretically on 1% agarose gel. As reported in Figure 4.11., the DNA amount in the supernatant decreases during the entrapping step for PEI-MA 4 hydrogels (lane 3, 4, 5, 6). The PEI-MA 5 gel shows a slower entrapping since any visible difference in DNA is visible in its supernatant (lane 7, 8, 9, 10). Moreover the DNA integrity is preserved during the entrapment as well as upon the elution step (lane 12, 13).

Table 4.4. - *Plasmid DNA (µg/mg) entrapped and released from PEI-MA 3 (blue line), PEI-MA 4 (red line) and PEI-MA 5 (green line) hydrogels; percentages of plasmid DNA entrapped and released.*

	pUC18 entrapped (µg/mg)	pUC18 entrapped (%)	pUC18 released (µg/mg)	pUC18 released (%)
PEI-MA 3	13.3	69.2	10.7	80.9
PEI-MA 4	15.8	82.3	10.9	82.4
PEI-MA 5	14.6	76.0	10.4	78.5

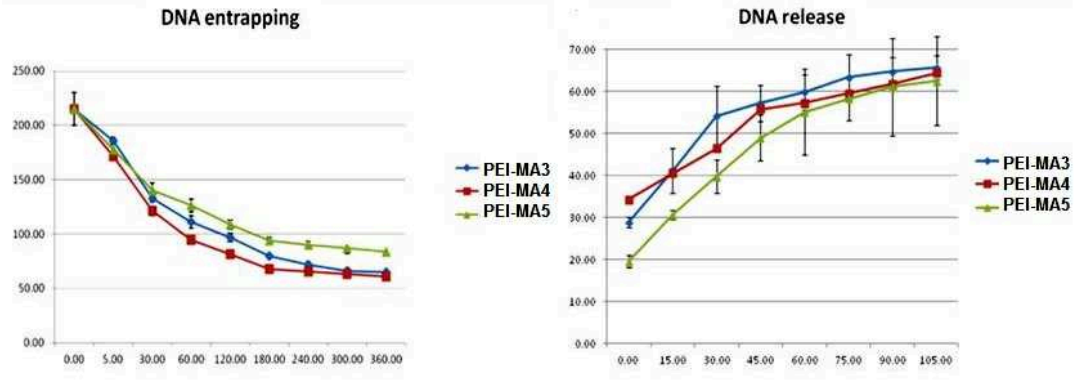

Figure 4.10.– plasmid DNA entrapping and release kinetics using elution buffer obtained from 10 mM NaCl in 50mM NaOH with final pH of 12.57.

.

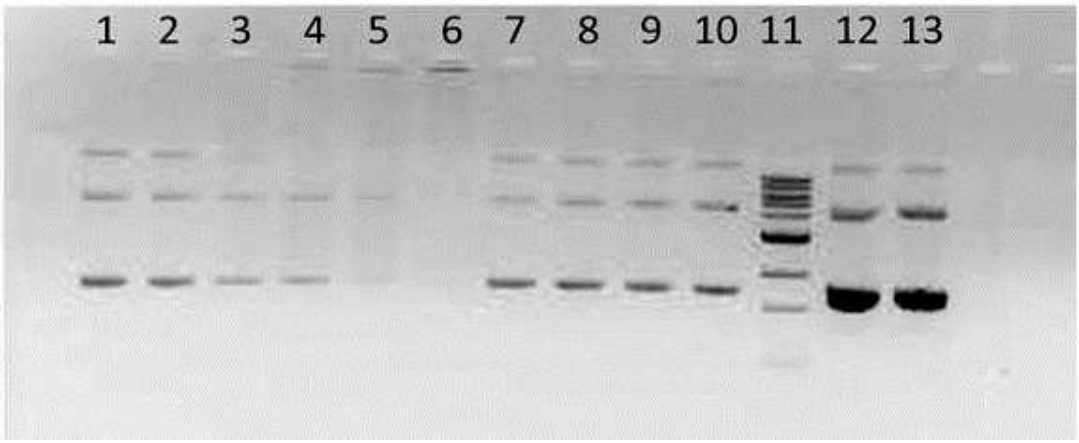

Figure 4.11. – Electrophoresis experiments on agarose gel to demonstrate that DNA integrity is preserved during entrapment as well as upon elution step. 1-2) DNA sample T_0 ; 3-4-5) PEI-MA 4 supernnatant during entrapping DNA; 6-7-8) PEI-MA 5 surnatant during entrapping DNA; 9-10) PEI-MA 3 surnatant during entrapping DNA; 11) DNA molecular weight ladder; 12) Eluted DNA from PEI-MA 4 and 13) Eluted DNA from PEI-MA 5.

4.5. Conclusions

Hydrogels based on branched PEI were synthetized, characterized and investigated for releasing plasmid DNA in a controlled manner. These hydrogels were prepared after chemical modification of primary and secondary amines of the branched PEI with methacrylate groups. The supramolecular nature of the prepared hydrogels was verified from to absence of characteristics peaks of the eventual crosslinking evidence by ^{1}H-NMR analysis and also by observing the conformational changes of the network assembly after varying temperature. We concluded that the introduction of methacrylic groups on primary and secondary amine of the starting PEI material significantly changed the anphiphilic nature of branched PEI , and with the addition of hydrophobic groups a fine balance with hydrophilic interaction was obtained, which resulted in a supramolecular architecture. PEI-MA hydrogels swelled to a large extent in water and its swelling properties can be modulated by the amount of methacrylic groups introduced in the polymer structure. Interestingly, PEI-MA hydrogels

showed periodic properties due to the different contributes in terms of chemical modifications as verified by ^{1}H-NMR analysis. Surprisingly, in our reaction conditions the methacrylation process was more predominant on secondary amines of the starting material than on primary amines. This behaviour is related to the hydrogen interactions between primary amines as the gel was prepared in DCM. PEI-MA 4 hydrogels showed the larger swelling factor and through NMR analysis it was verified that the ratio between secondary and tertiary methacrylated amines was of 8:15, differently from other hydrogels where this ratio was similar for PEI-MA 3 and 5, and not for PEI-MA 2 and PEI-MA 7 due to the use of methacrylic anhydride in excess, which increased the mathacrylation on primary amine groups of the startingPEI material. The ratio 8:15 is indicative of the consolidation of the π-stacking interaction between one secondary and two tertiary methacrylated amines after reaction. The swelling behaviour of the hydrogels was confirmed in the morphological analysis where for PEI-MA 4 a pseudo-spherical pore structure as opposed to channel formation in the other hydrogels could be assessed. In SAXS measurements the self-assembly of PEI building blocks in overlapping lamellae with a characteristics repeating distance of about 9 nm, due to the presence of π-stacking interaction, was determined. The pH-dependent properties were also estimated for PEI-MA 3, 4 and 5 hydrogels showed different values in terms of buffering capacity, Further, these hydrogels showed ability to entrap and release plasmid supercoiled DNA of 2800 pb without denaturing its structure. Entrapping kinetics for PEI-MA 4 showed a rapid DNA absorption up to 14 μg per mg of dried hydrogel, whereas in releasing kinetic it was observed that the plasmid was released not only through electrostatic interactions but also by diffusion mechanism due to plasmid size. These interesting chemical and physical properties and unusual behaviour of supramolecular PEI-based hydrogels make them a sophisticated potential platform where the function, activity and mobility of biomolecules can be manipulated for significant advances in bio-

nanotechnology and nanomedicine. In this scientific contest the use of supramolecular hydrogels results still today a great challenge and their development can be useful for a wide variety of future applications.

4.6. References

1. Seiffert, S.; Sprakel, J., Physical chemistry of supramolecular polymer networks. *Chemical Society Reviews* **2012,** *41* (2), 909-930.
2. Ionov, L., Biomimetic Hydrogel-Based Actuating Systems. *Advanced Functional Materials* **2013**, n/a-n/a.
3. Roy, D.; Cambre, J. N.; Sumerlin, B. S., Future perspectives and recent advances in stimuli-responsive materials. *Progress in Polymer Science* **2010,** *35* (1), 278-301.
4. Peng, F.; Li, G.; Liu, X.; Wu, S.; Tong, Z., Redox-Responsive Gel− Sol/Sol− Gel Transition in Poly (acrylic acid) Aqueous Solution Containing Fe (III) Ions Switched by Light. *Journal of the American Chemical Society* **2008,** *130* (48), 16166-16167.
5. von Gröning, M.; de Feijter, I.; Stuart, M. C.; Voets, I. K.; Besenius, P., Tuning the aqueous self-assembly of multistimuli-responsive polyanionic peptide nanorods. *Journal of Materials Chemistry B* **2013**.
6. Martin, J. E.; Patil, A. J.; Butler, M. F.; Mann, S., Guest-Molecule-Directed Assembly of Mesostructured Nanocomposite Polymer/Organoclay Hydrogels. *Advanced Functional Materials* **2011,** *21* (4), 674-681.
7. Zhang, J.; Liu, H.-J.; Yuan, Y.; Jiang, S.; Yao, Y.; Chen, Y., Thermo-, pH-, and Light-Responsive Supramolecular Complexes Based on a Thermoresponsive Hyperbranched Polymer. *ACS Macro Letters* **2012,** *2* (1), 67-71.
8. Stuart, M. A. C.; Huck, W. T.; Genzer, J.; Müller, M.; Ober, C.; Stamm, M.; Sukhorukov, G. B.; Szleifer, I.; Tsukruk, V. V.; Urban, M., Emerging applications of stimuli-responsive polymer materials. *Nature materials* **2010,** *9* (2), 101-113.
9. Hoffman, A. S., Hydrogels for biomedical applications. *Advanced drug delivery reviews* **2012**.
10. Appel, W. P.; Nieuwenhuizen, M. M.; Meijer, E., Multiple Hydrogen-Bonded Supramolecular Polymers. *Supramolecular Polymer Chemistry* **2012,** *1*, 3.
11. Li, F.; Zhu, Y.; You, B.; Zhao, D.; Ruan, Q.; Zeng, Y.; Ding, C., Smart Hydrogels Co-switched by Hydrogen Bonds and π–π Stacking for

Continuously Regulated Controlled-Release System. *Advanced Functional Materials* **2010,** *20* (4), 669-676.
12. Huang, F.; Scherman, O. A., Supramolecular polymers. *Chemical Society Reviews* **2012,** *41* (18), 5879-5880.
13. Aida, T.; Meijer, E.; Stupp, S., Functional supramolecular polymers. *Science* **2012,** *335* (6070), 813-817.
14. Brunsveld, L.; Folmer, B.; Meijer, E.; Sijbesma, R., Supramolecular polymers. *Chemical Reviews* **2001,** *101* (12), 4071-4098.
15. Appel, E. A.; del Barrio, J.; Loh, X. J.; Scherman, O. A., Supramolecular polymeric hydrogels. *Chemical Society Reviews* **2012,** *41* (18), 6195-6214.
16. Komatsu, H.; Matsumoto, S.; Tamaru, S.-i.; Kaneko, K.; Ikeda, M.; Hamachi, I., Supramolecular hydrogel exhibiting four basic logic gate functions to fine-tune substance release. *Journal of the American Chemical Society* **2009,** *131* (15), 5580-5585.
17. van Gemert, G. M.; Peeters, J. W.; Söntjens, S. H.; Janssen, H. M.; Bosman, A. W., Self-Healing Supramolecular Polymers In Action. *Macromolecular Chemistry and Physics* **2012,** *213* (2), 234-242.
18. Banerjee, S.; Das, R. K.; Maitra, U., Supramolecular gels 'in action'. *Journal of Materials Chemistry* **2009,** *19* (37), 6649-6687.
19. Mendes, A. C.; Baran, E. T.; Reis, R. L.; Azevedo, H. S., Self-assembly in nature: using the principles of nature to create complex nanobiomaterials. *Wiley Interdisciplinary Reviews: Nanomedicine and Nanobiotechnology* **2013**, n/a-n/a.
20. Shi, N. E.; Dong, H.; Yin, G.; Xu, Z.; Li, S. H., A Smart Supramolecular Hydrogel Exhibiting pH-Modulated Viscoelastic Properties. *Advanced Functional Materials* **2007,** *17* (11), 1837-1843.
21. Mintzer, M. A.; Simanek, E. E., Nonviral vectors for gene delivery. *Chemical Reviews* **2008,** *109* (2), 259-302.
22. Cui, X.; Yang, F.; Li, A.; Yang, X., Chip surface charge switch for studying histone–DNA interaction by surface plasmon resonance biosensor. *Analytical Biochemistry* **2005,** *342* (1), 173-175.
23. Chen, Y.; Pan, B.; Zhang, S.; Li, H.; Lv, L.; Zhang, W., Immobilization of polyethylenimine nanoclusters onto a cation exchange resin through self-crosslinking for selective Cu (II) removal. *Journal of hazardous materials* **2011,** *190* (1), 1037-1044.
24. Nguyen, D. N.; Green, J. J.; Chan, J. M.; Langer, R.; Anderson, D. G., Polymeric materials for gene delivery and DNA vaccination. *Advanced Materials* **2009,** *21* (8), 847-867.
25. Dai, Z.; Gjetting, T.; Mattebjerg, M. A.; Wu, C.; Andresen, T. L., Elucidating the interplay between DNA-condensing and free polycations in gene transfection through a mechanistic study of linear and branched PEI. *Biomaterials* **2011,** *32* (33), 8626-34.

26. Boussif, O.; Lezoualc'h, F.; Zanta, M. A.; Mergny, M. D.; Scherman, D.; Demeneix, B.; Behr, J. P., A versatile vector for gene and oligonucleotide transfer into cells in culture and in vivo: polyethylenimine. *Proceedings of the National Academy of Sciences* **1995,** *92* (16), 7297-7301.
27. Tang, M. X.; Szoka, F. C., The influence of polymer structure on the interactions of cationic polymers with DNA and morphology of the resulting complexes. *Gene Ther* **1997,** *4* (8), 823-32.
28. Godbey, W.; Wu, K. K.; Mikos, A. G., Poly (ethylenimine) and its role in gene delivery. *Journal of Controlled Release* **1999,** *60* (2), 149-160.
29. Dunlap, D. D.; Maggi, A.; Soria, M. R.; Monaco, L., Nanoscopic structure of DNA condensed for gene delivery. *Nucleic Acids Res* **1997,** *25* (15), 3095-101.
30. Boussif, O.; Zanta, M. A.; Behr, J.-P., Optimized galenics improve in vitro gene transfer with cationic molecules up to 1000-fold. *Gene Therapy* **1996,** *3* (12), 1074-1080.
31. Suh, J.; Paik, H.-J.; Hwang, B. K., Ionization of Poly (ethylenimine) and Poly (allylamine) at Various pH′ s. *Bioorganic Chemistry* **1994,** *22* (3), 318-327.
32. Han, S. C.; He, W. D.; Li, J.; Li, L. Y.; Sun, X. L.; Zhang, B. Y.; Pan, T. T., Reducible polyethylenimine hydrogels with disulfide crosslinkers prepared by michael addition chemistry as drug delivery carriers: synthesis, properties, and in vitro release. *Journal of Polymer Science Part A: Polymer Chemistry* **2009,** *47* (16), 4074-4082.
33. Ahn, C.-H.; Chae, S. Y.; Bae, Y. H.; Kim, S. W., Biodegradable poly(ethylenimine) for plasmid DNA delivery. *Journal of Controlled Release* **2002,** *80* (1–3), 273-282.
34. Nimesh, S.; Aggarwal, A.; Kumar, P.; Singh, Y.; Gupta, K.; Chandra, R., Influence of acyl chain length on transfection mediated by acylated PEI nanoparticles. *International journal of pharmaceutics* **2007,** *337* (1), 265-274.
35. Luten, J.; van Nostrum, C. F.; De Smedt, S. C.; Hennink, W. E., Biodegradable polymers as non-viral carriers for plasmid DNA delivery. *Journal of Controlled Release* **2008,** *126* (2), 97-110.
36. van Gaal, E. V.; Oosting, R. S.; Hennink, W. E.; Crommelin, D. J.; Mastrobattista, E., Junk DNA enhances pEI-based non-viral gene delivery. *International journal of pharmaceutics* **2010,** *390* (1), 76-83.
37. Başer, B.; Demirel, G. B.; Caykara, T., DNA adsorption on poly (N, N-dimethylacrylamide)-grafted chitosan hydrogels. *Journal of Applied Polymer Science* **2011,** *120* (3), 1420-1425.
38. Zhong, L.; Scharer, J.; Moo-Young, M.; Fenner, D.; Crossley, L.; Honeyman, C. H.; Suen, S.-Y.; Chou, C. P., Potential application of hydrogel-based strong anion-exchange membrane for plasmid DNA purification. *Journal of Chromatography B* **2011,** *879* (9–10), 564-572.

39. Paciello, A.; Cusano, A. M.; Santonicola, M. G., Bioactive and photoactive PEI hydrogels as platforms for biomolecule immobilization. *European Cells and Materials* **2013,** *26 (Suppl. 6)*, 52.
40. Forrest, M. L.; Meister, G.; Koerber, J.; Pack, D., Partial Acetylation of Polyethylenimine Enhances In Vitro Gene Delivery. *Pharmaceutical Research* **2004,** *21* (2), 365-371.
41. Tan, S.; Erol, M.; Attygalle, A.; Du, H.; Sukhishvili, S., Synthesis of positively charged silver nanoparticles via photoreduction of AgNO3 in branched polyethyleneimine/HEPES solutions. *Langmuir* **2007,** *23* (19), 9836-43.
42. von Harpe, A.; Petersen, H.; Li, Y.; Kissel, T., Characterization of commercially available and synthesized polyethylenimines for gene delivery. *Journal of Controlled Release* **2000,** *69* (2), 309-322.
43. Beaucage, G., Small-angle scattering from polymeric mass fractals of arbitrary mass-fractal dimension. *Journal of Applied Crystallography* **1996,** *29* (2), 134-146.
44. Zhou, S.; Zhao, Y.; Cai, Y.; Wang, D.; Xu, D., Lamellar architecture and crystalline transformation in supramolecular complexes of highly-branched polyethyleneimine-octadecanoic acid. *Chemical Communications* **2003,** (15), 1932-1933.

5. CHAPTER 3

A supramolecular two-photon-active hydrogel from polyethyleneimine for photo-conjugation at near-infrared wavelengths*

5.1. Abstract

The precise distribution of extracellular bioactive signals is crucial for cellular responses in a myriad of processes that include adhesion, differentiation and ultimately tissue organization. The patterning of chemical and biochemical signals within hydrogels allow to adding complexity towards their use as cell microenvironments for biomedical applications. Therefore, cell-instructive materials and cell recognition are mains aspect to consider for exploit cellular guidance behaviour. Here, we present a three-dimensional photopatterning system that utilizes photo-conjugation at near-infrared wavelengths and permits extensive modifications of supramolecular PEI-based hydrogels. This method combined with chemically activated hydrogel network promoted biomolecular immobilization using an easy conjugation procedure and without the addition of chemical activators. We demonstrated three-dimensional photopatterning abilities of the hydrogel by means of multi-photon microscopy experiments. At the same time, we established that the hydrogel platform showed 3D patterning capabilities in presence of molecular probes with free carboxylic acid and their derivates, or hydroxyl groups. In particular, we also demonstrated that RGD peptide could be photo-conjugated at micro spatial resolution and the chemical selectivity of the method allows to immobilize multiple signals, due to the number of

---

The work in this chapter has been submitted for publication by A. Paciello and M. G. Santonicola.

---

affinity reactive handles accessible for secondary reaction on the hydrogel. In addition, the method permits to exploit photobleaching of fluorescent probes to generate patterns and concentration gradients with submicron spatial resolution. In the end, in combination with bioactive molecules, these hydrogels represent a novel cell-instructive platform that can be selectively encoded with active signals, with relevant applications in biotechnology and medicine.

5.2. Introduction

The ability of patterning hydrogel materials on the nano- and microscale has become a key strategy in the fabrication of advanced biomaterials presenting controlled and predetermined spatial patterns of biological cues, most notably for guiding cell growth and differentiation.[1-3] In particular, laser irradiation has emerged has an easy and direct approach to selectively functionalize soft transparent materials with sub-micron resolution,[4] thus offering the possibility for the precise immobilization of bioactive signals into three-dimensional scaffolds. Despite the highly relevant applications, today most of the available photopatterning strategies rely on materials that are cross-linked under light irradiation after addition of a photoinitiator.[5] One of the major limitations of this process is that photoactive initiators mostly respond to UV radiation, which is limited by its cytotoxicity and very low tissue penetration power. Supramolecular polymeric hydrogels are three-dimensional networks of macromolecules held together through a delicate balance of non-covalent interactions such as hydrogen bonding, hydrophobic effects, and electrostatic forces.[6] In aqueous solutions, where these interactions can be strong, supramolecular polymers self-assemble into robust, yet adaptive structures with exceptional water-entrapping properties,[7] thus generating highly biocompatible materials.[8-9] Due to their adaptive properties and to the versatility of bioconjugation strategies for macromolecules,[10-12]

supramolecular hydrogels formed by natural and synthetic polymers are extensively investigated by the biomedical research community in the bottom-up fabrication of biomaterials for tissue engineering and drug delivery.[13] In this work, we report a simple and effective method to generate a supramolecular photo-responsive hydrogel on which micropatterns of biomolecules can be written using near-infrared (NIR) light. To our knowledge, our approach represents the first supramolecular hydrogel based on chemically modified polyethyleneimine that can be permanently patterned with bioactive molecules in the near-infrared region. We show that this method allows for an easy and precise modulation of the hydrogel surface properties on the micrometer scale by direct laser patterning in multiphoton microscopy without the need of additional photoinitiator molecules active under UV irradiation, which are often toxic in biological systems. The novel hydrogel that we present has the potential to overcome the limitations posed by currently available photopatternable hydrogels in biomedical applications, most notably tissue engineering, opening the way for *in vivo* micropatterning applications of these materials.

4.3. Materials and methods

5.3.1. Chemicals and general materials

Branched polyethylenimine (MW~25,000 Da average, Mn~10,000 by GPC), methacrylic anhydride (94%,d=1.035 g/cm^3), ethanol absolute, 6 aminofluorescein, methacryloxyethyl thiocarbonate rhodaamine B, RGD, biotin free carboxylic group, and biotin free amine group were purchased from Sigma-Aldrich. ATTO 647N free carboxylic group, ATTO 647N free amine group and streptavidin labelled with ATTO 647N were purchased from ATTO-TEC GmbH. Alexa Fluor®350 carboxylic acid succinimidyl

ester was purchased from Invitrogen Life Technology. Dichloromethane (DCM) stabilized with extra dry amilene, triethylamine (TEA) and ultrapure water (Super purity Solvent,SpS) were purchased from Romil Pure Chemistry. Deuterium oxide (100 atom% D) was purchased from ARMAR Chemicals Switzerland. Reagents and solvents were used without further purification unless otherwise specified. Spectra/Por® Dialysis membrane with cut-off MWCO:12-14,000 Da was purchased from Spectrum Laboratories, Inc.

5.3.2. Hydrogel synthesis

PEI-MA hydrogels were prepared by reaction of 25-KDa branched PEI with methacrylic anhydride and triethylamine in dichloromethane. Branched PEI (1 g, 4.0×10^{-5} mol) was first dried under vacuum and then dissolved in 3 mL of dichloromethane under argon flow. After 30 min, methacrylic anhydride (148 µL, 9.9×10^{-4} mol) and triethylamine (10 µL, 7.2×10^{-5} mol) were added, and the mixture was kept stirring for 18 h at room temperature under argon. After synthesis, the hydrogel material was first dried under vacuum for 12 h to remove excess dichloromethane. Next, the gel was dialyzed for one week against ultrapure water and ethanol in several cycles using Spectra/Por 2 dialysis membranes (12,000-14,000 MWCO, Spectrum Laboratories) to remove unreacted methacrylic anhydride and triethylamine. After purification, the PEIMA hydrogel was dried under vacuum at room temperature and stored at -20 °C until further use.

5.3.4. Hydrogel characterization

^{1}H NMR spectra were recorded using a Varian Unity INOVA 700-MHz spectrometer. Spectra were acquired at 25 °C using D_2O as solvent. PEI and

methacrylated PEI samples were first dried in vacuum for 24 h and then dissolved in D_2O (100% D, Armar Chemicals). The extent of methacrylation of PEI was determined by peak integration following the procedure reported by Forrest *et al.*[14] Fourier transform infrared (FTIR) spectroscopy of dried methacrylated PEI was performed on a Nicolet 6700 spectrometer (Thermo Scientific) equipped with a single-reflection attenuated total reflectance accessory (Smart iTR) under ambient conditions. Spectra were collected in the range 600-4000 cm^{-1} with a resolution of 4 cm^{-1} and averaging over 128 scans. The ATR correction (germanium crystal) and baseline correction were applied to the data before analysis.

5.3.5. Swelling studies

For analyzing the hydrogel swelling in water, methacrylated PEI samples were dried in vacuum and dry weights (W_d) were measured in glass vials. Next, the samples were incubated in ultrapure water at ambient temperature for 5 days to reach equilibrium swelling state. Excess water was removed from the vials and the swollen hydrogel sample weights (W_s) were measured. The swelling ratio was calculated as W_s/W_d averaging the weights of five different samples.

4.3.6. Morphological analysis

The hydrogel morphology was investigated by confocal laser scanning microscopy using an inverted Leica TCS SP5 confocal and multiphoton microscope (Leica Microsystems) equipped with a HeNe/Argon/MP laser source for fluorescence images and differential interference contrast optics for transmission images. Hydrogel samples were first rehydrated in pure water for four days, and then incubated in a 1 mM solution of the fluorescent

dye Alexa Fluor® 350 succinimidyl ester overnight. Stained hydrogel samples were gently rinsed.

4.3.7. Photopatterning experiments

Patterning of the PEI hydrogels was performed using the inverted Leica TCS SP5 microscope equipped with a multiphoton laser source covering the wavelength range 680-1000 nm. A 40× water immersion objective (Leica HCX PL APO CS 40×/1.10 W UV and Leica HCX IRAPO L 25×/0.95 W) was used. Experiments were conducted at 20 °C with the hydrogel material sealed in a closed cell of PDMS and glass coverslips to prevent water evaporation. Before investigations under the microscope, hydrogel samples were left to equilibrate in the probe solutions overnight at room temperature. The following probes were used: 6 fluorescein free amine group, methacryloxyethyl thiocarbonate rhodaamine B, Alexa Fluor®350 carboxylic acid succinimidyl ester, ATTO 647N with free COOH, free amino group, biotin-COOH, biotin-NH_2 and RGD. Biotin detection after photopatterning was revealed by fluorescent assay using streptavidin labeled with ATTO 647N. The images were analyzed with ImageJ software (U.S. National Institutes of Health, http://imagej.nih.gov/ij/) to compare fluorescence intensities in different region of interests (ROI) after photopatterning.

5.4. Result and discussion

5.4.1. General synthetic scheme

Polyethyleneimine (PEI) is a cationic polyelectrolyte containing a large number of secondary and tertiary amines. PEI macromolecules and its derivatives have been predominantly used as non-viral gene carriers because they form stable complexes with nucleic acids by electrostatic interactions.[15-

[16] Supramolecular PEI-MA hydrogels were prepared from partial methacrylation of branched PEI (M_w ~ 25 kDa) followed by several purification steps. A schematic of the hydrogel synthesis from reaction of branched PEI with bifunctional methacrylic anhydride (MAAH) in dichloromethane is illustrated in Figure 5.1.a. In our approach, we control the self-assembly properties of branched PEI by reducing the electrostatic surface charge of the macromolecules while adding terminal hydrophobic moieties that drive and sustain the formation of the hydrogel network as illustrated in Figure 5.1.b. More important, the methacrylation process confers photosensitivity in the near-IR range to the hydrogel material as illustrated in Figure 5.1.c.

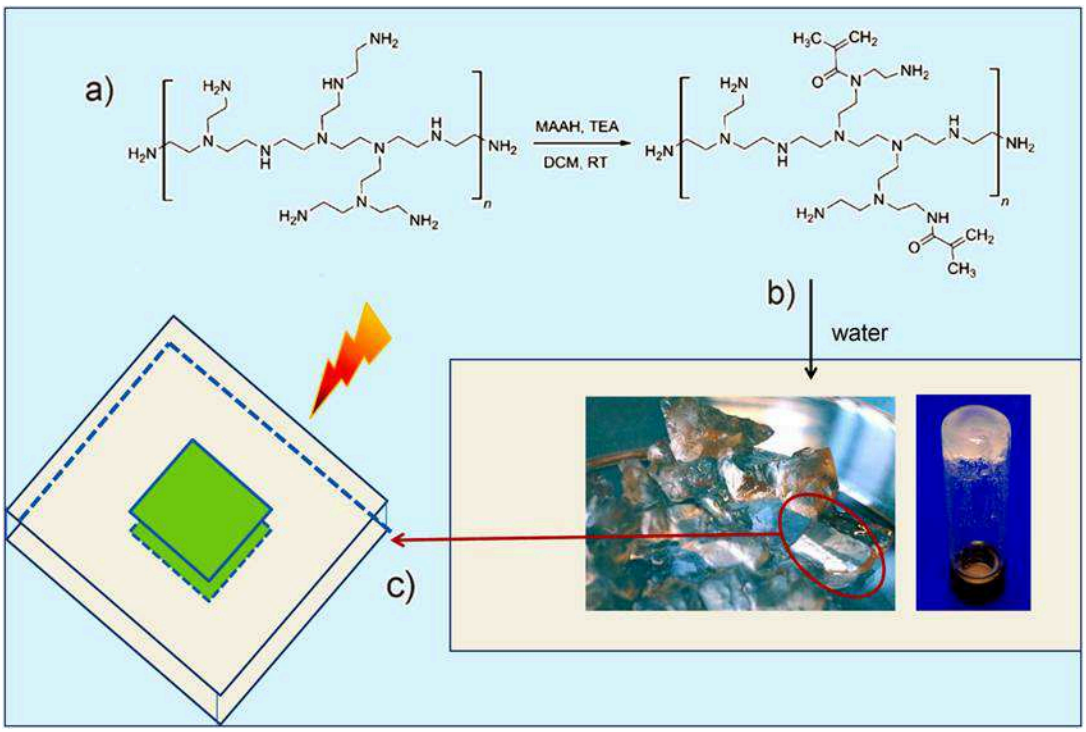

Figure 5.1. - Preparation of photoactive supramolecular hydrogels by methacrylation of branched PEI: **a)** reaction scheme of branched PEI (M_w ~ 25 kDa) with methacrylic anhydride and triethylamine in dichloromethane; **b)** photograph of PEI-MA hydrogel after swelling in water overnight; **c)** laser patterning.

5.4.2. Hydrogel characterization

The modified PEI macromolecules were characterized by ATR-FTIR and ^{1}H NMR spectroscopy to investigate and quantify the methacrylation process at the level of the PEI amine groups. In ATR-FTIR spectroscopy, the spectrum of branched PEI in the fingerprint region (Figure 5.2.b) shows typical absorbance bands at 1123 cm^{-1} for C–N stretching vibrations of secondary amines, at 1298 cm^{-1} for C–N stretching vibrations of primary amines and CH bending vibrations, at 1458 cm^{-1} for N–H bending of secondary amines and CH_2 scissoring vibrations, and at 1585 cm^{-1} for N–H bending vibrations of primary amines.[17-18] After reaction with methacrylic anhydride, the appearance of strong absorption bands in the region 1600–1700 cm^{-1} and at 1542 cm^{-1} indicate formation of amide groups. The peak at 1652 cm^{-1} and 1615 cm^{-1} can be assigned to the C=O stretching vibration of the amide groups (amide I band), whereas the peak at 1542 cm^{-1} is related to the C–N stretching vibration (amide II band). FTIR measurements also show a decrease of the absorption bands at ~1300 cm^{-1} and at ~1100 cm^{-1} after reaction, which confirms that methacrylation occurs at both primary and secondary amines of PEI. Next, we investigated the extent of the PEI amines methacrylation using NMR spectroscopy. The relative ratio of the different amine functional groups in the commercial PEI starting material follows the ratio of 31% primary, 39% secondary and 30% tertiary amines, as determined from ^{13}C NMR analysis previously.[19] This ratio corresponds to a branching factor (% secondary / % tertiary amines) of 1.30, meaning that nearly every second nitrogen forms a branch. After chemical modification of PEI with methacrylic anhydride, we determined the extent of secondary and tertiary amide formation by ^{1}H NMR analysis using a procedure adapted from the literature,[14] in particular by analysis of δ 1.70-1.75 peaks corresponding to methacrylated secondary amines [–NH–$COC(CH_2)CH_3$] and δ 2.0-2.1 peaks corresponding to methacrylated tertiary amines [>N– $COC(CH_2)CH_3$]

(Figure 5.2.a). From this analysis, it was determined that the overall methacrylation extent of branched PEI amines amount to 25.3%, and that PEI primary amines undergo methacrylation to a lower extent (30%) than secondary amines (41%) when reacting under our protocol conditions. This asymmetry in the reactivity of PEI amines is a relevant feature for the self-assembly of the modified PEIMA macromolecules into an hydrogel network, as the hydrogen bonding interactions at the level of methacrylated secondary amines [–NH–COC(CH_2)CH_3] contributes to sustain the hydrogel structure in water.

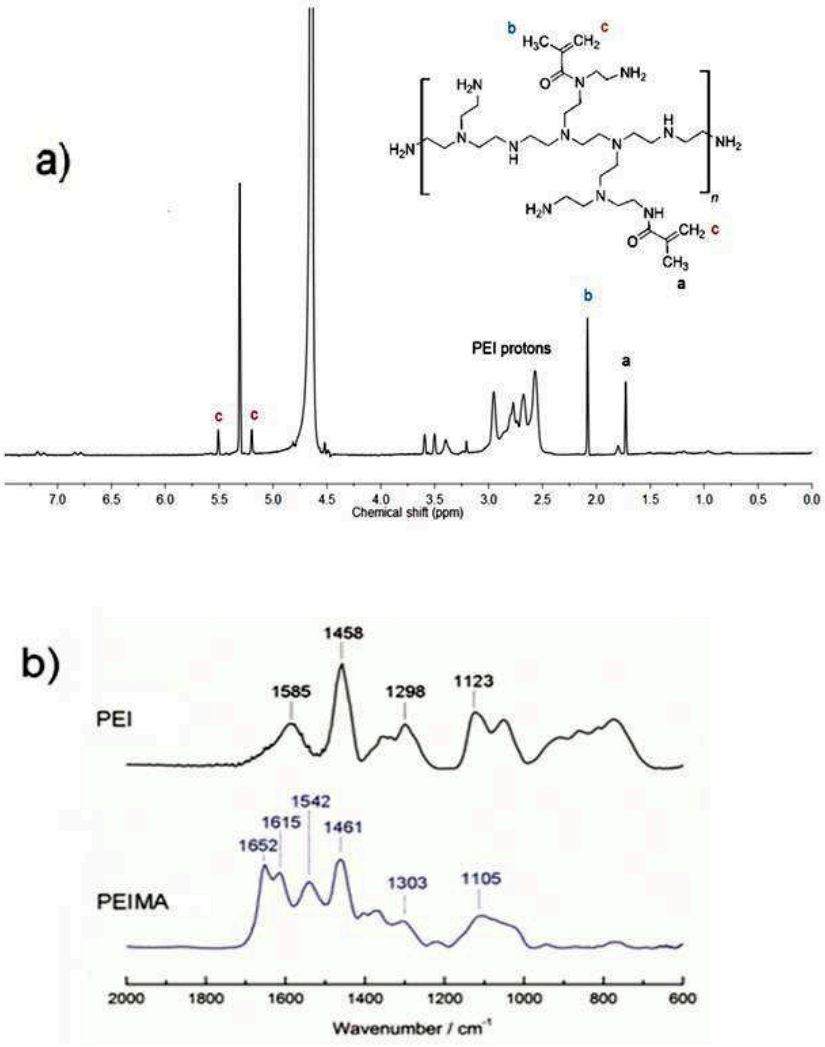

Figure 5.2. a) ^{1}H NMR spectra at 700 MHz of methacrylated branched PEI in D_2O at 25 °C. The peaks at 2.5-3.0 ppm were assigned to protons of PEI backbone, the characteristic peak at 1.70-1.75 ppm (a) to methacrylated secondary amines [–NH–COC(CH_2)CH_3] and the peak at 2.0-2.1 ppm (b) to methacrylated tertiary amines [>N– COC(CH_2)CH_3]. **b)** ATR-FTIR absorbance spectra of dried PEI and methacrylated PEI (PEIMA) collected under ambient conditions.

4.4.3. Swelling behavior

Methacrylated PEI- macromolecules self-assemble in water to form a supramolecular hydrogel material characterized by an equilibrium swelling factor W_s/W_d of 20.6, which corresponds to a water content value of 95.1 wt%. Due to their large water retention, these hydrogels show promising features in terms of biocompatibility for potential biomedical applications.[20-21] The self-assembly of the modified macromolecules in water into supramolecular structures is driven by a delicate balance between association interactions and repulsive interactions.[22] The high swelling values are also consistent with a significant charge density that is present on the PEI network after methacrylation at the reaction conditions that we use. By linking reaction conditions to the hydrogel charge density and to the methacrylation extent of the primary and secondary amines, superabsorbent hydrogels with controlled water retention properties can be synthesized.

4.4.4. Morphological evaluation

The microstructure of PEI-MA hydrogels was investigated at various *xy* planes within the sample by laser scanning confocal microscopy using the amine-specific fluorescent dye Alexa Fluor®350 succinimidyl ester (Figure 5.3.a-f). After equilibrating the hydrogel in water for several days, z-stacks of 10-μm-thick sections of the material were acquired, revealing the presence of large interconnected pores within the hydrogel structure. The large open-network porosity is of the order of several 100 μm, making these hydrogels particularly suitable as cell microenvironments.

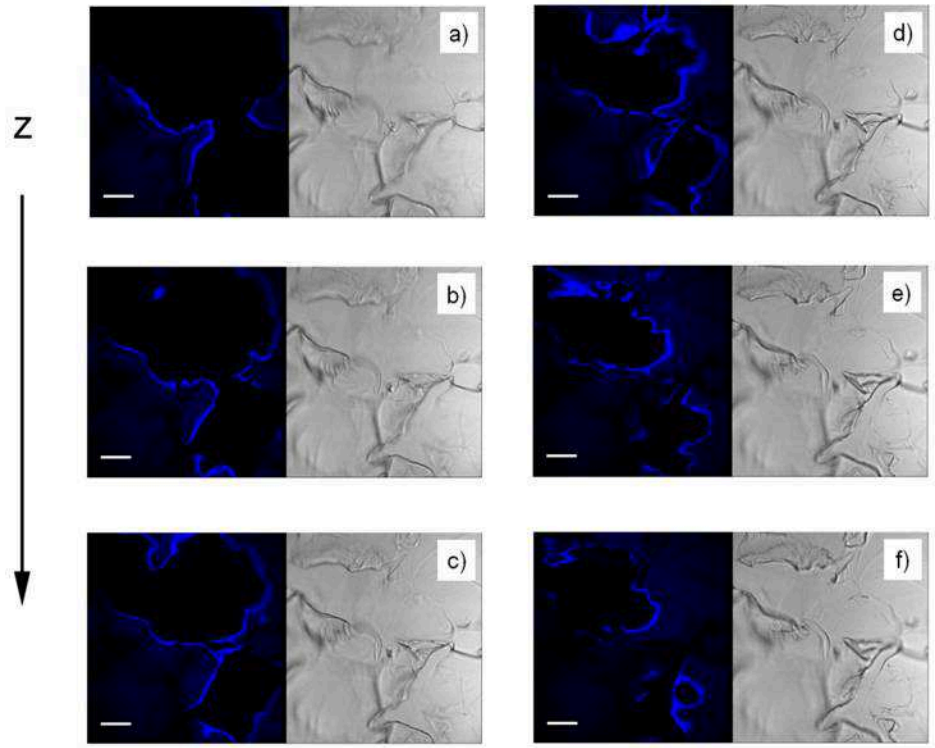

Figure 5.3. - Confocal fluorescence microscopy images (left panels) and white light transmission images (right panels) showing the porous microstructure of the supramolecular PEIMA hydrogel labeled with Alexa Fluor® 350 dye. The sequence shows a z-stack of 10-µm-thick sections across 50 µm of hydrogel sample. All scale bars are 100 µm.

4.4.5. Photopatterning experiments

The two-photon-triggered patterning of the PEI-MA supramolecular hydrogel is demonstrated in confocal microscopy experiments using wavelengths in the 680-1000 nm range. Several molecular probes with various functional groups, with and without fluorescence properties, were tested during the experiments. The hydrogel samples were immersed in water containing the dissolved probe for several hours before the photo-conjugation experiments. Figure 5.4. shows the results from the direct photo-conjugation of PEI-MA hydrogels to several fluorescent probes using two-photon laser irradiation. As reported in the literature, the fluorophores can be excited at resonance

causing photobleaching and attachment for passive substrate preparation via a mechanism involving for example oxygen or radical formation.[4, 23] We used this method to exploit photobleaching of fluorescent molecules to generate patterns and concentration gradients with submicron spatial resolution. In our cases, we observed that photobleaching of fluorophores also generated non fluorescent pattern on hydrogel surfaces. We also demonstrated that several fluorescent probes with opportune chemical groups were useful to give photopatterning. Therefore, we verified that only molecules having carboxylic groups and their derivates, and hydroxyl groups were able to react at the hydrogel interface, probably through radical-mediated photocoupling reaction or Michael-type addition on alkene of the methacrylate groups. As negative control, when the gel was immersed in a solution containing fluorescent probes such as ATTO 647N free amine group or 5(6)-carboxy-X-rhodamine were not able to bound to the hydrogels. In particular, for 5(6)-carboxy-X-rhodamine, even if it presents a carboxylic group in its structure, this is a photo-labile group because it is not covalently bonded to molecule structure. Thus, it did not show the capability to give patterns on the hydrogel and their photo-bleaching was not observable as it was not immobilized.

Figure 5.5. shows the results from the direct photo-conjugation of PEI-MA hydrogels to several non fluorescent biomolecules using two-photon laser irradiation. PEI-MA hydrogels can be photo-patterned only in presence of molecular probes with free carboxylic acid groups or hydroxyl groups, such as biotin-COOH or RGD (Figure 5.5.a-e). When the gel is immersed in a solution containing amine-terminated molecules, such as biotin-NH_2, no patterning is visible (Figure 5.5.b). Control experiments for the hydrogel photo-conjugation were conducted in pure water and resulted in the absence of any hydrogel patterning after two-photon irradiation at wavelengths of 680 nm or 1000 nm (Figure 5.6.a-b). Further, in order to assess whether modifications at the PEI-MA hydrogel interfaces were induced by localized laser heating, we performed patterning experiments in a temperature-

controlled cell and the hydrogel sample was monitored in time. We found no differences in the morphology of the imprinted gel surface up to 30 min after the laser writing experiment. Effective biomolecules photo-conjugation triggered by the two-photon laser irradiation at the hydrogel surface was verified using biotin-COOH as binding probe, and subsequent selective recognition of the biotin-patterned hydrogel by streptavidin-labeled ATTO dyes. Figure 5.7. shows the results of such experiments with fluorescent strep-ATTO-647N that is bound to the photo-patterned biotin-rich area of the hydrogel. It should be noted that we selected the ATTO 647N dyes due to their cationic nature, so that electrostatic adsorption onto the positively charged PEIMA hydrogel could be minimized. As additional investigation, selected areas of the PEIMA hydrogel were photo-patterned with the carboxylated biotin probe for longer times in order to generate areas with higher density of immobilized biotin. After recognition by the streptavidin-labeled ATTO dye, the hydrogel interface was analyzed in fluorescence microscopy experiments. Here the intensity signal from the fluorescent dye in the different areas was quantified in grayscale histograms. Results indicate that it is possible to control the density of the probe that is photo-conjugated to the PEI-MA hydrogel by tuning the exposure time to the near-infrared irradiation (Figure 5.7.b2 and c) as well as with different wavelenghts of the laser source (Figure 5.8.). It is the first time to our knowledge that two-photon 3D patterning has been demonstrated on a highly hydrated self-assembled matrix such as that of the PEI-MA hydrogels, which are characterized by water content of about 95 wt%. These photoactive hydrogels can thus open new avenues of applications, in particular as cell-instructive hydrogels that can be sequentially patterned with 3D topographical cues when immersed in solutions of bioactive molecules terminated by carboxyl or hydroxyl moieties. Previously, two-photon absorption photolithography has been used to create 3D bioactive patterns of integrin ligands and signaling factors in PEGDA hydrogels.[24-25] Under laser irradiation and favored by the

basic environment of the PEI-MA hydrogel, a Michael-type addition reaction between the hydroxyl group of the molecular probe and the carbon-carbon bond of the methacrylate functional groups on the hydrogel surface occurs. Unlike previously reported Michael-type reactions,[26] however, the photo-sensitive reaction that we observe on the PEI-MA hydrogels is induced by near-infrared radiation (680-1000 nm) and requires no additional photoinitiator in solution. The versatile PEI-MA hydrogels can be patterned in the presence of molecular probes with free carboxylic acid groups and their activated substitutions (e.g. succinimidyl ester), as well as free hydroxyl groups. In the first case, the formation of a covalent bond between the deprotonated carboxylic acid groups of the probe and the backbone amine groups of the PEI hydrogel is the most favorable mechanism. In fact, this binding is initiated by the high energy of the multiphoton laser irradiation, and it offers a clean and efficient alternative to currently available conjugation strategies,[27-28] such as those based on EDC/NHS activating systems. On the other hand, in the presence of hydroxyl-terminated molecules the hydrogel basic environment favors the addition reaction of the deprotonated -OH or radical -ȮH groups with the double bonds available on the modified PEI hydrogel to favor metal-free click-chemistry reactions.[29]

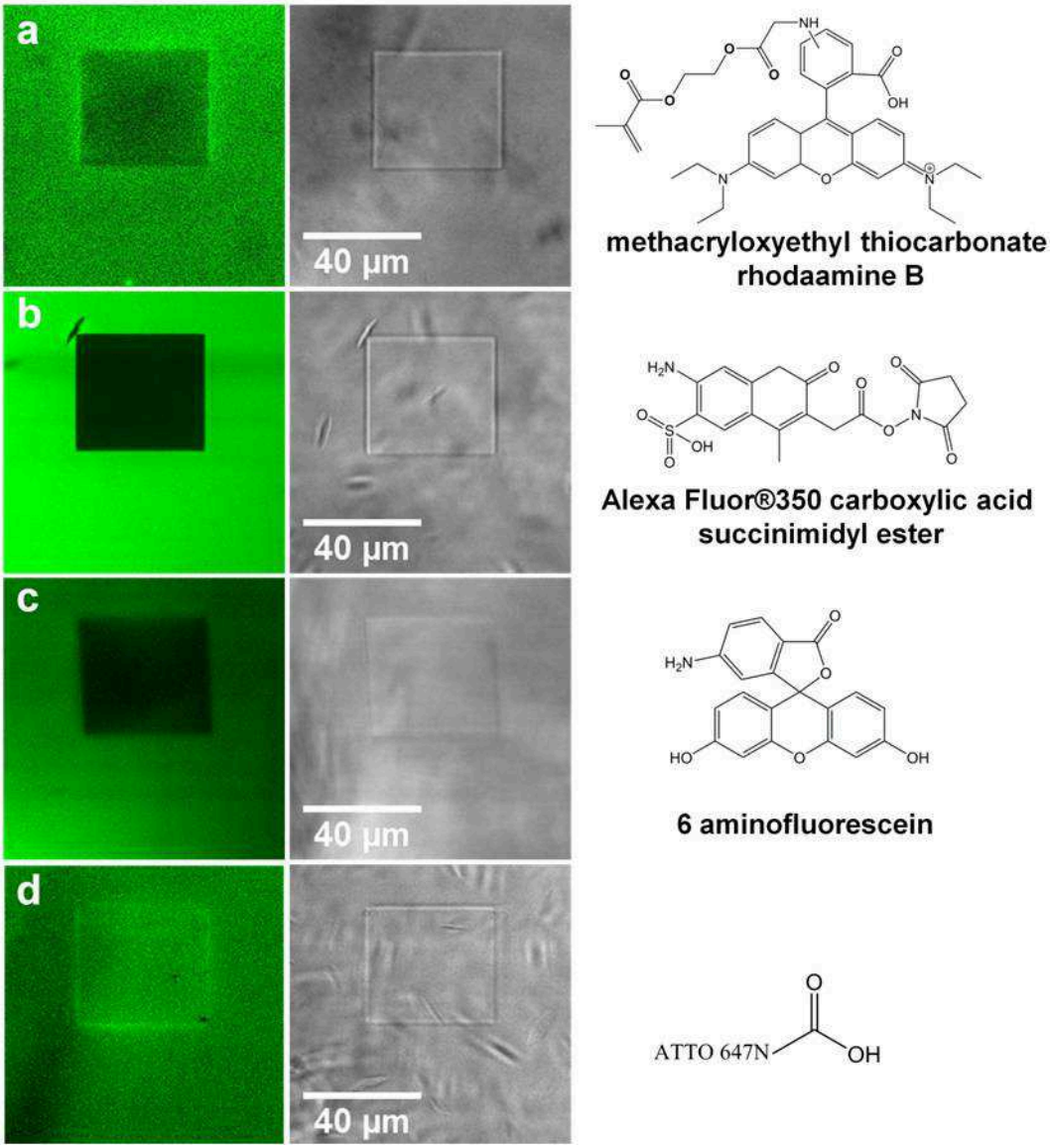

Figure 5.4. – Fluorescence and white light trasmission images of photopatterning by two-photon near-IR activation at λ = 1000 nm. Left: fluorophores photobletching, right: direct photopatterning of PEI-MA hydrogels in solutions. a) methacryloxyethyl thiocarbonate rhodaamine B shows labile photobleaching and pronounced pattern, b) Alexa Fluor®350 carboxylic acid succinimidyl ester shows pronounced photobleaching and pattern, c) 6 aminofluorescein shows labile photobleaching and pattern probably due to low yield of Michael-type addition and d) ATTO 647N free carboxylic group shows resistance to photobleaching but exaltation of fluorescence of the dye bound in pronounced pattern.

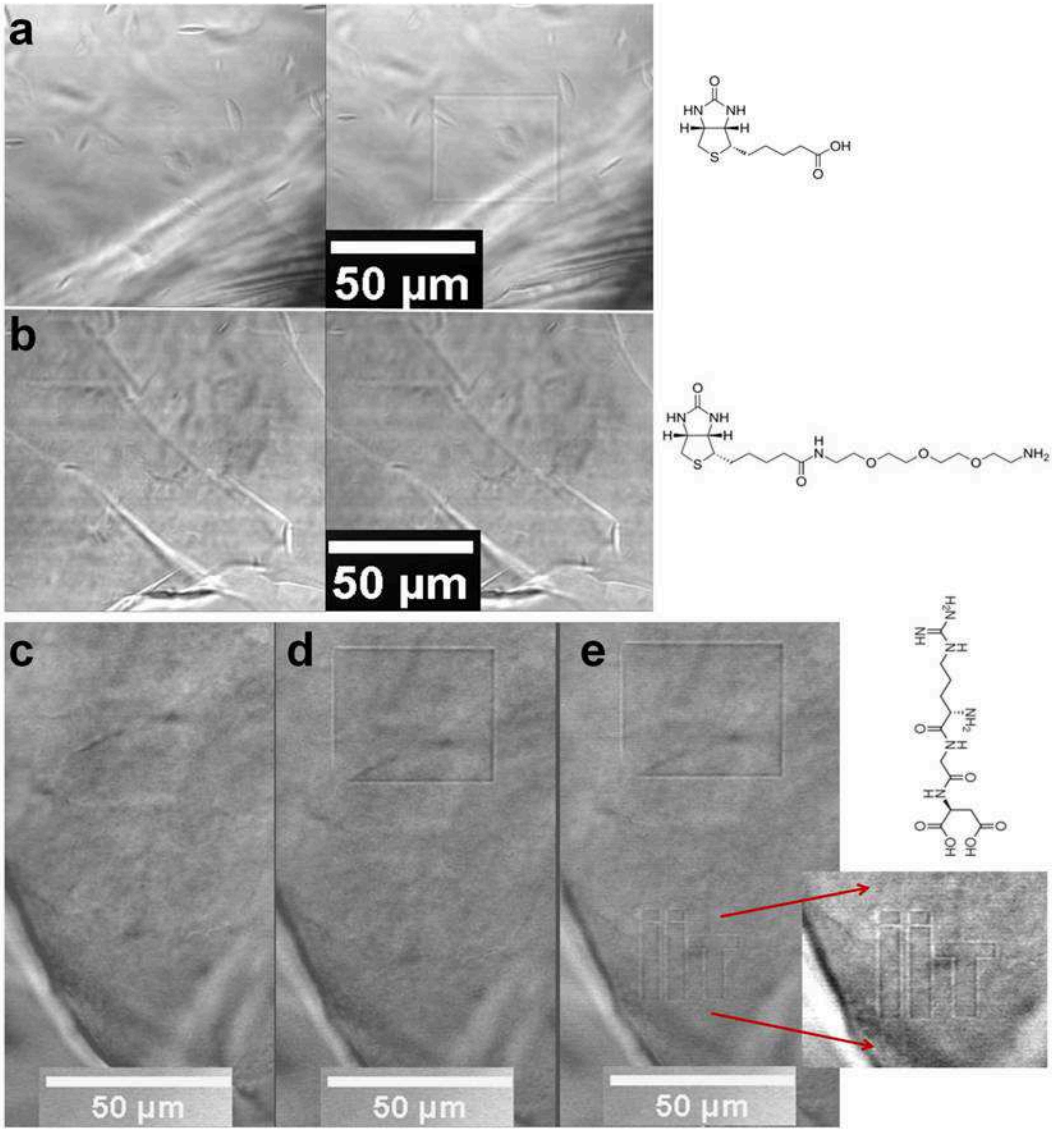

Figure 5.5. - Top: white light transmission images of direct photopatterning of PEI-MA hydrogels in solutions of (a) biotin-COOH and in comparison with experiments in (b) biotin-NH_2 solution where no patterning can be observed. Bottom: white light transmission images of direct photopatterning of PEI-MA hydrogels in solutions of RGD. c) Hydrogel surface without photoactivation, b) direct photopatterning and c) direct photopatterning of hydrogel at micro spatial resolution.

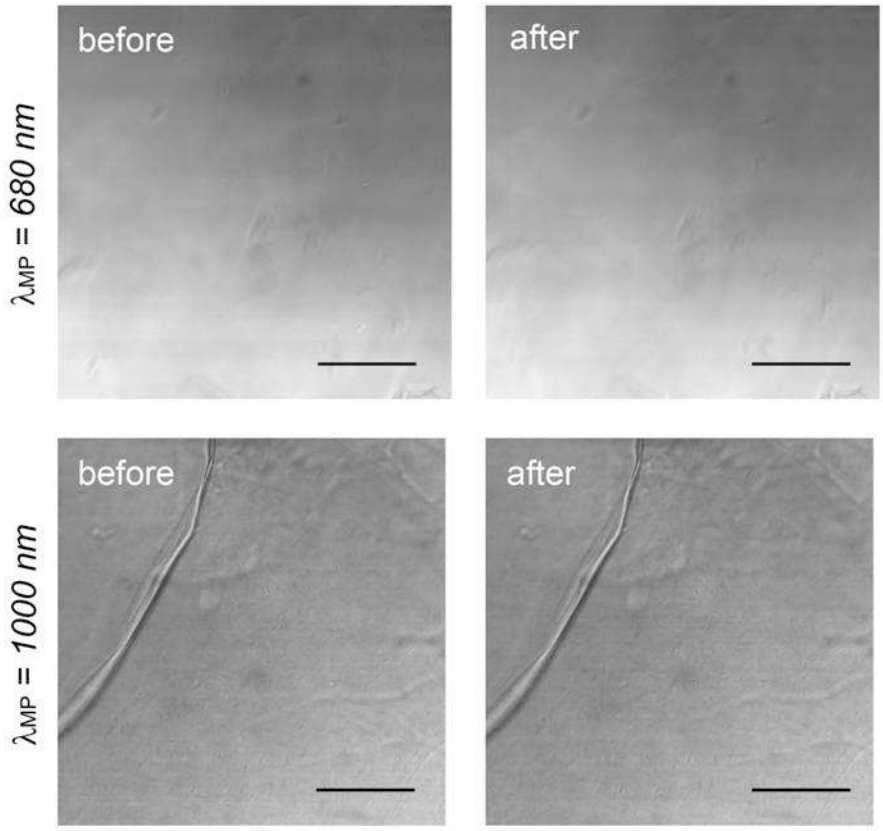

Figure 5.6. - White light transmission images of PEI-MA hydrogel in solution without functional probes. No imprinting is visible before and after multiphoton laser irradiation at wavelengths of 680 nm (top) and 1000 nm (bottom). Scale bars are 100 μm.

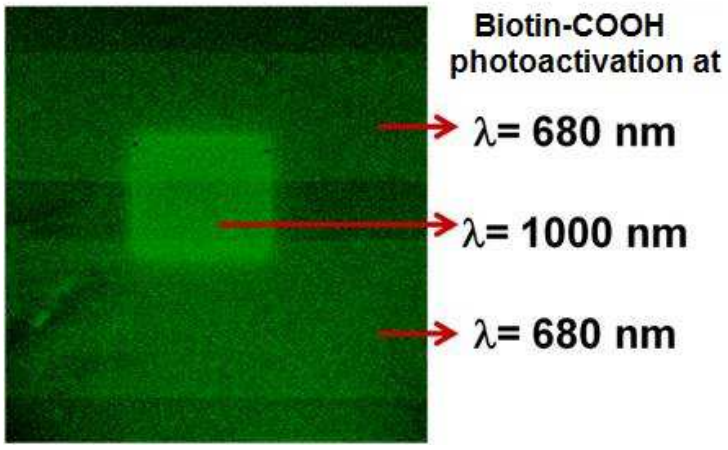

Figure 5.8. - Fluorescent images of direct photopatterning of PEI-MA hydrogels in solutions of biotin-COOH by two-photon near-IR activation at λ= 680 nm and 1000 nm and recognition of the biotin-patterned hydrogel interface with fluorescent streptavidin (strep-ATTO-647N). Image shows fluorescent intensity relative to photoactivation with different wavelenghts of the laser source.

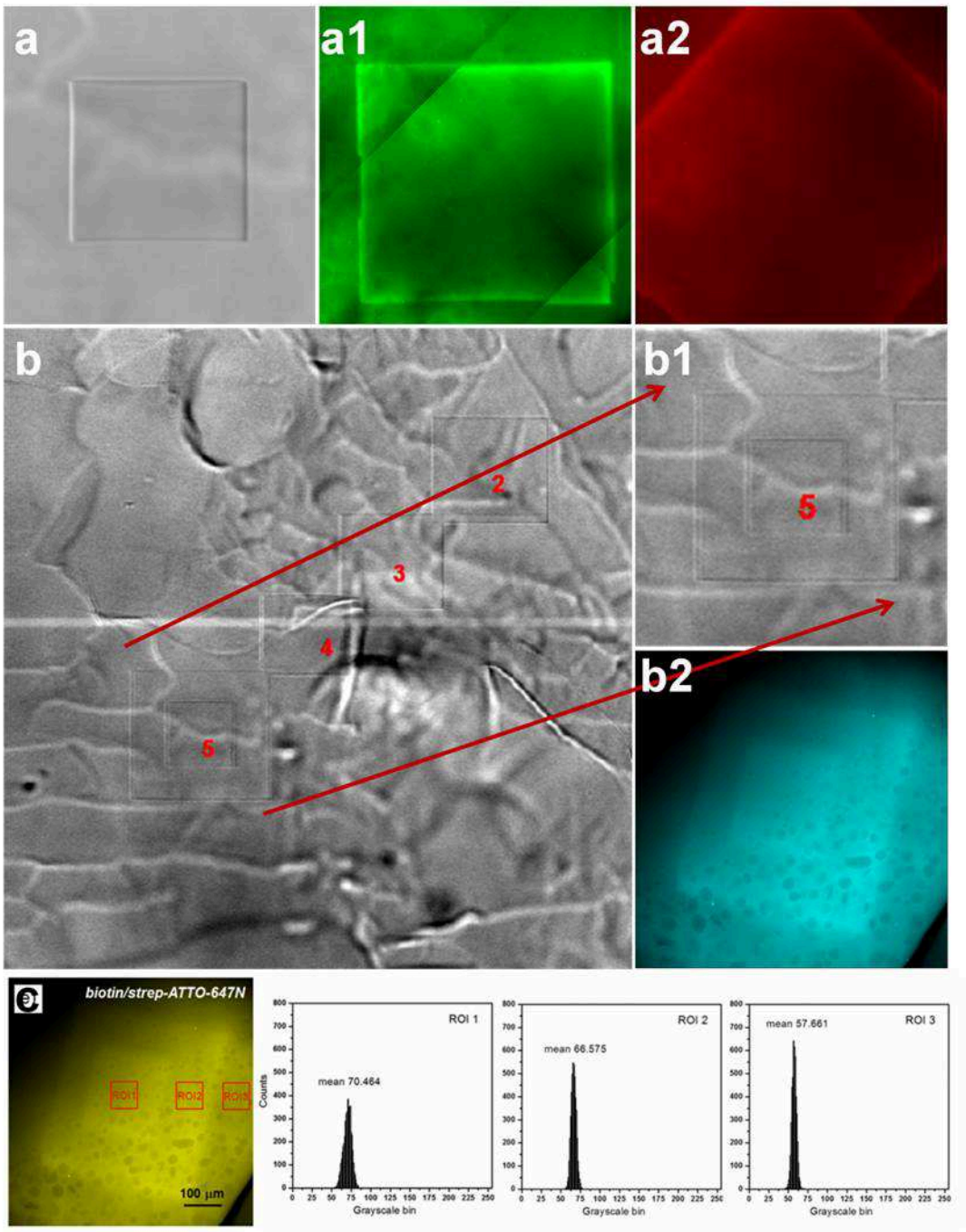

Figure 5.7. - White light transmission images of direct photopatterning by two-photon near-IR activation at λ = 1000 nm of PEI-MA hydrogels in solutions of (a, b and b1) biotin-COOH; a1, a2 and b2) fluorescence images and sequential patterning of PEI-MA hydrogels with biotin-COOH and recognition using strep-ATTO-647N; c) grayscale histograms corresponding to fluorescence intensities from selected ROIs (70×70 μm^2) showing the effect of the additional patterning on the intensity signal from the fluorescent dye.

5.5. Conclusions

In conclusion, we have prepared a novel supramolecular hydrogel that self-assembles from methacrylated branched PEI and where three-dimensional patterns of functional molecules can be permanently written using two-photon laser irradiation. The PEI-MA hydrogels present several advantages. First, they can be patterned under near-infrared radiation without the use of additional photoinitiator molecules, which are often not biocompatible and cytotoxic. In addition, they represent a versatile platform for the facile and rapid patterning of several types of probes as RGD peptide. Our confocal microscopy experiments show that bioactive molecules with free carboxylic acid groups, as well as free hydroxyl groups, can be used for the patterning of these hydrogels. The entire process is completed within few minutes and can be reiterated with solutions of different probes to create multifunctional materials with programmed patterns on the microscale. The novel PEI-MA hydrogels represent an efficient and versatile platform for the creation of three-dimensional patterned structures with immobilized bioactive cues with microscale resolution. We can anticipate that cell-active topographic features with well-controlled architectures can be delivered to these hydrogels on demand, leading to the fabrication of multifunctional cell-instructive materials at the point of use.

5.6. References

1. Sands, R. W.; Mooney, D. J., Polymers to direct cell fate by controlling the microenvironment. *Current Opinion in Biotechnology* **2007,** *18* (5), 448-453.
2. Comisar, W. A.; Kazmers, N. H.; Mooney, D. J.; Linderman, J. J., Engineering RGD nanopatterned hydrogels to control preosteoblast behavior: A combined computational and experimental approach. *Biomaterials* **2007,** *28* (30), 4409-4417.

3. Kilian, K. A.; Bugarija, B.; Lahn, B. T.; Mrksich, M., Geometric cues for directing the differentiation of mesenchymal stem cells. *Proceedings of the National Academy of Sciences* **2010,** *107* (11), 4872-4877.
4. Belisle, J. M.; Correia, J. P.; Wiseman, P. W.; Kennedy, T. E.; Costantino, S., Patterning protein concentration using laser-assisted adsorption by photobleaching, LAPAP. *Lab on a Chip* **2008,** *8* (12), 2164-2167.
5. Culver, J. C.; Hoffmann, J. C.; Poché, R. A.; Slater, J. H.; West, J. L.; Dickinson, M. E., Three-Dimensional Biomimetic Patterning in Hydrogels to Guide Cellular Organization. *Advanced Materials* **2012,** *24* (17), 2344-2348.
6. Appel, E. A.; del Barrio, J.; Loh, X. J.; Scherman, O. A., Supramolecular polymeric hydrogels. *Chem. Soc. Rev.* **2012,** *41* (18), 6195-6214.
7. Leenders, C. M.; Mes, T.; Baker, M. B.; Koenigs, M. M.; Besenius, P.; Palmans, A. R.; Meijer, E., From supramolecular polymers to hydrogel materials. *Materials Horizons* **2014,** *1* (1), 116-120.
8. Aida, T.; Meijer, E.; Stupp, S., Functional supramolecular polymers. *Science* **2012,** *335* (6070), 813-817.
9. Appel, E. A.; Loh, X. J.; Jones, S. T.; Dreiss, C. A.; Scherman, O. A., Sustained release of proteins from high water content supramolecular polymer hydrogels. *Biomaterials* **2012,** *33* (18), 4646-4652.
10. Siegwart, D. J.; Oh, J. K.; Matyjaszewski, K., ATRP in the design of functional materials for biomedical applications. *Progress in Polymer Science* **2012,** *37* (1), 18-37.
11. Deng, X.; Lahann, J., A Generic Strategy for Co-Presentation of Heparin-Binding Growth Factors Based on CVD Polymerization. *Macromol. Rapid Commun.* **2012,** *33* (17), 1459-1465.
12. Azagarsamy, M. A.; Anseth, K. S., Bioorthogonal Click Chemistry: An Indispensable Tool to Create Multifaceted Cell Culture Scaffolds. *ACS Macro Letters* **2013,** *2* (1), 5-9.
13. Hoffman, A. S., Hydrogels for biomedical applications. *Advanced Drug Delivery Reviews* **2002,** *54* (1), 3-12.
14. Forrest, M. L.; Meister, G.; Koerber, J.; Pack, D., Partial Acetylation of Polyethylenimine Enhances In Vitro Gene Delivery. *Pharmaceutical Research* **2004,** *21* (2), 365-371.
15. Pack, D. W.; Hoffman, A. S.; Pun, S.; Stayton, P. S., Design and development of polymers for gene delivery. *Nature Reviews Drug Discovery* **2005,** *4* (7), 581-593.
16. Nguyen, D. N.; Green, J. J.; Chan, J. M.; Langer, R.; Anderson, D. G., Polymeric Materials for Gene Delivery and DNA Vaccination. *Adv. Mater.* **2009,** *21* (8), 847-867.
17. Tan, S.; Erol, M.; Attygalle, A.; Du, H.; Sukhishvili, S., Synthesis of Positively Charged Silver Nanoparticles via Photoreduction of AgNO3 in

Branched Polyethyleneimine/HEPES Solutions. *Langmuir* **2007,** *23* (19), 9836-9843.
18. Larkin, P. J., *Infrared and Raman Spectroscopy; Principles and Spectral Interpretation*. Elsevier: Amsterdam, 2011.
19. von Harpe, A.; Petersen, H.; Li, Y.; Kissel, T., Characterization of commercially available and synthesized polyethylenimines for gene delivery. *Journal of Controlled Release* **2000,** *69* (2), 309-322.
20. Deligkaris, K.; Tadele, T. S.; Olthuis, W.; van den Berg, A., Hydrogel-based devices for biomedical applications. *Sensors and Actuators B: Chemical* **2010,** *147* (2), 765-774.
21. Hoare, T. R.; Kohane, D. S., Hydrogels in drug delivery: Progress and challenges. *Polymer* **2008,** *49* (8), 1993-2007.
22. Steed, J. W., Supramolecular gel chemistry: developments over the last decade. *Chemical Communications* **2011,** *47* (5), 1379-1383.
23. Holden, M. A.; Cremer, P. S., Light Activated Patterning of Dye-Labeled Molecules on Surfaces. *Journal of the American Chemical Society* **2003,** *125* (27), 8074-8075.
24. Hahn, M. S.; Miller, J. S.; West, J. L., Three-Dimensional Biochemical and Biomechanical Patterning of Hydrogels for Guiding Cell Behavior. *Advanced Materials* **2006,** *18* (20), 2679-2684.
25. Leslie-Barbick, J. E.; Shen, C.; Chen, C.; West, J. L., Micron-Scale Spatially Patterned, Covalently Immobilized Vascular Endothelial Growth Factor on Hydrogels Accelerates Endothelial Tubulogenesis and Increases Cellular Angiogenic Responses. *Tissue Engineering Part A* **2011,** *17* (1-2), 221-229.
26. Mather, B. D.; Viswanathan, K.; Miller, K. M.; Long, T. E., Michael addition reactions in macromolecular design for emerging technologies. *Progress in Polymer Science* **2006,** *31* (5), 487-531.
27. DeForest, C. A.; Anseth, K. S., Cytocompatible click-based hydrogels with dynamically tunable properties through orthogonal photoconjugation and photocleavage reactions. *Nature chemistry* **2011,** *3* (12), 925-931.
28. Piston, D. W.; Kremers, G.-J.; Benninger, R. K.; Davidson, M. W., Photoactivation in fluorescence microscopy. *Microscopy Today* **2009,** *17* (4), 8-13.
29. Becer, C. R.; Hoogenboom, R.; Schubert, U. S., Click Chemistry beyond Metal-Catalyzed Cycloaddition. *Angewandte Chemie International Edition* **2009,** *48* (27), 4900-4908.

6. CONCLUSION

(...reaching the aims)

In the first part of the PhD project is been designed and synthesized a novel biomedical device able to operate as wound dressing after surgical or accidental damage of human derma and cornea of the eye. DVS crosslinked hyaluronic acid microbeads were prepared simultaneously combining single emulsion technique and crosslinking reaction. Microbeads prepared with different crosslinking were decorated on their surfaces with a peptide able to recognize specific molecular target on tissues. The peptide from fibronectin isolated since 1984 resulted to be selective and specific for collagen type I binding-sites. In this study, to improve peptides mobility, spatial control and distance from microbeads surface, the peptide sequence is been extended with spacer PEG-based at *N*-teminal region.

Interesting goals have been achieved:

- Preparation of a mimetic materials, having microspheres form (cMB-CIFB), capable to gloss over a specific rule. Microbeads resulted to be able to recognize in selective and specific manner collagen type I in biological tissues as derma and cornea of the eye.
- These microbeads HA-based are able to assemble in continuous layer when were instilled on surfaces of damaged tissues. This layer comes from microbeads deformation and HA layer thickness results to be correlated to crosslinking degree and forces exerted by peptides.
- HA layer is originated by many deformable spherical entities. The assembling of these micro-particles is responsible of a continuous layer formation and the recognition interactions are responsible to firmly hold the layer on tissue.

- This novel qualified material finds useful medical application in clinical post surgery recovering when collagenous tissues are been damaged by surgical and accidental trauma.
- This novel device results to be able to explain corneal wound dressing as temporary substitutes of epithelium and having behavior for cells guidance in tissue regeneration.

In second part of this PhD project, are been designed and synthesized novel supramolecular hydrogels based on PEI branched modified on primary and secondary amines with methacrylic groups. Five supramolecular hydrogels PEI-based are been investigated and chemically characterized. PEI-Ma building blocks are capable to form a supramolecular network, self-assembled in hierarchical architectures. The supramolecular nature of hydrogels prepared was verified by ^{1}H-NMR analysis from absence of crosslinking pick evidence and by fluorescence microscopy verifying that the assembling of PEI gels structure resulted different under temperature variation. PEI-MA hydrogels swollen in large extend of water and swelling properties can be modulated by amount of methacrylic groups introduced. Furthermore PEI Hydrogels resulted to be pH responsive materials.

Interesting goals have been achieved:

- Hydrogels showen periodic properties as verified by ^{1}H-NMR analysis due to different contributes in terms of chemical modifications.
- In the used reaction conditions the methacrylation of the starting PEI branched material was be more predominant on secondary that primary amines.
- The swelling factor depended by secondary and tertiary methacrylated amines ratio and the maximum of swelling factor was observed for PEI-MA 4 when amines methacrylated ratio was of 8:15.

- The different methacrylated degree is correlated to morphological aspects in terms of pore and channel sizes.
- Hydrogels have a predisposed ability to entrap and release plasmid supercoiled of 2800 pb without denature the DNA structure.
- The entrapping kinetic shown for PEI-MA 4 a rapid DNA absorption up to 14 μg per mg of dried hydrogel in 60 minutes.
- The releasing kinetic resulted to be influenced by diffusion mechanism due to plasmid size.
- Hydrogels have a predisposed ability to be tree-dimensional photo-patterned under near-infrared radiation without the use of additional photo-initiator or activator.
- Hydrogels shown a rapid photo-patterning of several types of biological probes as RGD peptide and biotin, extensively at the biomolecules that contain in their chemical structures free hydroxyl and carboxylic active groups.
- The entire patterning process can be completed within few minutes and can be reiterated with solutions of different probes to create multifunctional materials with programmed patterns on the microscale.
- Supramolecular hydrogels PEI-based could represent a sophisticated potential platform where the function, activity and mobility of biomolecules can be manipulated for significant advances in bio-nanotechnology and nanomedicine.
- Cell-active topographic features with well-controlled architectures can be delivered to these hydrogels on demand, leading to the fabrication of multifunctional cell-instructive materials at the point of use.